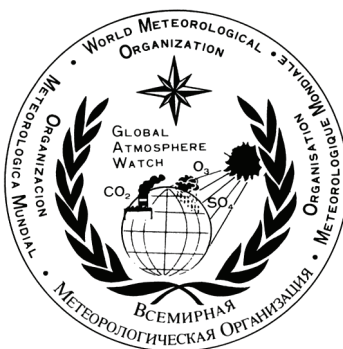


WORLD METEOROLOGICAL ORGANIZATION

GLOBAL ATMOSPHERE WATCH

WORLD DATA CENTRE FOR GREENHOUSE GASES



WMO WDCGG DATA SUMMARY

WDCGG No. 36

GAW DATA

Volume IV-Greenhouse Gases and Other Atmospheric Gases

**PUBLISHED BY
JAPAN METEOROLOGICAL AGENCY
IN CO-OPERATION WITH
WORLD METEOROLOGICAL ORGANIZATION**

MARCH 2012



Acknowledgements

This issue of *Data Summary* reports the latest status of greenhouse and some reactive gases in the global atmosphere. This *Data Summary* has been prepared by the World Data Centre for Greenhouse Gases (WDCGG), established under the Global Atmosphere Watch (GAW) Programme of the World Meteorological Organization (WMO) and operated by the Japan Meteorological Agency (JMA). Data summary is based on the data submitted by many contributors worldwide (Appendix: LIST OF CONTRIBUTORS). These contributors include both organizations and individuals involved in observations and research of greenhouse and some reactive gases at stations and laboratories operating within the framework of GAW and some other monitoring and research programmes. The WDCGG thanks all of these organizations and individuals, including those from the global air sampling network of the National Oceanic and Atmospheric Administration (NOAA), for their efforts in maintaining the observation programme and continuous provision of observational data. Not all of the contributors may be explicitly acknowledged in this publication, owing to lack of space, but all the organizations and individuals that have submitted data to the WDCGG are nevertheless here acknowledged as invaluable contributors to this latest issue of *Data Summary*.

CONTENTS

| | Page |
|--|------|
| SUMMARY ----- | 1 |
| 1. INTRODUCTION ----- | 3 |
| 2. ANALYSIS ----- | 5 |
| 3. CARBON DIOXIDE ----- | 7 |
| 4. METHANE ----- | 15 |
| 5. NITROUS OXIDE ----- | 21 |
| 6. HALOCARBONS AND OTHER HALOGENATED SPECIES ----- | 25 |
| 7. SURFACE OZONE ----- | 31 |
| 8. CARBON MONOXIDE ----- | 35 |
| 9. NITROGEN MONOXIDE AND NITROGEN DIOXIDE ----- | 41 |
| 10. SULPHUR DIOXIDE ----- | 45 |
| REFERENCES ----- | 49 |
| APPENDICES ----- | 53 |
| CALIBRATION AND STANDARD SCALES ----- | 54 |
| LIST OF OBSERVATING STATIONS ----- | 67 |
| LIST OF CONTRIBUTORS ----- | 79 |
| GLOSSARY ----- | 97 |
| LIST OF WMO/ WDCGG PUBLICATIONS ----- | 99 |

SUMMARY

This *Data Summary* reports the results of basic analyses of greenhouse and some reactive gas data submitted to the WMO World Data Centre for Greenhouse Gases (WDCGG). This issue covers observations from 1968 through 2010, based on data reported to the WDCGG by October 2011. The *Data Summary* includes analyses of global, hemispheric and latitudinal monthly mean mole fractions of greenhouse and some reactive gases, and provides information on the current state of mole fractions of these gases at the stations.

Although only monthly mean mole fractions were used for the analyses, the WDCGG greatly appreciates those stations that submit daily and hourly mean mole fractions, which are important for analysing variations on shorter time scales. All data submitted to the WDCGG are available on its web site, <http://ds.data.jma.go.jp/gmd/wdogg/>.

To represent dry mole fractions, this *Data Summary* uses the units ppm, ppb and ppt, which correspond to the SI units $\mu\text{mol/mol}$, nmol/mol and pmol/mol , respectively.

Variations in the mole fractions of some gases are presented as combinations of seasonal cycles and deseasonalized long-term trends. Growth rates are presented as time derivatives of the long-term trends. The analytical results are summarized below for each greenhouse and reactive gas.

Carbon Dioxide (CO₂)

The level of carbon dioxide (CO₂), which contributes the most to increases in anthropogenic induced radiative forcing, has been increasing since the beginning of the industrial era. The global average mole fraction of CO₂ reached a new high of 389.0 ppm in 2010, 139% of that in the pre-industrial period (1750). The annually averaged increase of 2.3 ppm from 2009 to 2010 was larger than the average growth rate for the 1990s (about 1.5 ppm/year) and for the past decade (about 2.0 ppm/year).

The global growth rate of CO₂ has a significant interannual variation driven by natural processes. Growth rates higher than 2 ppm/year in 1987/1988, 1997/1998, 2002/2003 and 2009/2010 resulted from warmer conditions caused by El Niño-Southern Oscillation (ENSO) events. The anomalously strong El Niño event in 1997/1998 resulted in greater annual increases in CO₂ worldwide in 1998 than during any other one-year period. The high growth rates in 2006 may have been related to the global high temperature during the same year. The exceptionally low growth rates in 1992, including negative values in northern high latitudes, may have been due to low global temperatures following the eruption of Mount Pinatubo

in 1991. Variations in CO₂ mole fraction can be seen both on seasonal and long-term scales. The seasonal amplitudes are large in northern high and mid-latitudes and small in the Southern Hemisphere. In southern low latitudes, there is no clear annual cycle, but a semiannual cycle can be determined.

Methane (CH₄)

Methane (CH₄) is the second most significant greenhouse gas which is largely influenced by anthropogenic activity and whose level has been increasing since the beginning of the industrial era. The annual average mole fraction was 1808 ppb in 2010, an increase of 5 ppb since 2009. The mole fraction is now 258% of that in the pre-industrial period. This is the fourth year of strong methane increases after the levelling-off in the beginning of this century.

The latitudinal gradient of CH₄ mole fraction is large from the northern mid-latitudes to the tropics, suggesting that the major sources of CH₄ are located in the Northern Hemisphere.

CH₄ growth rates decreased significantly in some years, including 1992, when negative values were recorded in northern high and mid-latitudes. However, both hemispheres experienced high growth rates in 1998, caused by an exceptionally high global mean temperature. The global growth rates were generally low from 1999 to 2006, except during the El Niño event of 2002/2003. The global growth rate averaged over the period 1984–1990 was 11.5 ppb/year, but decreased markedly in the 1990s. The average global growth rate for the period 2000–2010 was 2.6 ppb/year, but in the last four years through 2010, the global mole fraction increased by a total of 24 ppb.

CH₄ mole fractions vary seasonally, being relatively high in winter and low in summer. Unlike CO₂, the seasonal amplitudes of CH₄ are large, not only in the Northern Hemisphere but also in southern high and mid-latitudes as those are connected with a chemical sink of methane. In southern low latitudes, a distinct secondary maximum in boreal winter overlies the annual cycle.

Nitrous Oxide (N₂O)

Nitrous oxide (N₂O) is an important greenhouse gas whose level is increasing globally. N₂O data submitted to the WDCGG show that mole fractions are increasing in both hemispheres. The global mean mole fraction reached a new high of 323.2 ppb in 2010, 0.8 ppb higher than that in the previous year. This mole fraction corresponds to 120% of that in the pre-industrial period. The mean growth rate of the global mean mole fraction over the period 2000–2010 was 0.75 ppb/year and the inter-hemispheric gradient

in N_2O is 1.1 ppb (averaged over the years 1980 to 2010), indicating that majority of N_2O sources are situated in the Northern hemisphere.

Halocarbons and Other Halogenated Species

Halocarbons, most of which are anthropogenic and generated from 20th Century, are potent greenhouse gases, with some also acting as ozone-depleting compounds. Levels of some halocarbons (e.g. CFCs) increased in the 1970s and 1980s, but this increase has almost ceased by now, due to the production and consumption control of halocarbons under the Montreal Protocol on Substances that Deplete the Ozone Layer and its subsequent Adjustments and Amendments. However, some substances targeted by the Kyoto Protocol but not regulated by the Montreal Protocol, such as HFCs and SF_6 , are increasing.

The mole fraction of CFC-11 peaked around 1992 and then started decreasing. The growth rate of CFC-12 increased until around 2005 and then started decreasing gradually. The mole fraction of CFC-113 stopped increasing in the 1990s, followed by a slight decrease over the last decade. The mole fractions of HCFCs, used mainly as substitutes for CFCs, have increased significantly during the last decade, but the growth of HCFC-141b decelerated rapidly in the second half of the decade. The mole fraction of Halon-1211 has not increased since 2005, whereas the mole fraction of Halon-1301 is increasing. The mole fraction of CCl_4 was maximal around 1991 and has since decreased slowly. The mole fraction of CH_3CCl_3 peaked around 1992 and decreased thereafter. The mole fractions of HFC-134a, HFC-152a and SF_6 are increasing.

Surface Ozone (O_3)

Ozone (O_3) plays important roles in the atmospheric environment through radiative and chemical processes. It absorbs solar UV radiation in the stratosphere, influencing the vertical temperature profile as well as terrestrial IR radiation, and contributing to the greenhouse effect as a greenhouse gas. Ozone is also involved in the chemical transformations of the primary air pollutants, as its mole fraction in the boundary layer serves as an indicator of air quality.

The mole fraction of O_3 near the surface, so-called surface ozone, reflects various processes. While some of the O_3 in the troposphere comes from the stratosphere, the rest is chemically produced in the troposphere through oxidation of CO or hydrocarbons in the presence of NO_x .

The mole fraction of surface ozone is measured at many locations in various environments. Due to its uneven geographic distribution, however, it is difficult to identify a global long-term trend of surface O_3 (WMO, 2011b).

Carbon Monoxide (CO)

Carbon monoxide (CO) is not a greenhouse gas itself but influences the mole fractions of greenhouse gases by affecting hydroxyl radicals (OH). Its mole fractions in northern high latitudes have been increasing since the mid-19th century. In 2010, the global mean mole fraction of CO was about 93 ppb. The mole fraction is high in the Northern Hemisphere and low in the Southern Hemisphere, suggesting substantial anthropogenic emissions in the Northern Hemisphere.

There was a large fluctuation in growth rate of CO. High positive rates followed by high negative rates in northern latitudes and southern low latitudes from 1997 to 1999. The growth rates in the Northern Hemisphere increased again in 2002. Both growth rate increases are attributed to large scale biomass burnings related with El Niño events.

The monthly mean mole fractions show seasonal variations, with large amplitudes in the Northern Hemisphere and small amplitudes in the Southern Hemisphere with opposite phase.

Nitrogen Monoxide (NO) and Nitrogen Dioxide (NO_2)

Nitrogen oxides (NO_x , i.e., NO and NO_2) are not greenhouse gases but are involved in the photochemical production of ozone in the troposphere. In the presence of NO_x , CO and hydrocarbons are oxidized to produce ozone (O_3), which affects the Earth's radiative balance as a greenhouse gas and the oxidization capacity of the atmosphere by reproducing OH.

Most of the stations that have so far reported NO_x data to the WDCGG are located in Europe. NO_x has a large temporal and geographic variability, and it is difficult to identify its long-term global trend based on a spatially limited dataset.

Sulphur Dioxide (SO_2)

Sulphur dioxide (SO_2) is not a greenhouse gas but a precursor of atmospheric sulphate aerosols. Sulphate aerosols are produced by SO_2 oxidation through photochemical gas-to-particle conversion. SO_2 has also been a major source of acid rain and deposition throughout the industrial era.

Most of the stations reporting SO_2 data to the WDCGG are located in Europe. Global analysis can not be performed on this data set.

1. INTRODUCTION

Human activities have had major impacts on the global environment. Since the beginning of the industrial era, mankind has increasingly made use of land, water, minerals and other natural resources, and continuous growth of the world human population and economies may further increase our impact on the environment. As the climate, biogeochemical processes and natural ecosystems are closely interlinked, changes in any one of these may affect the others and be detrimental to humans and other organisms. Emissions of man-made gaseous species and particulate matter alter the energy balance of the atmosphere, which in turn has implications for the interactions in the system atmosphere - hydrosphere - biosphere. Complex interactions in this system, including numerous feedbacks, are not completely understood in particular due to the lack of observations.

The World Meteorological Organization (WMO) established the Global Atmosphere Watch (GAW) Programme in 1989 to promote systematic and reliable observations of the global environment, including but not limited to, greenhouse gases (*e.g.*, CO₂, CH₄, CFCs, and N₂O) and some reactive gases (*e.g.*, O₃, CO, NO_x, and SO₂) in the atmosphere. In October 1990, WMO designated the Japan Meteorological Agency (JMA) in Tokyo to serve as the World Data Centre for Greenhouse Gases (WDCGG). The WDCGG is responsible for collecting, archiving and providing data on greenhouse and reactive gases in the atmosphere and oceans from a number of observation sites throughout the world that participate in GAW and other scientific monitoring programmes (Appendix: LIST OF OBSERVING STATIONS). In August 2002, the WDCGG took over the role of the World Data Centre for Surface Ozone from the Norwegian Institute for Air Research (NILU).

With regard to the issue of climate change the Kyoto Protocol to the United Nations Framework Convention on Climate Change entered into force in February 2005. In March 2006, WMO commenced annual publication of the WMO Greenhouse Gas Bulletin, which summarizes the state of greenhouse gases in the atmosphere. The seventh issue of the Bulletin was published in November 2011. The WDCGG contributes to the production of the bulletin through timely and adequate collection and analysis of data in cooperation with the contributors of the data.

Since its establishment, the WDCGG has provided its users with data and other information through its regular publications, including the *Data Summary* and *DVD* (Appendix: LIST OF WMO WDCGG PUBLICATIONS). In accordance with the GAW Strategic Plan: (2008–2015) and its Addendum, all data and information have been made available on the WDCGG web site, improving the accessibility of data, information and products (WMO, 2007a; WMO, 2011a). The WDCGG published the Data Submission and

Dissemination Guide in 2007 (WMO, 2007b), which, with its revision in 2009 (WMO, 2009b), is designed to facilitate submission of observational data and access to archived data in the WDCGG.

The GAW Strategic Plan requests that World Data Centres assist data users by providing the data and analysis related to atmospheric observations. To this end, the WDCGG provides global and integrated diagnostics on the state of greenhouse and some reactive gases as analytical information in the *Data Summary*. The WDCGG global analysis methods have been described in a GAW technical report (WMO, 2009a). The content of the *Data Summary* is revised and improved based on comments from data contributors and scientists. We hope the diagnostic information presented here will promote the use of data on greenhouse and reactive gases and will enhance appreciation of the value of the GAW Programme.

All users are required to accept the following statement endorsed by the Commission for Atmospheric Sciences (CAS) at its thirteenth session: “For scientific purposes, access to these data is unlimited and provided without charge. By their use you accept that an offer of co-authorship will be made through personal contact with the data providers or owners whenever substantial use is made of their data. In all cases, an acknowledgement must be made to the data providers or owners and to the data centre when these data are used within a publication.” The WDCGG requests data users to make appropriate acknowledgements. The principal investigators and other contacts can be obtained from the WDCGG website, as well as from the GAW Station Information System (GAWSIS) website, <http://gaw.empa.ch/gawsis/>. Information on these websites is updated in cooperation with the data contributors and the WMO Secretariat.

Finally, the WDCGG would like to thank all data contributors worldwide, including those involved in on-site measurements, for their efforts in maintaining the observational programme and for continuous data provision.

Mailing address:

WMO World Data Centre for Greenhouse Gases
(WDCGG)

c/o Japan Meteorological Agency

1-3-4, Otemachi, Chiyoda-ku, Tokyo 100-8122, Japan

E-mail: wdcgg@met.kishou.go.jp

Telephone: +81-3-3287-3439

Facsimile: +81-3-3211-4640

Web Site: <http://ds.data.jma.go.jp/gmd/wdcgg/>

2. ANALYSIS

The WDCGG collects, archives and provides observational data on the dry mole fractions of greenhouse and some reactive gases, and publishes diagnostic information on these gases based on the reported data.

The long-term trends and seasonal variations in the mole fractions of CO₂, CH₄ and CO are calculated for the whole globe (global means) and for latitudinal belts (zonal means). Only global and hemispheric long-term trends are calculated for N₂O. Global long-term trends in the surface O₃, are not analysed due to its substantial spatial gradients, and its uneven geographic distribution which is poorly covered by observation sites. For halocarbons, NO_x and SO₂, only monthly mean mole fractions over time are presented without global, hemispheric or zonal averaging, due to insufficient number of reporting sites for each compound.

The units used in this analyses are ppm, ppb, and ppt, rather than the SI units of $\mu\text{mol/mol}$, nmol/mol , and pmol/mol , respectively.

The method of analysis for CO₂, CH₄, CO and N₂O are summarized below. The details of the global analysis methods for CO₂, CH₄, and N₂O are provided in the *Technical Report of Global Analysis Method for Major Greenhouse Gases by the World Data Centre for Greenhouse Gases*, published as a GAW technical report (WMO, 2009a). Additional uncertainty can be expected in the result of CO global analysis due to diversity of scales. When assessing long-term trends for CO₂, CH₄ and N₂O, the growth rates at both ends of the period were assumed to be simple linear extensions of the adjacent year, thus avoiding end effects. For simplicity, the rates for the rest of the period were approximated by linear expressions.

(1) Site selection

For CO₂, CH₄ and N₂O, the diagnostic analyses, including global, hemispheric and zonal means, were based on data from sites that have adopted a standard scale traceable to the Primary Standard designated under GAW. These analyses also utilize data on other standard scales that are convertible to the WMO/GAW scale through a proven equation. The letters encouraging data submitters on the most recent WMO scales are sent out regularly since 2010.

Selection of observation sites have also been based on whether they provide data representing a reasonably large geographical area, considering the fact that some sites may be susceptible to local sources and sinks. Sites are selected objectively using data submitted to the WDCGG. Only those sites for CO₂, CH₄ and CO that provide annual mean mole fractions falling within a range of $\pm 3\sigma$ from a curve fitted to the LOESS model

curve (Cleveland *et al.*, 1988) have been selected, with outliers rejected in an iterative manner. This procedure does not affect the datasets present in the WDCGG, and these data may be useful for purposes other than global analysis, such as sources and sinks identification.

The sites selected according to the above criteria are marked with asterisks in Plate 3.1 for CO₂, Plate 4.1 for CH₄, Plate 5.1 for N₂O and Plate 8.1 for CO, which represent 128, 125, 53 and 53 of the submitted datasets respectively.

(2) Analysis of long-term trends

The mole fractions of greenhouse and reactive gases over time, measured under unpolluted conditions, exhibit variations on different time scales. The two major components are seasonal variations and long-term trend. Various attempts have been made to divide measured data into these two components, including objective curve fitting (Keeling *et al.*, 1989), digital filtering (Thoning *et al.*, 1989; Nakazawa *et al.*, 1991), or both (Conway *et al.*, 1994; Dlugokencky *et al.*, 1994).

In this report, seasonal variations derived from components of Fourier harmonics and long-term trends are extracted by low-pass filtering with a cut-off frequency of 0.48 year^{-1} for each selected site. Details are described in WDCGG Data Summary No. 22 (WMO, 2000).

(3) Estimation for missing periods and gaps

The number and distribution of sites used to assess trends during the analysis period should be kept as constant as possible to avoid the effects of changes in the availability of data over time. However, only a small number of sites provided data throughout the entire analysis period; others may have covered shorter periods or had gaps in measurements due to different reasons. To use as many sites as possible, missing values were estimated for the calculation of zonal means, using interpolation and extrapolation as described below.

For the former, gaps were interpolated linearly based on the data, by subtracting the seasonal variation calculated from the longest consecutive period of data with Lanczos filters (Duchon, 1979). The subtracted variation was added back to the data to obtain estimated mole fractions in a single sequence.

For the latter, long-term trends calculated from the interpolated series of data were extrapolated based on zonal mean growth rates calculated from other sites in the same latitudinal zone. The seasonal variation was added to the extrapolated long-term trend to obtain estimated mole fractions for the entire period of analysis.

Using these statistical procedures, the future addition of new stations should not affect the consistency in global estimates over time.

(4) Calculation of global, hemispheric and zonal means

Zonal means were calculated by determining the arithmetic average of the mole fractions in each latitudinal zone, based on consistent datasets derived as above.

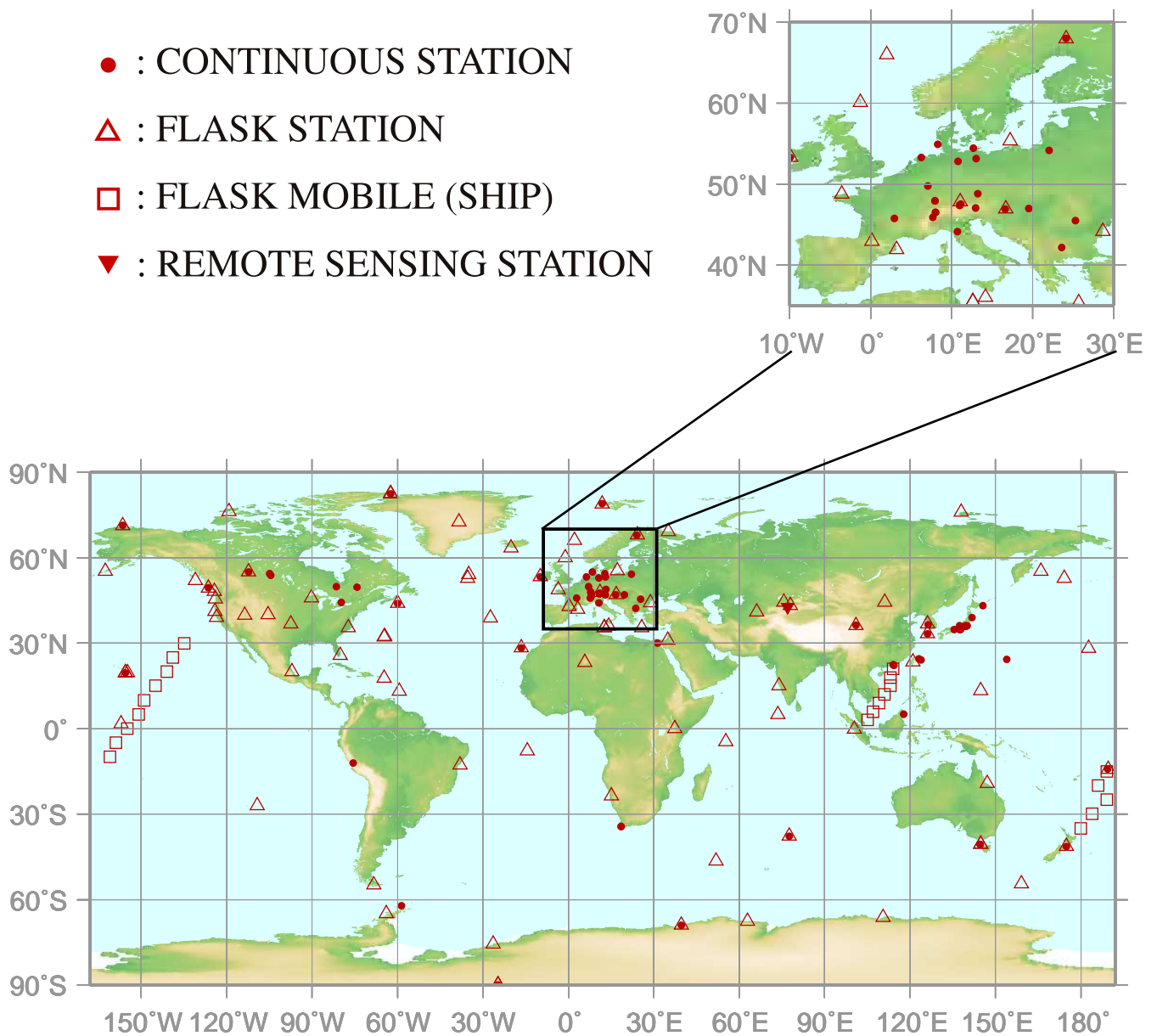
Global and hemispheric means were calculated as the weighted averages of the zonal means taking account of the area of each latitudinal zone.

Deseasonalized long-term trends and growth rates for the globe, each hemisphere and each latitudinal zone were calculated from the global, hemispheric and zonal means, respectively, using the low-pass filter mentioned above and the time derivatives after filtering.

3.

CARBON DIOXIDE (CO₂)

- : CONTINUOUS STATION
- △ : FLASK STATION
- : FLASK MOBILE (SHIP)
- ▼ : REMOTE SENSING STATION



This map shows locations of the stations that have submitted data for monthly mean mole fraction.

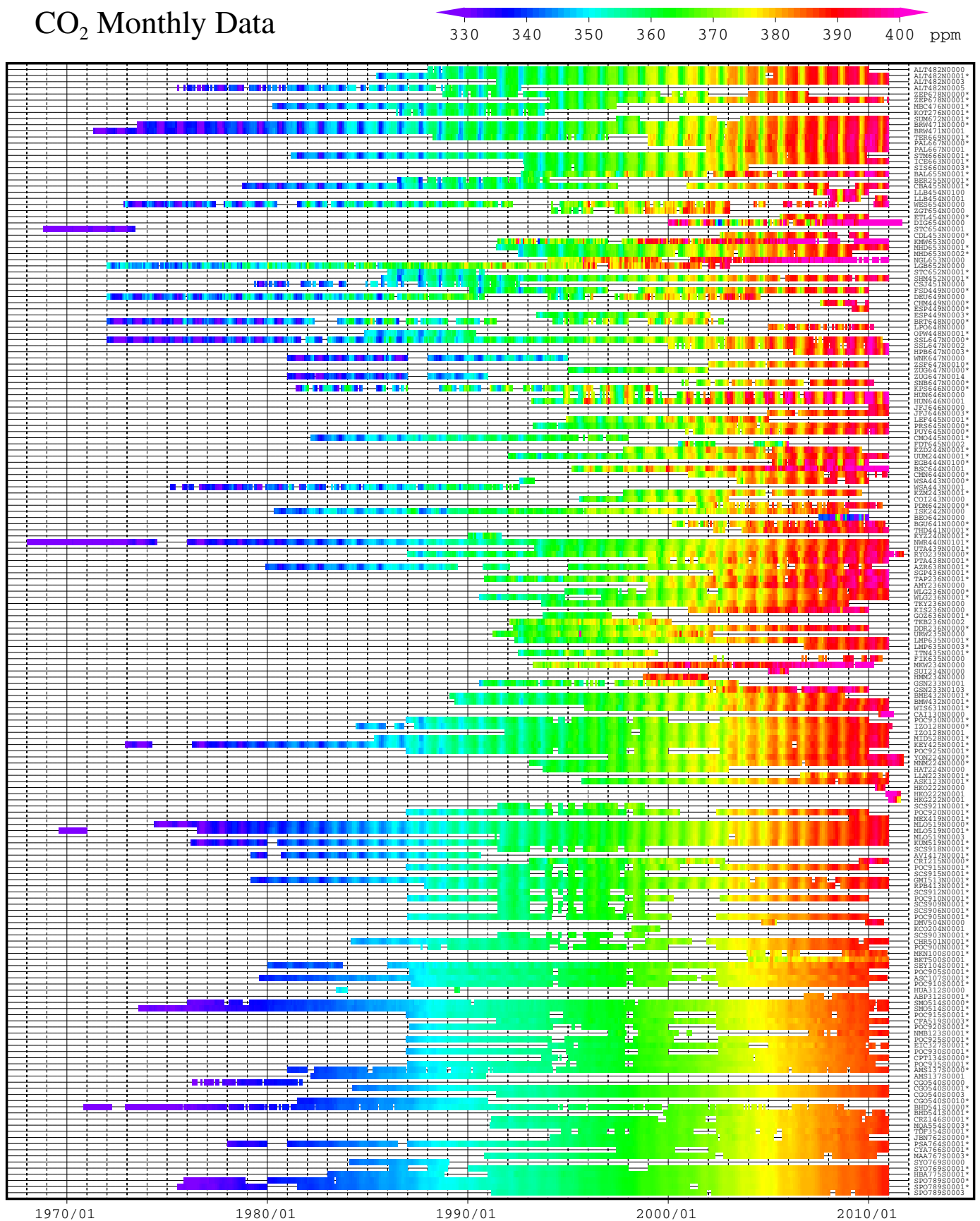
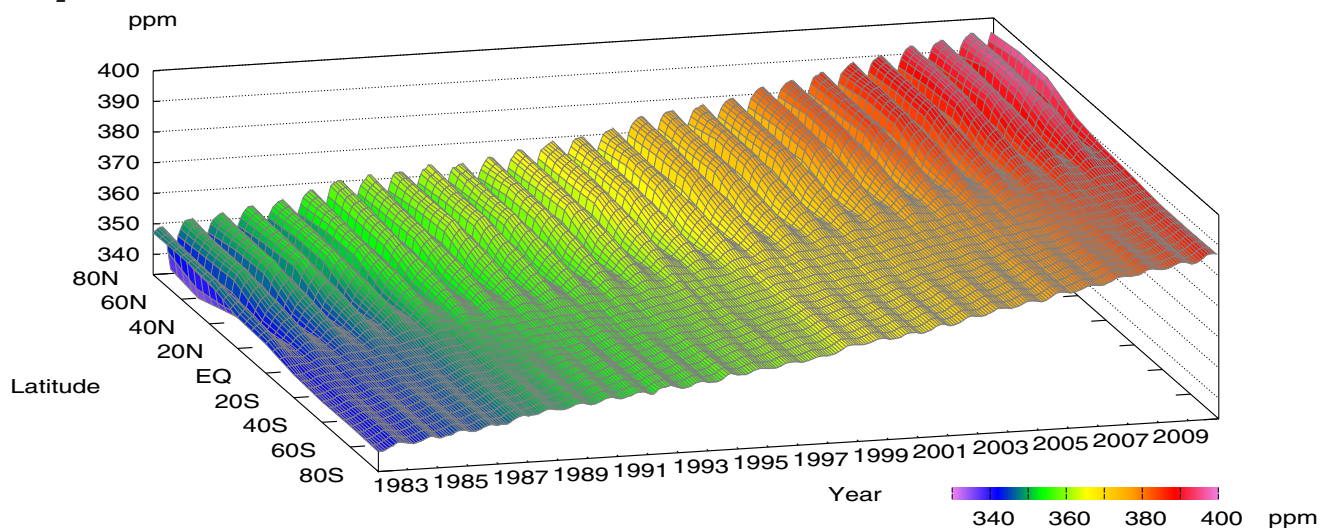
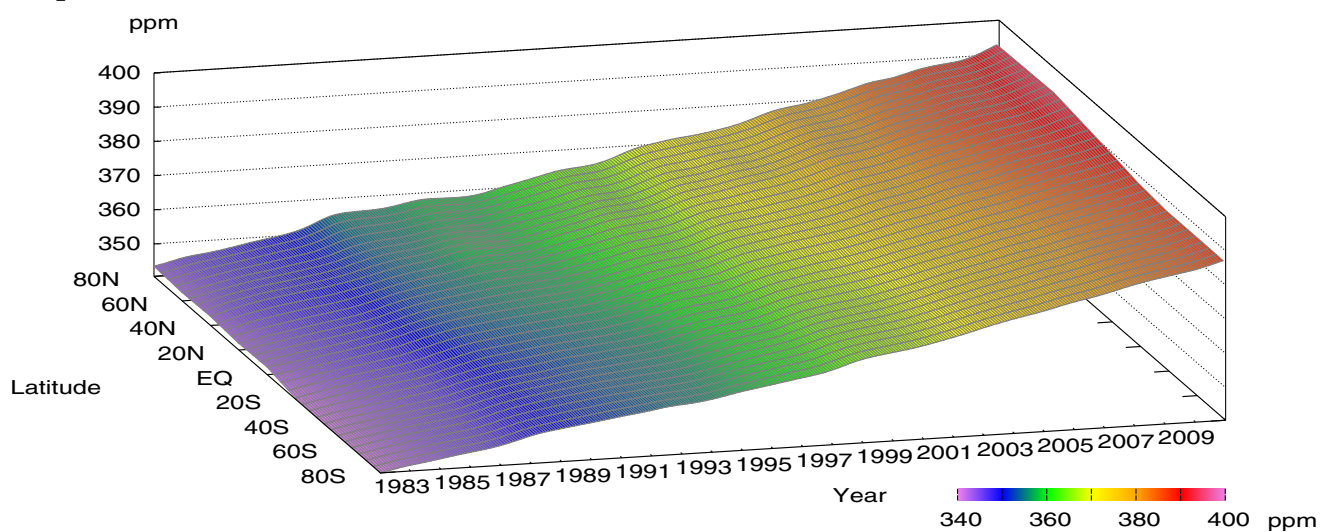


Plate 3.1 Monthly mean CO₂ mole fractions that have been reported to the WDCGG. The mole fractions are illustrated in different colors. The sites are listed in order from north to south. In the case where data are reported for two or three different altitudes, only the data at the highest altitudes are illustrated. In the case where monthly means are not reported, the WDCGG calculates them from hourly or other mole fractions reported to the WDCGG by simple arithmetic mean. The data from the sites with an asterisk at the end of the station index are used for the analysis shown in Plate 3.2. (see Chapter 2)

CO₂ mole fraction



CO₂ deseasonalized mole fraction



CO₂ growth rate

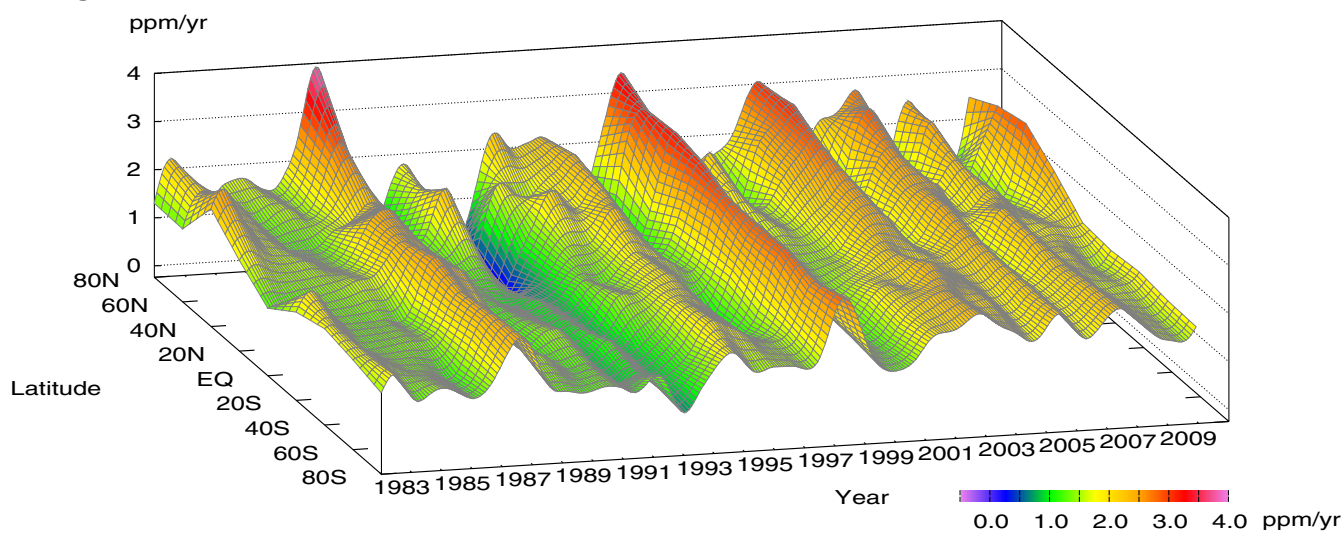


Plate 3.2 Variation of zonally averaged monthly mean CO₂ mole fractions (top), deseasonalized long-term trends (middle), and growth rates (bottom). The zonally averaged mole fractions are calculated for each 20° zone. The deseasonalized trends and growth rates are derived as described in Chapter 2.

3. CARBON DIOXIDE (CO₂)

Basic information on CO₂ with regard to environmental issues

Carbon dioxide (CO₂) has strong absorption bands in the infrared region and is the biggest anthropogenic contributor to the greenhouse effect. CO₂ accounted for about 64% of total increase in the radiative forcing due to long-lived greenhouse gases in the atmosphere from 1750 to 2010 (WMO, 2011b).

The balance between its emission and absorption over the continents and oceans determines the mole fraction of CO₂ in the atmosphere. About 762 gigatonnes of carbon are present in the atmosphere as CO₂ (IPCC, 2007) and annual anthropogenic emissions mainly due to fossil fuel combustion reached 8.4 ± 0.5 gigatonnes in 2009 (<http://www.globalcarbonproject.org>). Carbon in the atmosphere is exchanged with two other large reservoirs, the terrestrial biosphere and the oceans. CO₂ exchanges between the atmosphere and terrestrial biosphere occur mainly through absorption by photosynthesis and emission from the respiration of plants and the decomposition of organic soils. These biogenic activities vary seasonally, resulting in large seasonal variations in the level of CO₂. CO₂ exchange between the atmosphere and oceans occurs in direction determined by the gradient of CO₂ mole fraction, and varies in time and space.

The current mole fractions of atmospheric CO₂ far exceed historic records, dating back 650,000 years (Solomon *et al.*, 2007). Based on the results of ice core studies, the mole fraction of atmospheric CO₂ in pre-industrial times was about 280 ppm (IPCC, 2007). The emission of CO₂ due to human activities has increased dramatically since the beginning of the industrial era, impacting CO₂ exchange rates between different reservoirs and CO₂ levels not only in the atmosphere but in the oceans and terrestrial biosphere. The global carbon cycle, which is comprised mainly of CO₂, is not fully understood. About half of anthropogenic CO₂ emissions have remained in the atmosphere, with the remainder removed by sinks, including the terrestrial biosphere and oceans, and non-anthropogenic sources. However, the amount of CO₂ removed from the atmosphere varies significantly over time (Figure 3.1).

Carbon isotopic studies have shown the importance of the terrestrial biosphere and oceans as sources and sinks of CO₂ (Francey *et al.*, 1995; Keeling *et al.*, 1995; and Nakazawa *et al.*, 1993, 1997). In contrast, the atmospheric content of O₂ depends primarily on its removal by the burning of fossil fuels and on its release from the terrestrial biosphere. Therefore, the uptake of carbon by the terrestrial biosphere and oceans can be estimated from the combination of measurements of

O₂ (O₂/N₂) and CO₂ (Manning and Keeling, 2006). CO₂ equilibrates largely between the atmosphere and the ocean and, depending on associated increases in acidity and in ocean warming, typically about 20% of added tons of CO₂ remain in the atmosphere while about 80% are mixed into the ocean. A quasi-equilibrium amount of CO₂ is expected to be retained in the atmosphere by the end of the millennium that is surprisingly large: typically 40% of the peak concentration enhancement over preindustrial values (280 ppmv) (Solomon *et al.*, 2009).

Large amounts of CO₂ are exchanged among these reservoirs, and the global carbon cycle is coupled with the climate system on seasonal, yearly and decadal time scales. Accurate understanding of the global carbon cycle is essential for estimating future CO₂ mole fractions in the atmosphere.

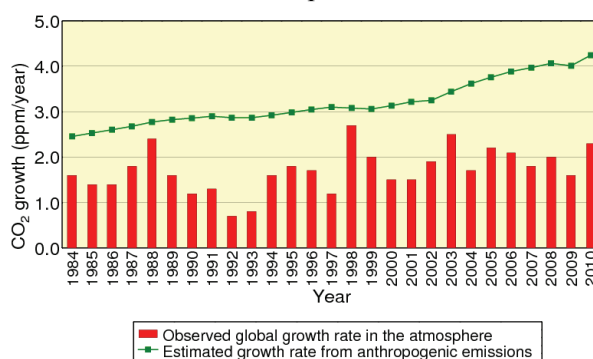


Fig. 3.1. Annual mean growth rates of CO₂ in the atmosphere, calculated from observational data (red columns) and from data for anthropogenic emissions (green curve). The estimated growth rates were calculated from CO₂ emissions (from CDIAC, Boden *et al.*, 2011). The values from 2009 to 2010 is quick estimation of Carbon Dioxide Information Analysis Center (CDIAC), expressed as moles divided by the total mass of gas in the atmosphere (5.2 petatonnes) converted to moles based on the mean molar weight of air (about 29). The observed growth rates were calculated by the WDCGG. The observational CO₂ abundance is expressed as mole fraction with respect to dry air, while the CO₂ amount calculated from anthropogenic emissions is based on the atmosphere, including water vapor, usually in a mole fraction less than 1%.

Mole fractions of CO₂ can be analyzed utilizing data submitted to the WDCGG from fixed stations and some ships. The observation sites from which data were used for the analysis are shown on the map at the beginning of this chapter. They include fixed stations performing continuous measurements as well as

flask-sampling stations, including those in the NOAA/ESRL cooperative air sampling network. In addition, mobile stations on ships and aircraft and other stations observing on an event basis report their data to the WDCGG (see Appendix: LIST OF OBSERVING STATIONS), which are not used for global analysis.

Annual variations of CO₂ mole fraction in the atmosphere

The monthly mean mole fractions of CO₂ used in the analysis are shown in Plate 3.1, with mole fraction levels illustrated in different colours. Global, hemispheric and zonal mean mole fractions were analysed based on data from selected stations under unpolluted conditions (see the caption to Plate 3.1). Latitudinally averaged mole fractions of atmospheric CO₂, together with their deseasonalized components and growth rates, are shown as three-dimensional representations in Plate 3.2. These plots show that the seasonal variations in mole fraction are large in northern high and mid-latitudes, but are indistinct in the Southern Hemisphere. The increases in the Northern Hemisphere precede those in the Southern Hemisphere by one or two years, and the interannual

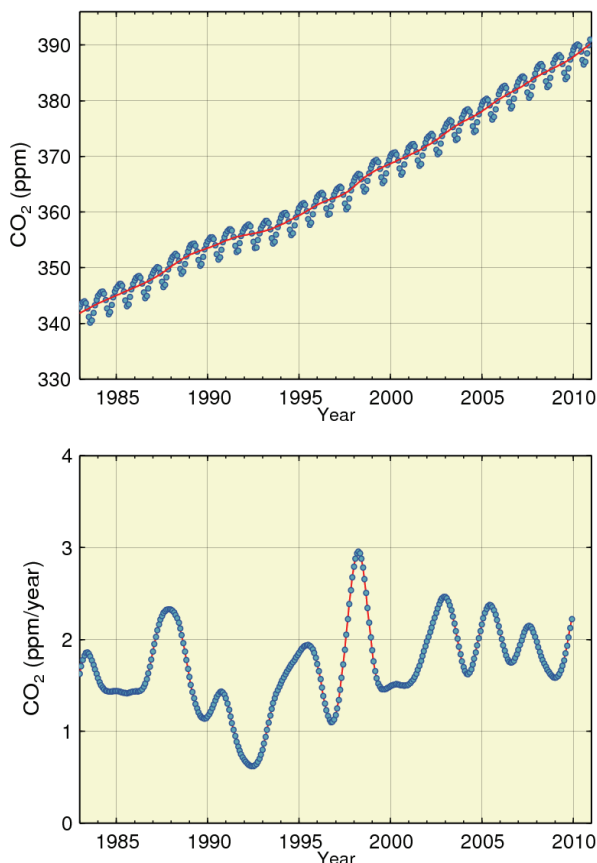


Fig. 3.2 Global monthly mean mole fraction of CO₂ from 1983 to 2010, including deseasonalized long-term trend shown as a red line (top) and annual growth rate (bottom).

variation in growth rate is larger in the Northern Hemisphere.

Figure 3.2 shows global monthly mean CO₂ mole fractions and their growth rates from 1983 to 2010. The global average mole fraction reached a new high of 389.0 ppm, in 2010 which is 138% of the pre-industrial level of 280 ppm. The annually averaged increase from 2009 to 2010 was 2.3 ppm, larger than the average of annual increases for the 1990s (about 1.5 ppm/year) and that of the past decade (about 2.0 ppm/year).

The global growth rate shows large interannual variations, with an instantaneous maximum of about 3 ppm/year in 1998 and a minimum below 1 ppm/year in 1992. There were short periods of high rates in 1987/1988, 1997/1998, 2002/2003, 2005/2006, 2007 and 2009/2010.

Figure 3.3 shows monthly mean mole fractions and long-term trends from 1983 to 2010 for each 30° latitudinal zone, indicating that there were clear long-term increases in both hemispheres and seasonal variations in the Northern Hemisphere.

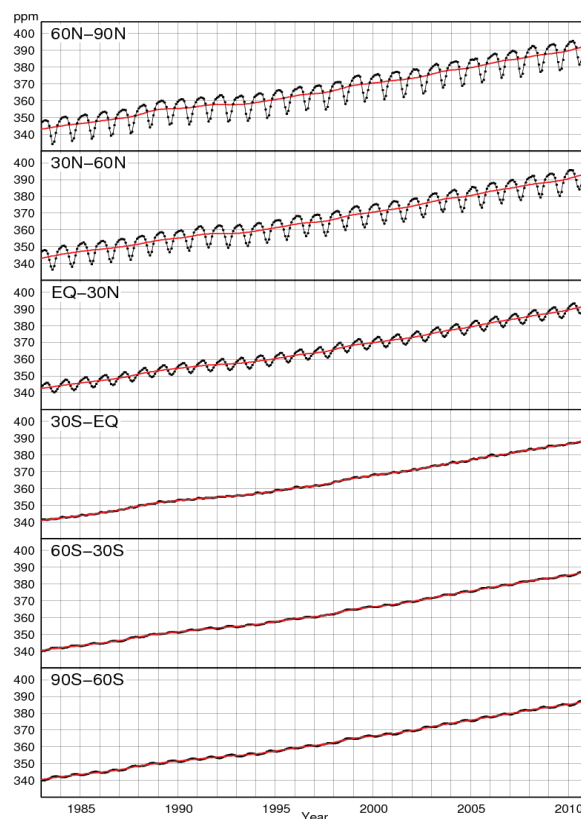


Fig. 3.3 Monthly mean mole fractions of CO₂ from 1983 to 2010 for each 30° latitudinal zone (dots) and their deseasonalized long-term trends (red lines).

As shown in Figure 3.4, the growth rates for each 30° latitude zone fluctuated between -0.3 and 3.6 ppm/year, with the largest interannual variability in northern high latitudes. High growth rates for all 30° latitude zones were observed in 1987/1988, 1997/1998, 2002/2003, 2005, 2007, with negative rates recorded in northern high latitudes in 1992.

Changes in growth rate are partly associated with El Niño-Southern Oscillation (ENSO). The El Niño events in 1982/1983, 1986–1988, 1991/1992, 1997/1998 and 2002/2003 coincided with high growth rates of CO_2 , with an exception in 1992. The growth rates of CO_2 observed by aircraft at high altitudes (8–13 km) over the Pacific Ocean were also associated with ENSO (Matsueda *et al.*, 2002). The latest El Niño event has occurred in 2009/2010.

During El Niño events, the up-welling of CO_2 -rich ocean water in the eastern equatorial Pacific is suppressed, resulting in reduced CO_2 emissions from this area. In contrast, El Niño events induce high temperature anomalies in many areas, particularly in the tropics, resulting in increased CO_2 emissions from the terrestrial biosphere due to the enhanced respiration of plants and activated decomposition of organic matter in soil (Keeling *et al.*, 1995). This effect is enhanced by the suppression of plant photosynthesis in areas of anomalously low precipitation, particularly in the tropics. These oceanic and terrestrial processes during El Niño events have opposing effects, but Heimann and Reichstein (2008) suggested that the latter was the main cause of the variation in the CO_2 growth rate.

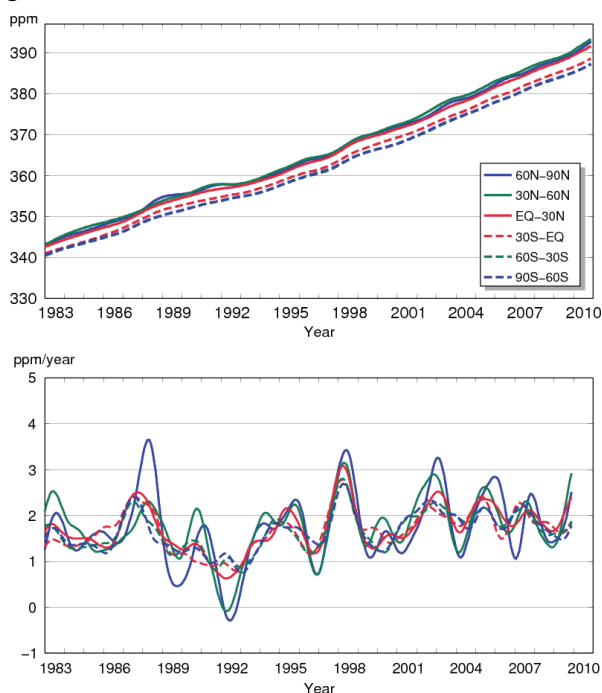


Fig. 3.4 Long-term trends in the mole fraction of CO_2 for each 30° latitudinal zone (top) and their growth rates (bottom).

However, an exceptionally low CO_2 growth rate occurred during the El Niño event in 1991/1992. The injection of 14–20 Mt of SO_2 aerosols into the stratosphere by the Mount Pinatubo eruption in June 1991 affected the radiation budget and atmospheric circulation (Hansen *et al.*, 1992; Stenchikov *et al.*, 2002), resulting in a drop in global temperature. Angert *et al.* (2004) suggested that the low CO_2 growth rate observed during this El Niño event was due to reduced CO_2 emissions caused by consequent changes in the respiration of terrestrial vegetation and the decomposition of organic matter (Conway *et al.*, 1994; Lambert *et al.*, 1995; Rayner *et al.*, 1999), and by enhanced CO_2 absorption due to intensive photosynthesis caused by an increase in diffuse radiation (Gu *et al.*, 2003).

Seasonal cycle of CO_2 mole fraction in the atmosphere

Figure 3.5 shows average seasonal cycles in the mole fraction of CO_2 for each 30° latitudinal zone. The seasonal cycles are clearly large in amplitude in northern high and mid-latitudes and small in the Southern Hemisphere. The seasonal cycle in the Northern Hemisphere is mainly dominated by the land biosphere (Nevison *et al.*, 2008), and it is characterized by rapid decreases from June to August and large returns from September to December.

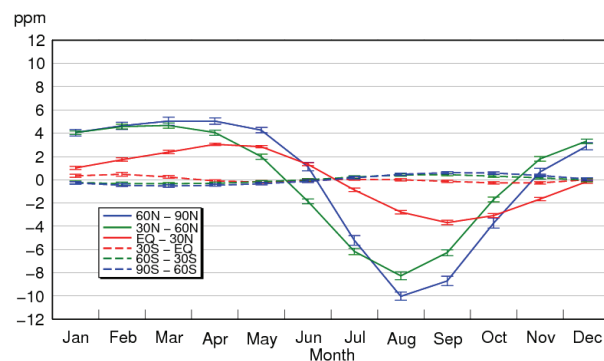


Fig. 3.5 Average seasonal cycles in the mole fraction of CO_2 for each 30° latitudinal zone obtained by subtracting long-term trends from the zonal mean time series. Error bar expresses standard deviation of each month.

The mole fractions of CO_2 in northern low latitudes lagged behind that in high latitudes by one or two months. Minimum values appeared in August in northern high and mid-latitudes and in September in northern low latitudes.

In the Southern Hemisphere, seasonal variations showed small amplitudes with a half-year delay due to small amounts of net emission and absorption by the terrestrial biosphere. Seasonal variations in both northern and southern mid-latitudes were apparently

superimposed in southern low latitudes (0–30°S). The direct influence of sources and sinks in the Southern Hemisphere may be partially cancelled by the propagation of an antiphase variation from the Northern Hemisphere.

Figure 3.6 shows latitudinal distributions of the mole fractions of CO₂ in January, April, July and October 2010, from sites marked with an asterisk in Plate 3.1. In latitudes north of 30°N, the mole fractions increased towards higher latitudes in January and April, and decreased towards higher latitudes in July, corresponding to the large seasonal variations in northern high and mid-latitudes, variations associated with activities of the terrestrial biosphere.

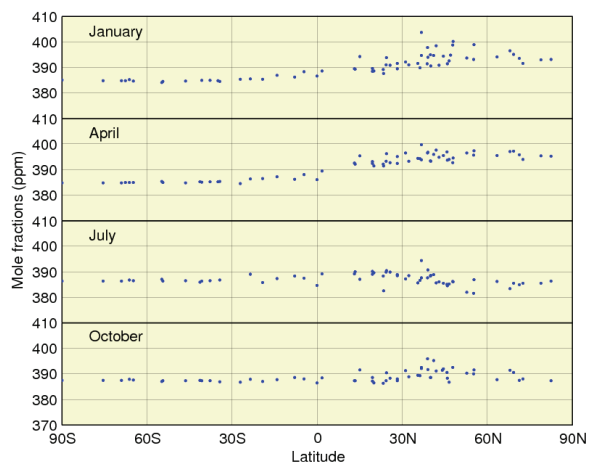


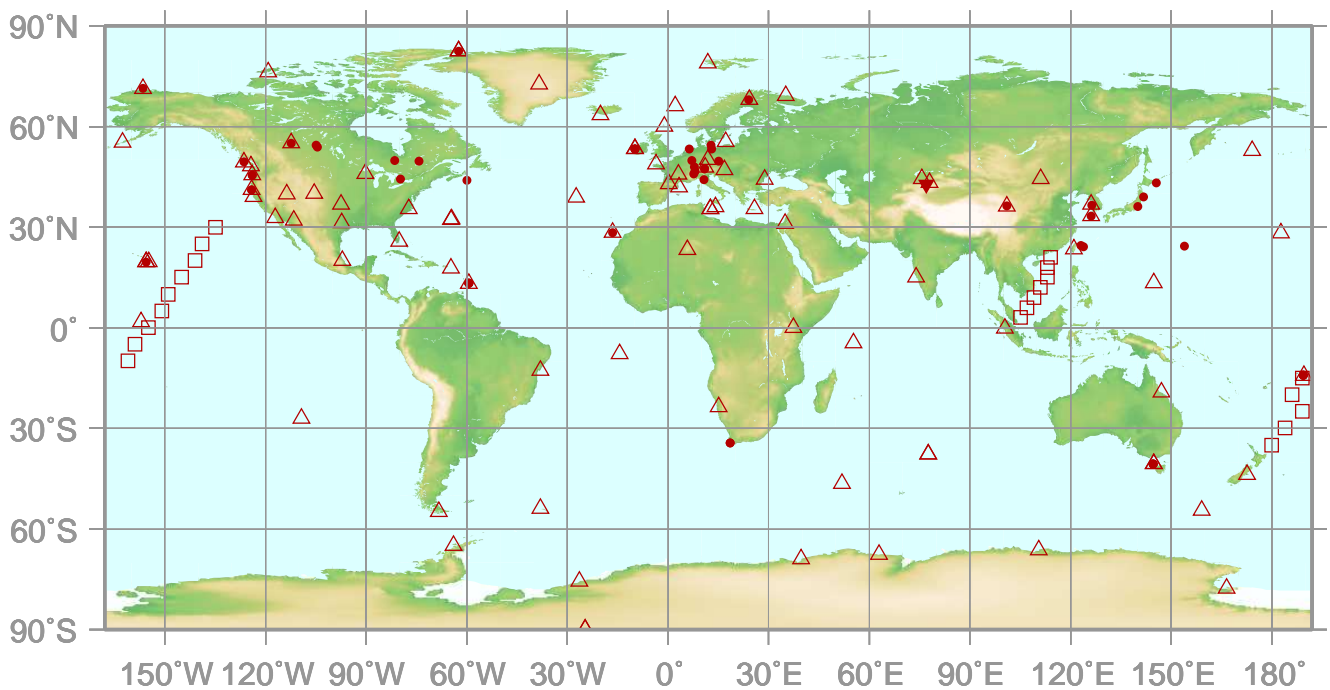
Fig. 3.6 Latitudinal distributions of the monthly mean mole fractions of CO₂ in January, April, July and October 2010.

4.

METHANE

(CH₄)

- : CONTINUOUS STATION
- △ : FLASK STATION
- : FLASK MOBILE (SHIP)
- ▼ : REMOTE SENSING STATION



This map shows locations of the stations that have submitted data for monthly mean mole fraction.

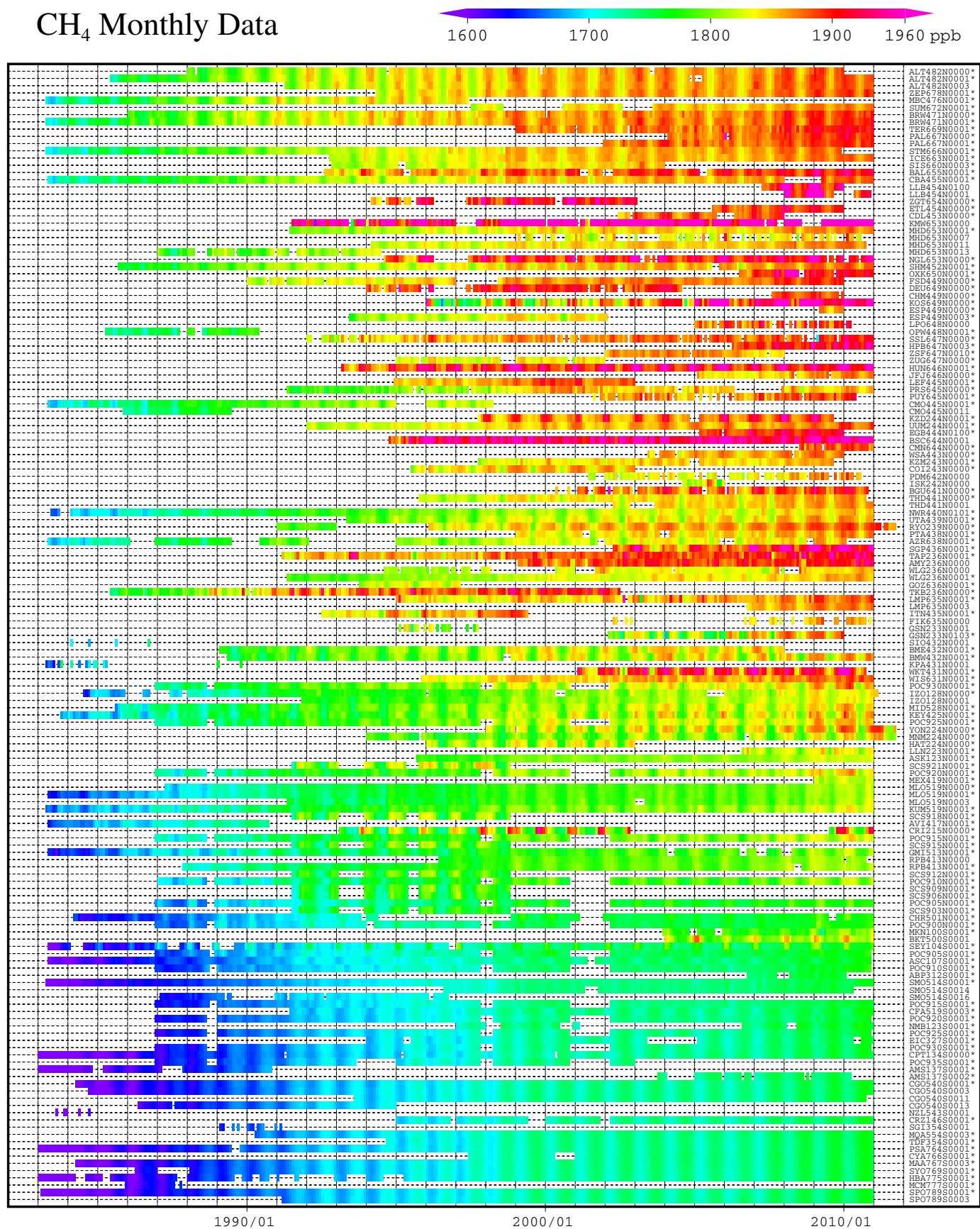
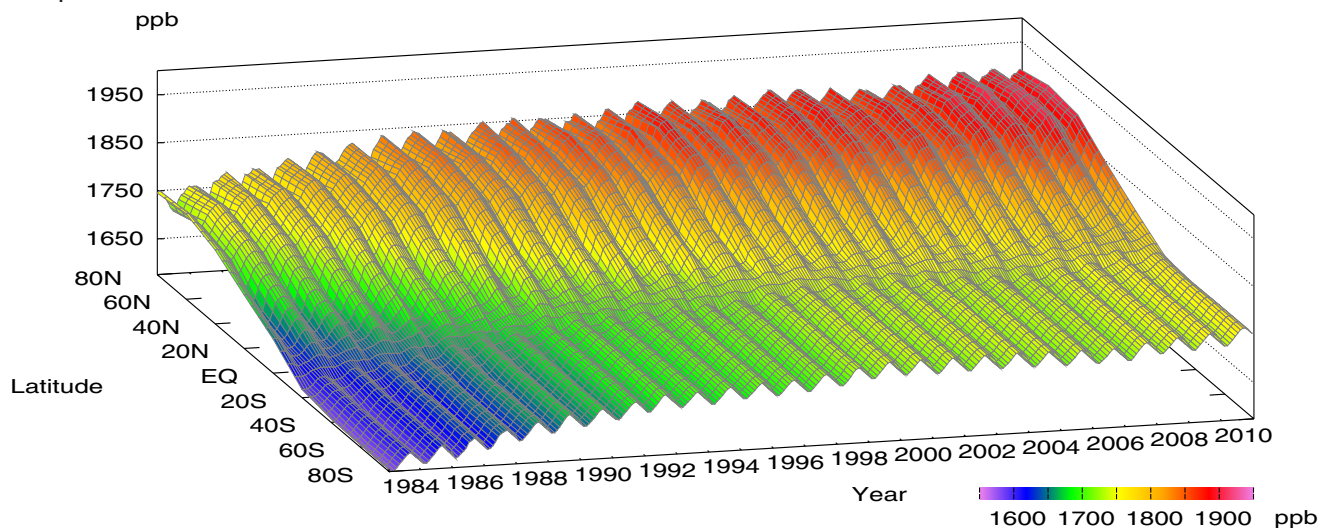
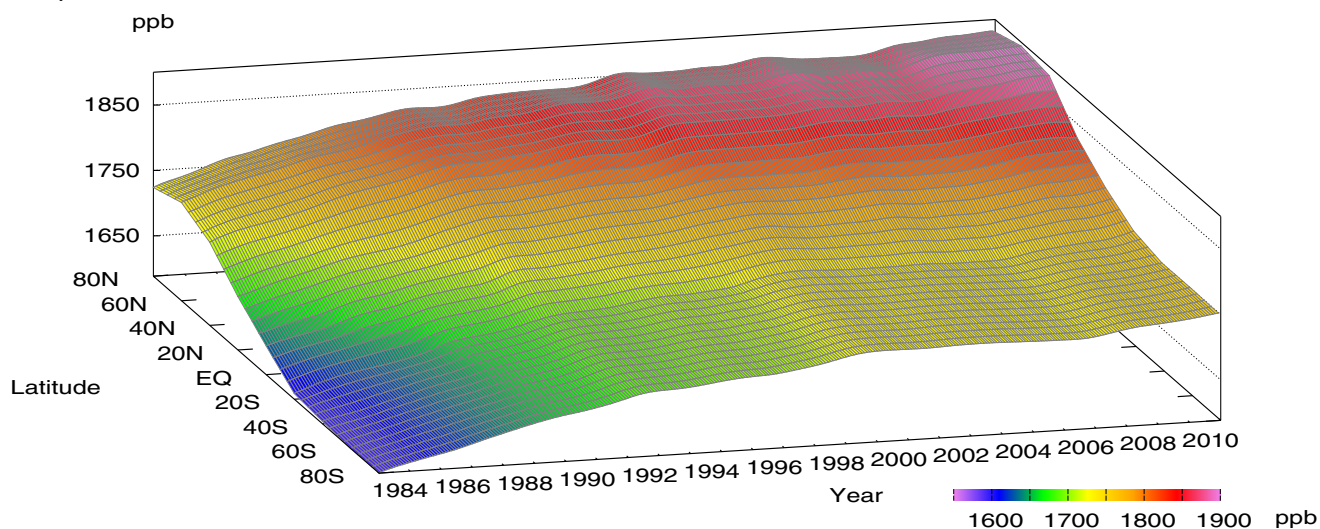


Plate 4.1 Monthly mean CH₄ mole fractions that have been reported to the WDCGG. The mole fractions are illustrated in different colors. The sites are listed in order from north to south. In the case where data are reported for two or three different altitudes, only the data at the highest altitudes are illustrated. In the case where monthly means are not reported, the WDCGG calculates them from hourly or other mole fractions reported to the WDCGG by simple arithmetic mean. The data from the sites with an asterisk at the end of the station index are used for the analysis shown in Plate 4.2. (see Chapter 2)

CH₄ mole fraction



CH₄ deseasonalized mole fraction



CH₄ growth rate

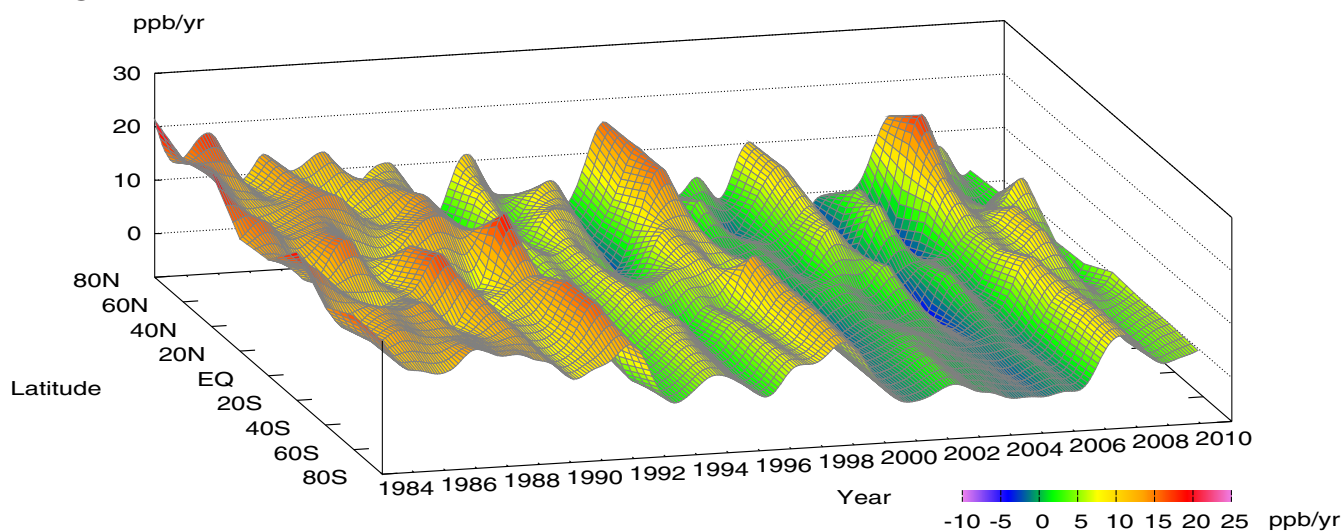


Plate 4.2 Variation of zonally averaged monthly mean CH₄ mole fractions (top), deseasonalized long-term trends (middle), and growth rates (bottom). The zonally averaged mole fractions are calculated for each 20° zone. The deseasonalized trends and growth rates are derived as described in Chapter 2.

4. METHANE (CH₄)

Basic information on CH₄ with regard to environmental issues

Methane (CH₄) is the second most important anthropogenic greenhouse gas, with an estimated global warming potential per molecule 25 times greater over a 100 year horizon and 72 times greater over a 20 years horizon than CO₂. Between 1750 and 2010, CH₄ accounted for about 18% of total increase in radiative forcing due to long-lived greenhouse gases in the atmosphere (WMO, 2011c).

Analyses of air trapped in ice cores from Antarctica and the Arctic revealed that the current atmospheric CH₄ mole fraction is the highest it has been over the last 650,000 years (Solomon *et al.*, 2007). The mole fraction of CH₄ remained steady at 700 ppb from 1000 A.D. until the start of the industrial era (Etheridge *et al.*, 1998), after which it began to increase. Measurements in ice cores have shown that the inter-pole differences in CH₄ mole fractions between Greenland and Antarctica ranged from 24 to 58 ppb between 1000 and 1800 A.D. (Etheridge *et al.*, 1998). This difference reached a value of 136 ppb as follows from the comparison of northern high and southern high latitude averaged over the years 1984 to 2010, Fig. 4.3. This fact reflects emissions from the Northern Hemisphere, where major anthropogenic and natural sources are situated.

CH₄ is emitted by both natural and anthropogenic sources, including natural wetlands, oceans, landfills, rice paddies, enteric fermentation, fossil fuel production and consumption and biomass burning. Denman *et al.* (2007) estimated the global emission of CH₄ is 582 teragrams (Tg) CH₄ per year, with more than 60% related to anthropogenic activities. CH₄ removed from the atmosphere by reaction with hydroxyl radicals (OH) in both the troposphere and stratosphere, and by reaction with chlorine atoms and O(¹D), an excited state of oxygen, in the stratosphere. CH₄ is one of the most important sources of water vapour in the stratosphere and has an atmospheric lifetime of about 10 years. More information regarding sources and sinks of CH₄ must be collected to better understand the budget of atmospheric CH₄.

Mole fractions of CH₄ are analyzed by using data submitted to the WDCGG from fixed stations and some ships. These observational sites are shown on the map at the beginning of this chapter.

Annual variation of CH₄ mole fraction in the atmosphere

The monthly mean mole fractions of CH₄ used in this analysis are shown in Plate 4.1, with the mole fraction levels illustrated in different colours. Global, hemispheric and zonal mean mole fractions have been

calculated based on data from selected stations under unpolluted conditions (see the caption for Plate 4.1). Latitudinally averaged atmospheric CH₄ mole fractions, together with their deseasonalized components and growth rates, are shown as three-dimensional representations in Plate 4.2. These plots show that the seasonal variations in CH₄ mole fractions are larger in the Northern than in the Southern Hemisphere and that the increase in the Northern Hemisphere propagates to the Southern Hemisphere. The growth rates vary on a global scale. These features are similar to those for CO₂ (see Section 3). There is a large latitudinal gradient in CH₄ mole fraction from the northern mid-latitudes to the tropics, suggesting major sinks in the tropics, where the mole fraction of OH radicals is higher.

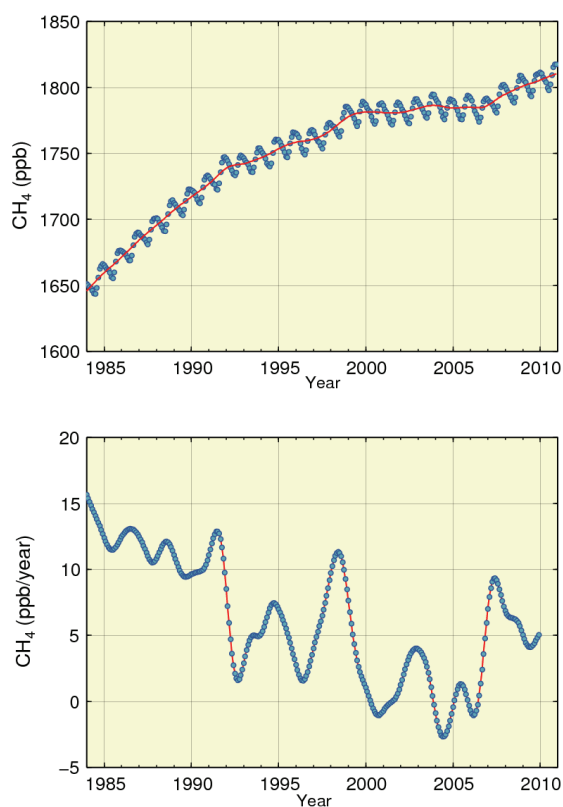


Fig. 4.1 Global monthly mean mole fraction of CH₄ from 1984 to 2010, including deseasonalized long-term trend in red line (top) and annual growth rate (bottom).

Figure 4.1 shows global monthly mean mole fractions and the global growth rates for CH₄ from 1984 to 2010. The mean mole fraction was 1808 ppb in 2010, an increase of 5 ppb since 2009. Mole fraction did not change much between 1999 and 2006. The average growth rate over the period 2000–2010 was

2.6 ppb/year. The current mole fraction is 258% of its pre-industrial level, 700 ppb.

Figure 4.2 shows monthly mean mole fractions from 1984 to 2010 for each 30° latitudinal zone. The smallest magnitude of the seasonal variations is registered in the latitudinal zone between the equator and 30°S.

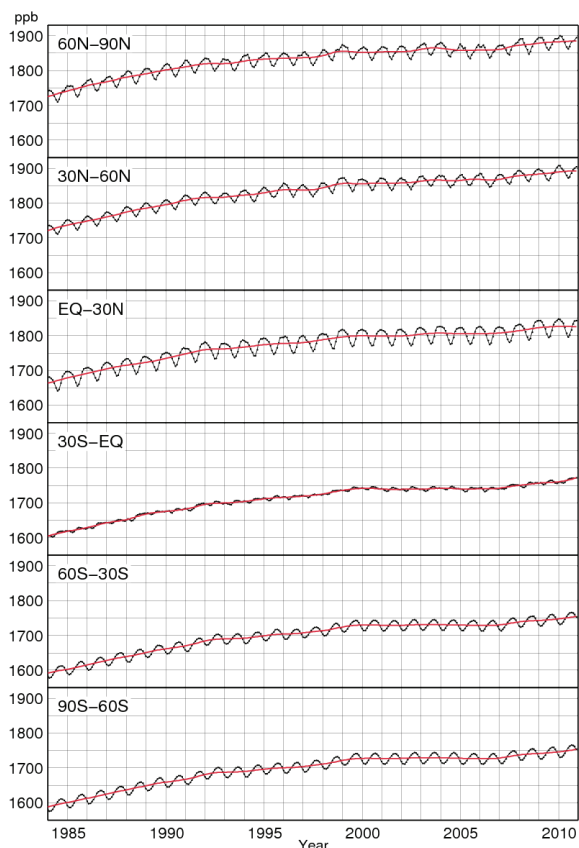


Fig. 4.2 Monthly mean mole fractions of CH_4 from 1984 to 2010 for each 30° latitudinal zone (dots) and their deseasonalized long-term trends (red lines) .

Figure 4.3 summarizes deseasonalized long-term trends for each 30° latitudinal zone and their growth rates. As it is the most distinctly seen in the deseasonalized long-term trends, a latitudinal gradient between the northern high and mid-latitudes with higher mole fractions and the southern latitudes with lower mole fractions is clearly pronounced, while mole fractions in most latitudinal belts have similar tendency. In the 1990s, the growth rates clearly decreased in all latitudinal zones, while remaining positive nevertheless. The declined growth rate was especially evident during the second half of 1992 in 1996, and almost even in 1999 and in 2004/2005, when growth rates were less than 5 ppb/year in all latitudes. In 1998, the global growth rate increased to about 11 ppb/year (Fig. 4.1). Maximum increases occurred in northern high and mid-latitudes, where the growth rates were over 15

ppb/year. In 2000 and 2001, the global growth rate decreased to around -1 ppb/year. Around 2002/2003, the growth rates increased in the Northern Hemisphere, especially in northern high and mid-latitudes where they reached about 10 ppb/year. The global growth rate was -3 ppb/year in 2004 and 1 ppb/year in 2005. Despite the large growth rates in 1998 and 2002/2003, during El Niño events, the global mean mole fraction was relatively stable between 1999 and 2006. However, the global mean mole fraction increased again by a total of 24 ppb in the four years starting in 2007.

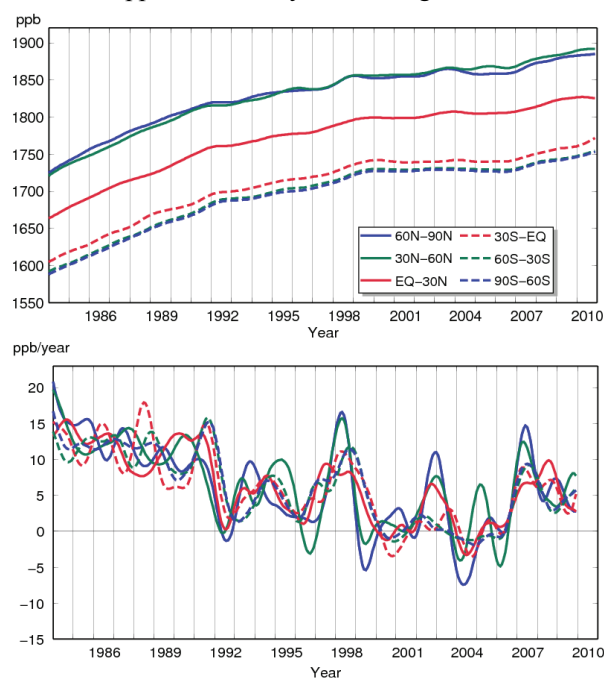


Fig. 4.3 Long-term trends in the mole fraction of CH_4 for each 30° latitudinal zone (top) and their growth rates (bottom).

The large increase in CH_4 growth rate in 1991 may have been caused by decreased levels of OH radicals in the atmosphere due to reduced UV radiation resulting from the eruption of Mount Pinatubo in 1991 (Dlugokencky *et al.*, 1996), and the subsequent decrease in 1992 may have been due to an increase in OH radicals resulting from the depletion of stratospheric ozone following this eruption (Bekki *et al.*, 1994).

In 1998, the growth rates were high in all latitudes, which may have been due to increased emissions in northern high latitudes and tropical wetlands caused by high temperatures and increased precipitation, as well as by biomass burning in boreal forests, mainly in Siberia (Dlugokencky *et al.*, 2001). In contrast, Morimoto *et al.* (2006) estimated from isotope observations that the contribution of biomass burning to the increase in 1998 was about half that of wetlands. The growth rates were low from 1999 to 2006, with an exception during the El Niño event of 2002/2003. The causes of these decreases in CH_4 growth rates remain

unclear.

Since 2007, atmospheric CH₄ has increased significantly throughout the entire monitoring network (Rigby *et al.*, 2008; Dlugokencky *et al.*, 2009). Although these increases may have been caused by emissions from natural sources in northern latitudes and the tropics, the reasons for renewed methane growth are not fully understood (WMO, 2011b).

The WMO/GAW observational network includes the observation of carbon stable isotopes in methane, with 19 datasets submitted to the WDCGG. Such observations can be useful for the identification of primary methane sources.

Seasonal cycle of CH₄ mole fraction in the atmosphere

Figure 4.4 shows seasonal cycles in the mole fraction of CH₄ for each 30° latitudinal zone. The seasonal cycles are driven mainly by reaction with OH radicals, a major CH₄ sink in the atmosphere. Seasonal cycles are also affected by the magnitude and timing of CH₄ emissions from sources such as wetlands and biomass burning as well as by its atmospheric transport. The seasonal cycles are large in amplitude in the Northern Hemisphere. Unlike CO₂, amplitudes were also large in southern high and mid-latitudes. Seasonally, the Northern Hemisphere shows minima in summer and maxima in winter, while the Southern Hemisphere shows a seasonal cycle lagging two-thirds to three-quarter years behind. The seasonal variations in the mole fraction of CH₄ were almost consistent with those of the OH radical that reacts with CH₄. Southern low latitudes have a distinct antiphase annual component with that of the seasonal cycle arising from southern mid-latitudes. The maximum in the former component occurs in boreal winter due to the interhemisphere transportation of CH₄ from the Northern Hemisphere.

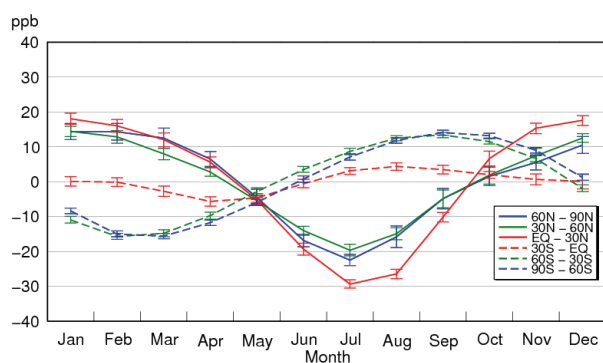
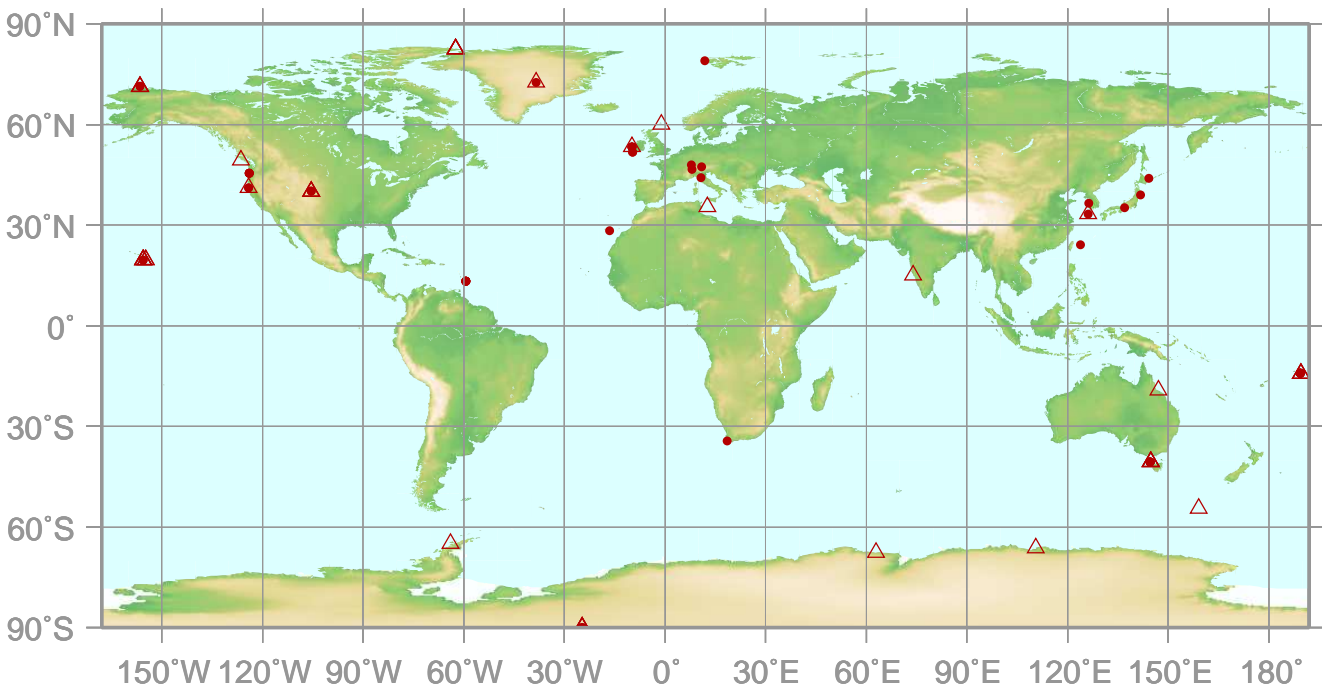


Fig. 4.4 Average seasonal cycles in the mole fraction of CH₄ for each 30° latitudinal zone obtained by subtracting long-term trends from the zonal mean time series. The standard deviation is indicated by vertical error bars.

5. DISCUSSION

- : CONTINUOUS STATION

 : FLASK STATION



This map shows locations of the stations that have submitted data for monthly mean mole fraction.

N₂O Monthly Data

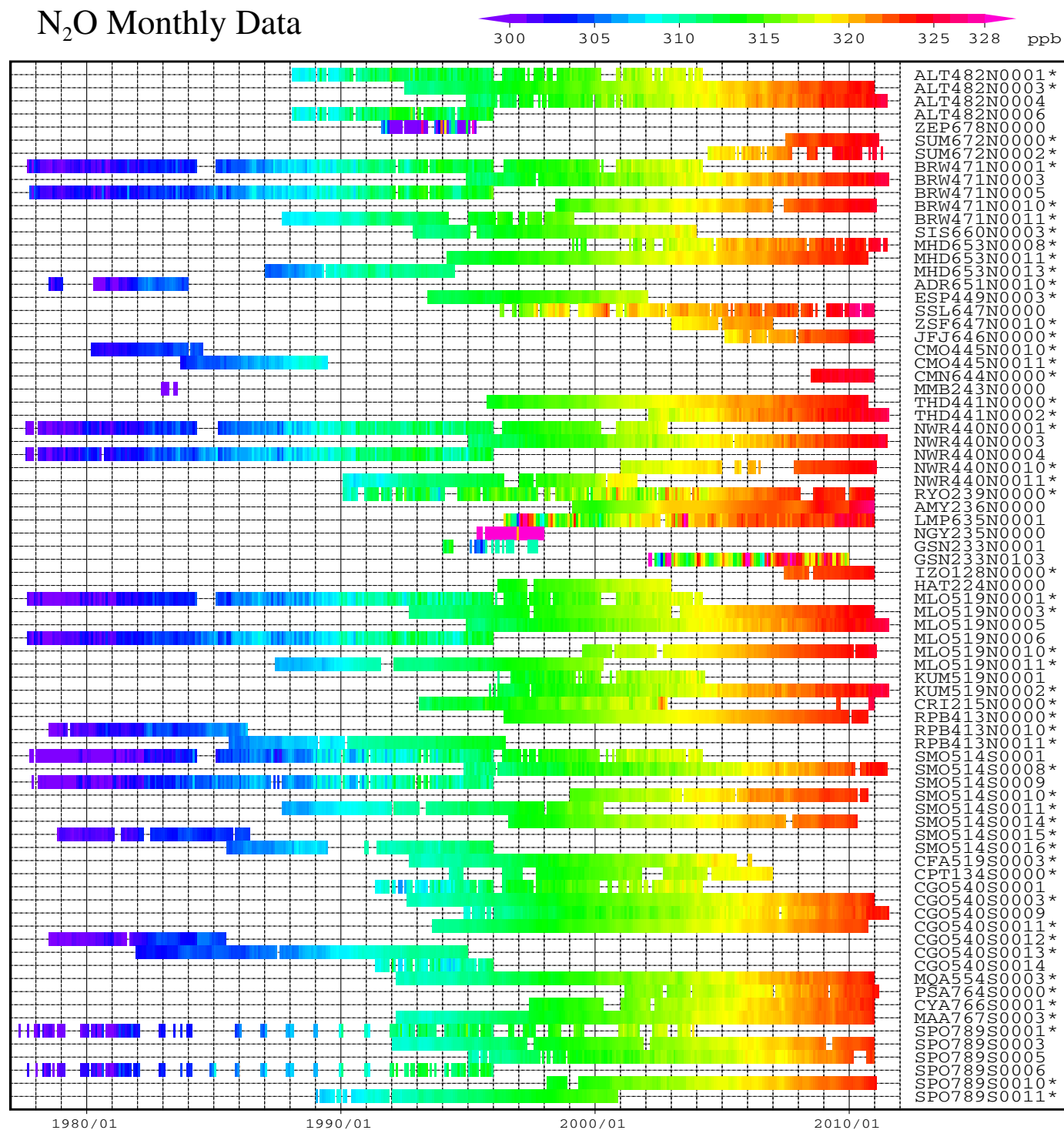
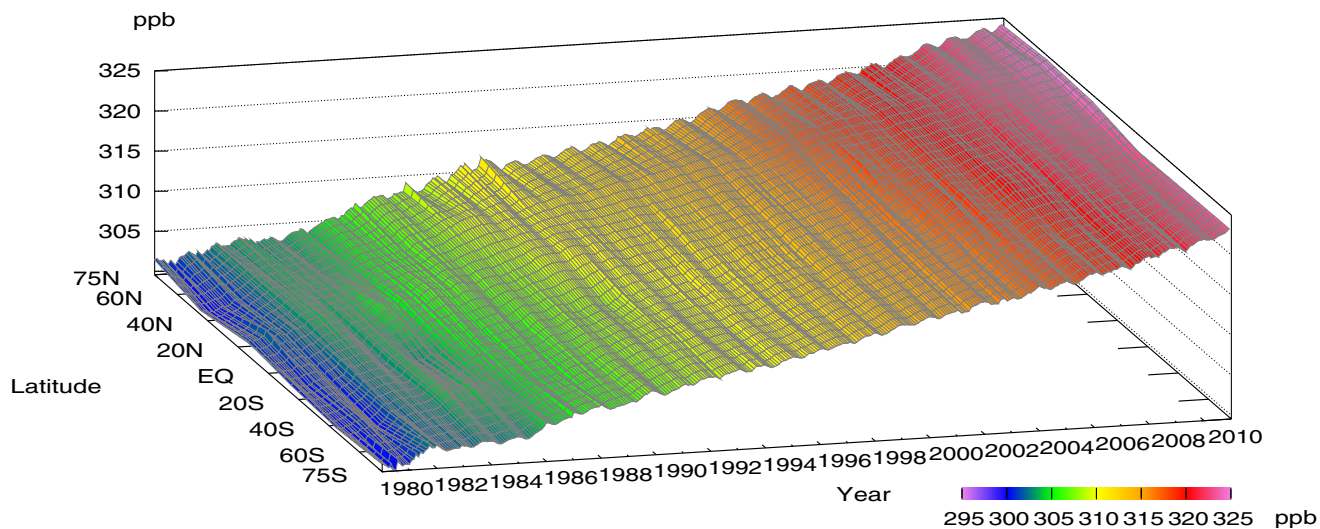
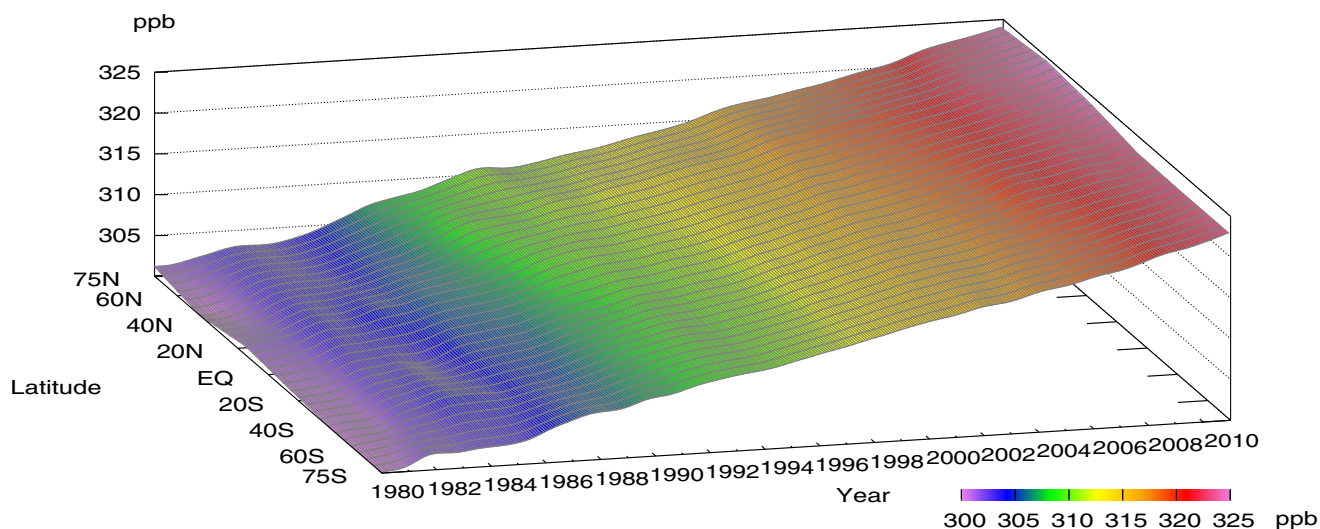


Plate 5.1 Monthly mean N₂O mole fractions that have been reported to the WDCGG. The mole fractions are illustrated in different colors. The sites are listed in order from north to south. The data from the sites with an asterisk at the end of the station index are used for the analysis shown in Fig.5.1. (see Chapter 2)

N₂O mole fraction



N₂O deseasonalized mole fraction



N₂O growth rate

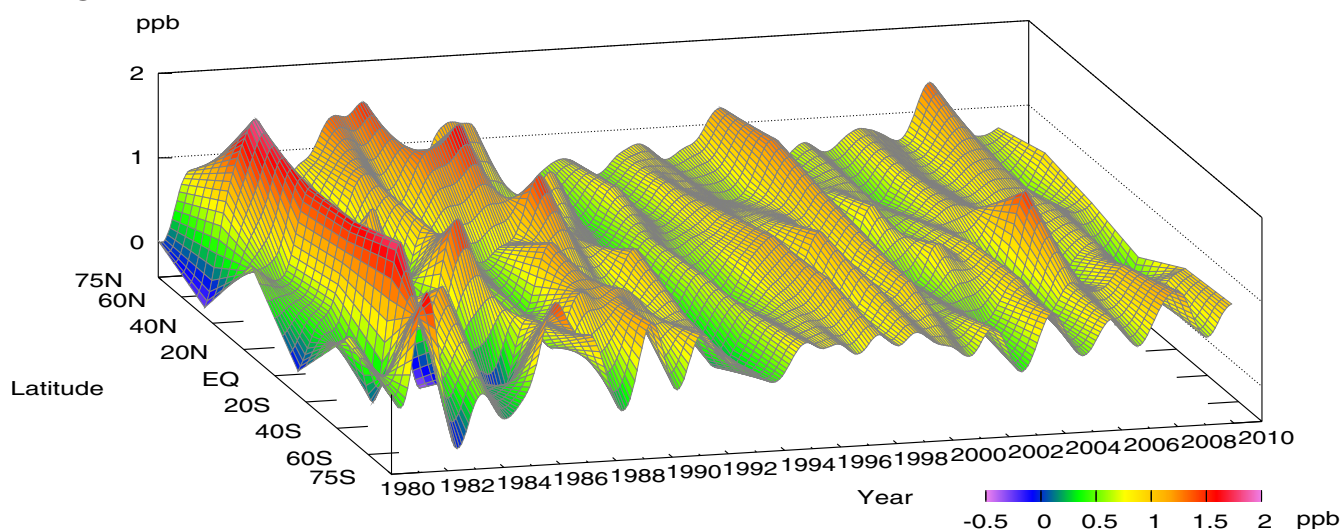


Plate 5.2 Variation of zonally averaged monthly mean N₂O mole fractions (top), deseasonalized long-term trends (middle), and growth rates (bottom). The zonally averaged mole fractions are calculated for each 30° zone. The deseasonalized trends and growth rates are derived as described in Chapter 2.

5. NITROUS OXIDE (N₂O)

Basic information on N₂O with regard to environmental issues

Nitrous oxide (N₂O) is a relatively stable greenhouse gas in the troposphere with an “adjustment-time” of 114 years. Between 1750 and 2010, N₂O accounted for about 6 % of total increase in radiative forcing due to long-lived greenhouse gases (WMO, 2011c). N₂O is the third most important anthropogenic greenhouse gas in the atmosphere. The mole fraction of N₂O in the atmosphere has increased steadily from about 270 ppb in pre-industrial times to its current value, which is 20% higher. N₂O is emitted into the atmosphere from natural and anthropogenic sources, including the oceans, soil, combustion of fuels, biomass burning, use of fertiliser and various industrial processes. The amount of N₂O emitted into the atmosphere by human activities is approximately equal to that derived from natural systems (oceans, chemical oxidation of ammonia in the atmosphere, and soils). Most of the anthropogenic N₂O found in the atmosphere comes from the transformation of fertilizer nitrogen into N₂O and its subsequent emission from agricultural soils. N₂O breaks down mainly by photo-dissociation in the stratosphere, forming nitrogen oxides that trigger ozone depleting reactions, so it plays an important role in ozone depletion (Ravishankara et al., 2009). However, the cycling of N₂O as a part of global nitrogen cycle is not well understood yet.

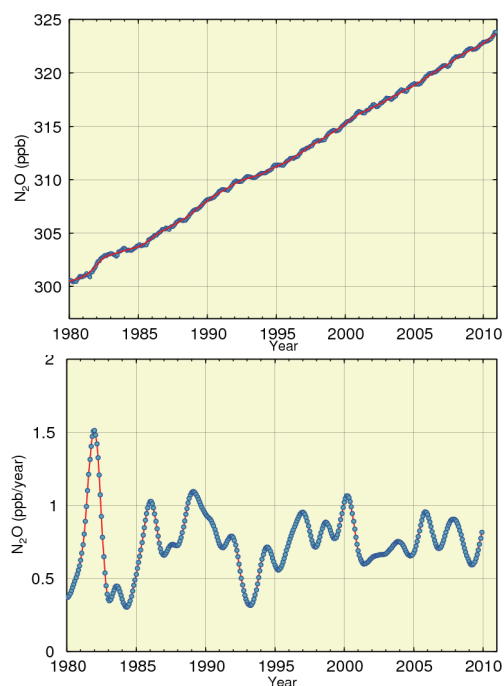


Fig. 5.1 Global monthly mean mole fraction of N₂O from 1980 to 2010, including deseasonalized long-term trend shown as a red line (top) and annual growth rate (bottom).

Annual variation of N₂O mole fraction in the atmosphere

Mole fractions of N₂O are analysed by using the data submitted to the WDCGG from fixed stations and some ships. The observational sites that supplied data used for this analysis are shown on the map at the beginning of this chapter. The monthly mean mole fractions of N₂O used in the global analysis are shown in Plate 5.1, with the various mole fraction levels illustrated in different colours. The data submitted to the WDCGG show that N₂O mole fractions have increased at almost all stations. Latitudinally averaged atmospheric N₂O mole fractions, together with their deseasonalized components and growth rates, are shown as three-dimensional representations from 1980 to 2010 in Plate 5.2. Figure 5.1 shows global monthly mean N₂O mole fraction from 1980 to 2010 and its long-term trend. The global mean mole fraction reached a new high of 323.2 ppb in 2010, an increase of 0.8 ppb over the previous year. The mean growth rate of the global mean mole fraction during the period 2000 to 2010 was 0.75 ppb/year. Atmospheric growth rate showed substantial variability (from 0.6 to 1.0 ppb/year) from the beginning of observations. There was an inter-hemispheric gradient in the mole fraction of N₂O, of 1.1ppb averaged over the years 1980 to 2010 (Figure 5.2 upper panel) indicating that majority of the N₂O sources is situated in the Northern Hemisphere (mostly agriculture).

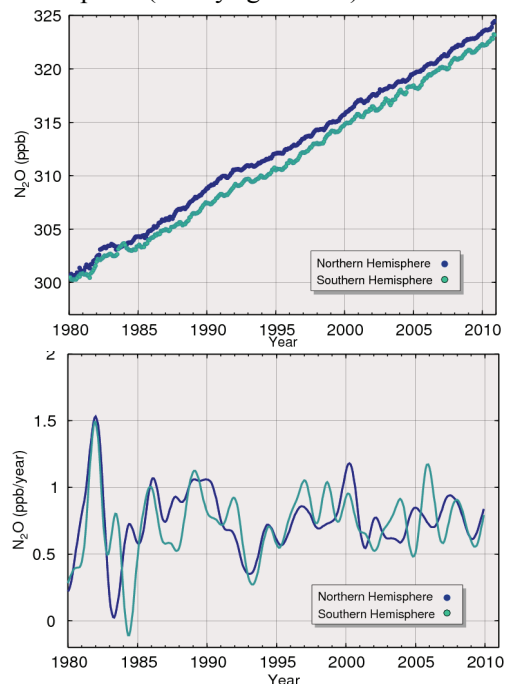


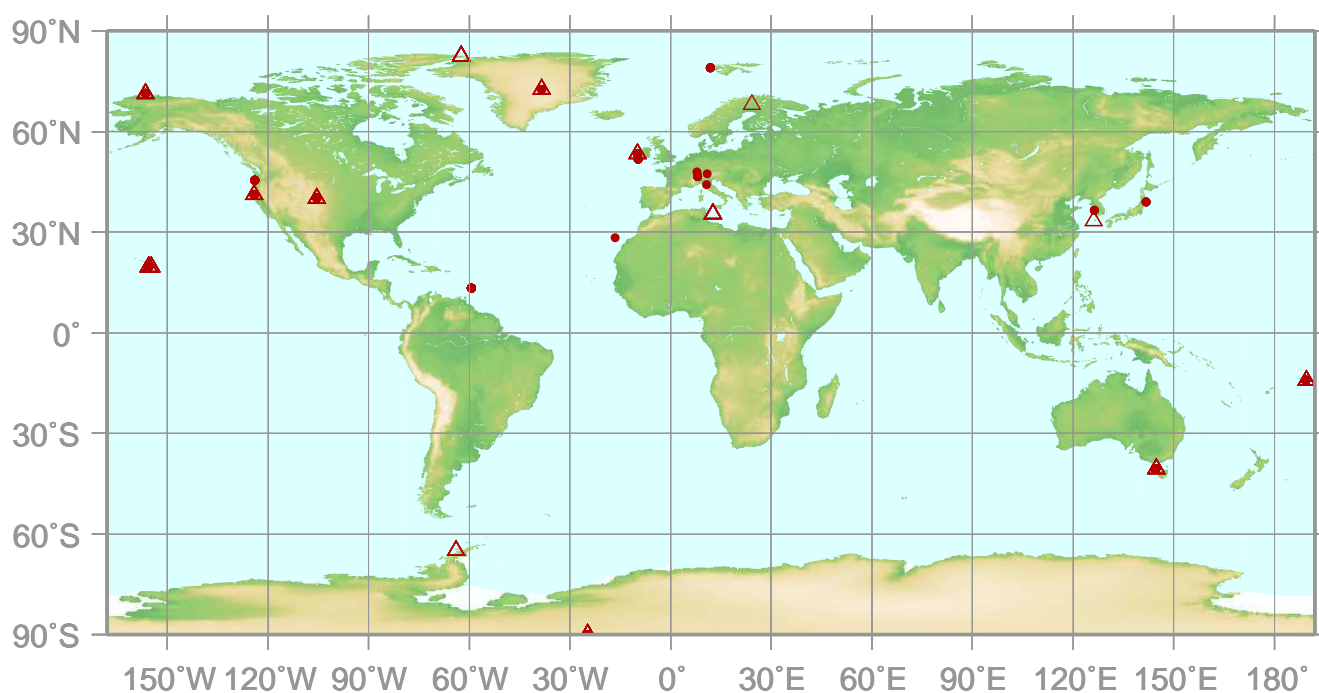
Fig. 5.2 Monthly mean mole fractions of N₂O from 1980 to 2010 (top) and annual growth rates (bottom), averaged over the Northern and Southern Hemispheres.

6.

HALOCARBONS AND OTHER HALOGENATED SPECIES

● : CONTINUOUS STATION

△ : FLASK STATION



This map shows locations of the stations that have submitted data for monthly mean mole fraction.

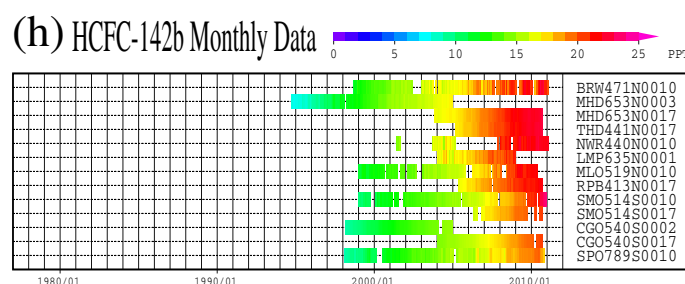
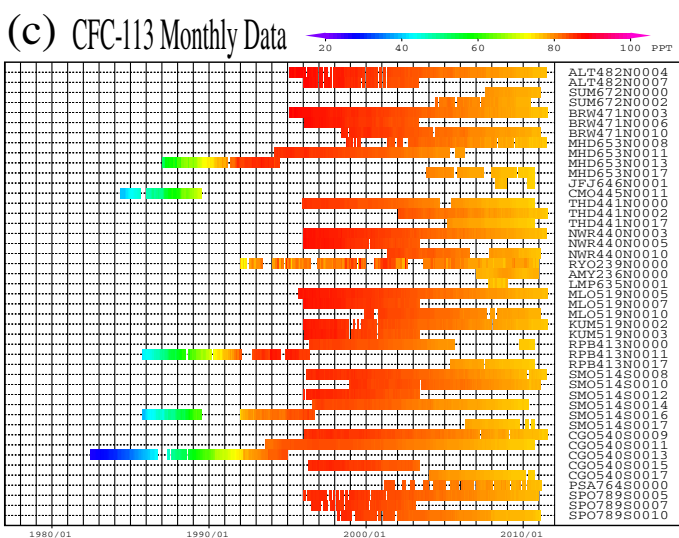
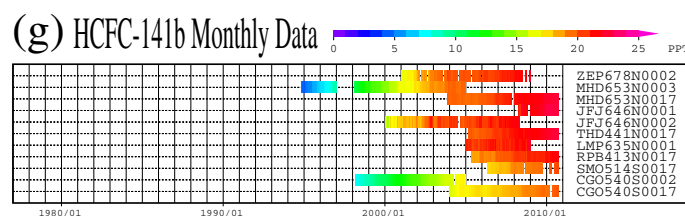
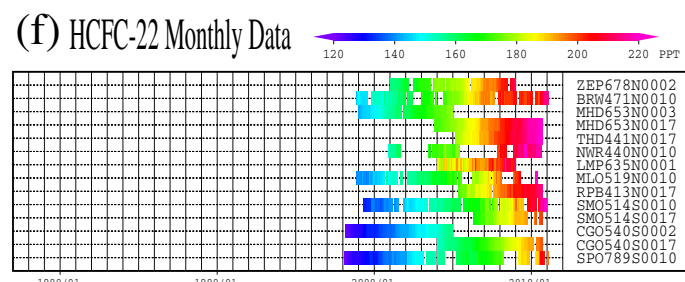
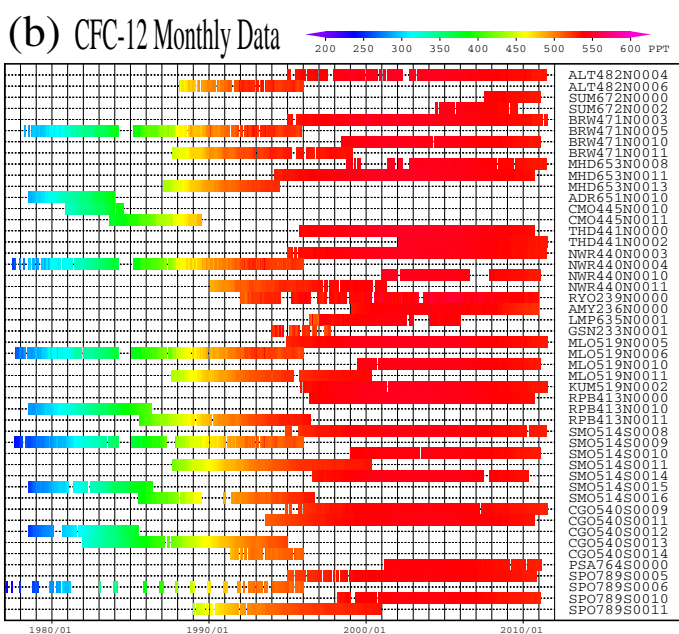
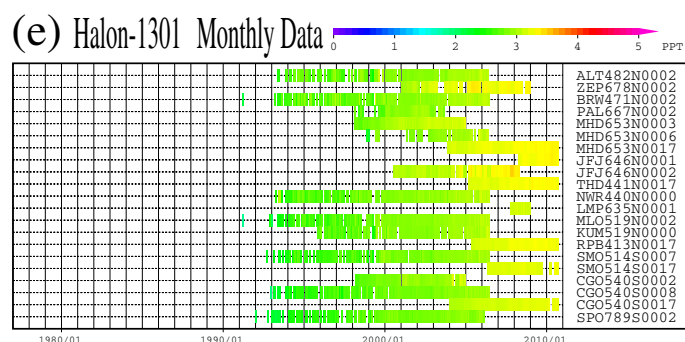
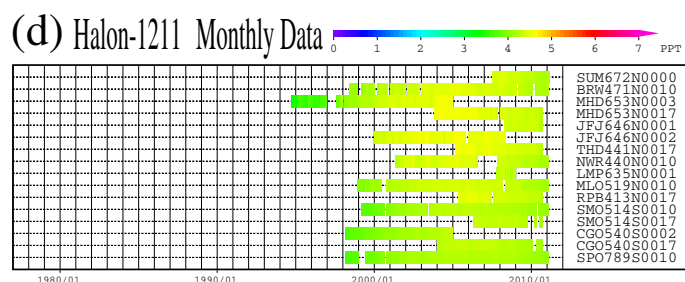
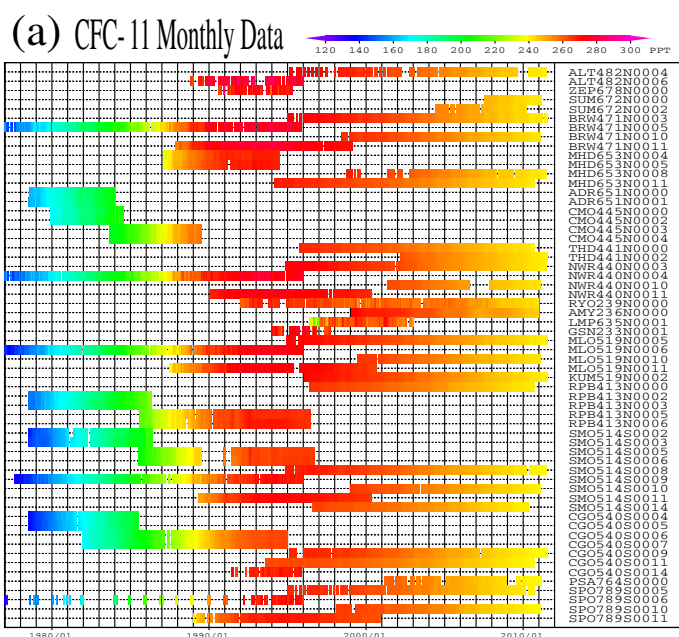


Plate 6.1 Monthly mean (a) CFC-11, (b) CFC-12, (c) CFC-113, (d) Halon-1211, (e) Halon-1301, (f) HCFC-22, (g) HCFC-141b, (h) HCFC-142b mole fractions that have been reported to the WDCGG. The mole fractions are illustrated in different colors. The sites are listed in order from north to south.

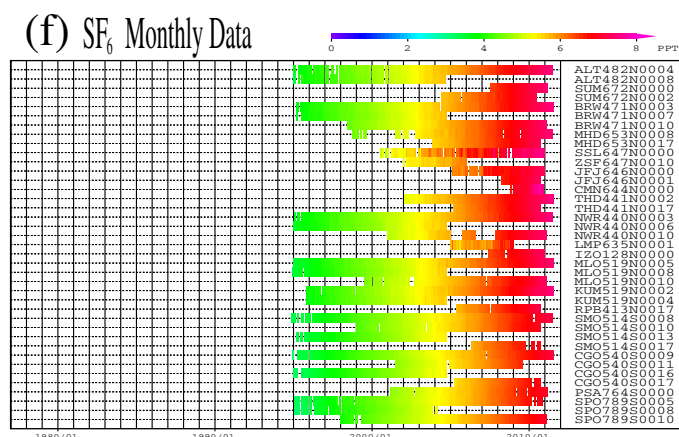
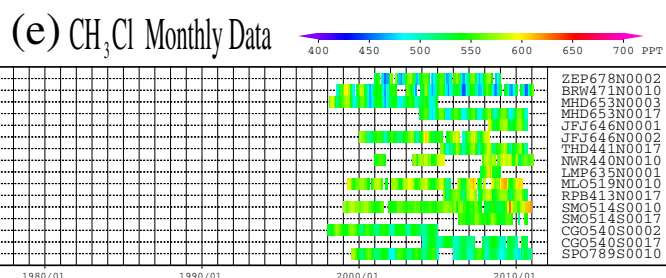
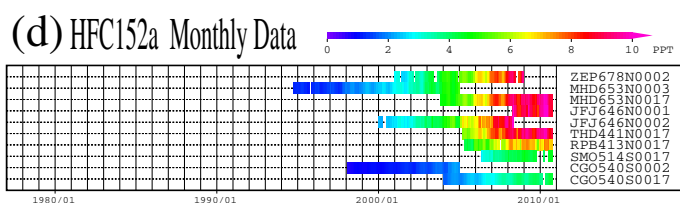
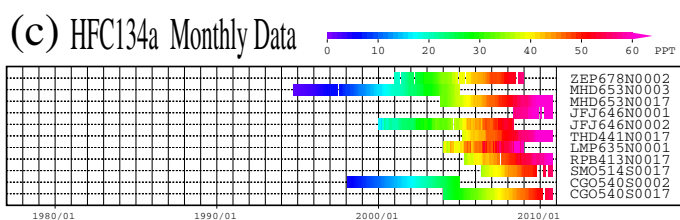
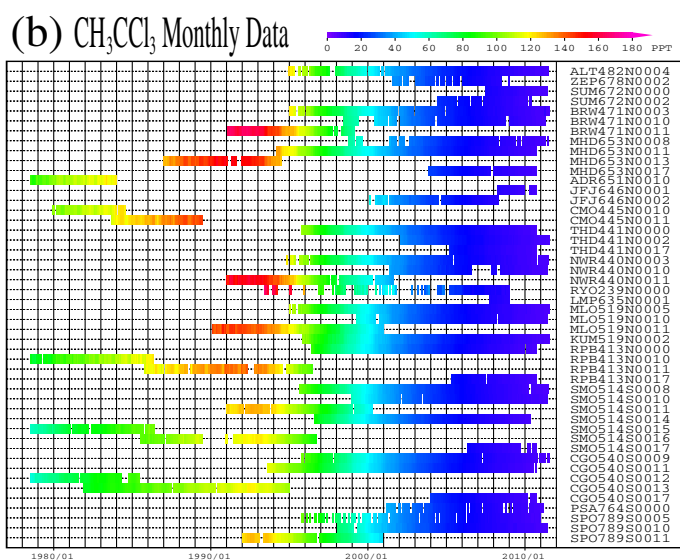
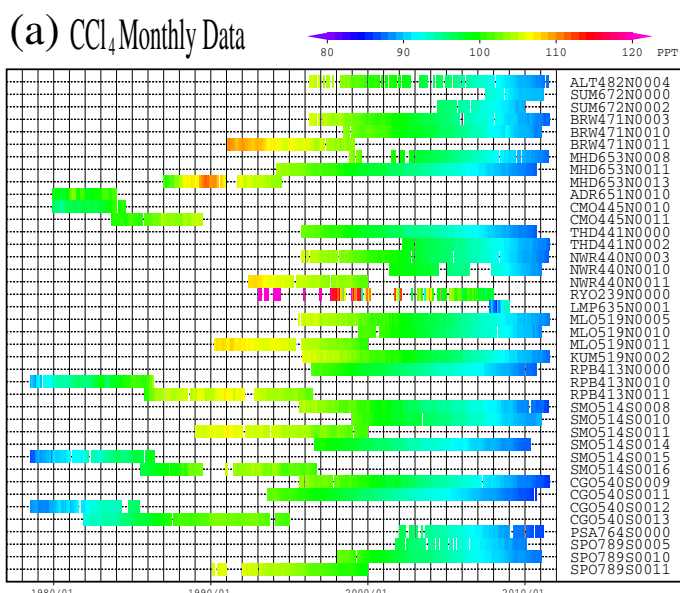


Plate 6.2 Monthly mean (a) CCl₄, (b) CH₃CCl₃, (c) HFC134a, (d) HFC152a, (e) CH₃Cl, (f) SF₆ mole fractions that have been reported to the WDCGG. The mole fractions are illustrated in different colors. The sites are listed in order from north to south.

6. HALOCARBONS AND OTHER HALOGENATED SPECIES

Basic information on halocarbons with regard to environmental issues

Halocarbons are carbon compounds containing one or more halogens, *i.e.*, fluorine, chlorine, bromine or iodine, with most being industrial products. Halocarbons are classified into chlorofluorocarbons (CFCs), which contain fluorine and chlorine; the hydrochlorofluorocarbons (HCFCs), which contain hydrogen in addition to fluorine and chlorine; and the halons, which contain bromine and other halogens. Perfluorocarbons (PFCs) are carbon compounds in which all hydrogen atoms are replaced by fluorine atoms, and hydrofluorocarbons (HFCs) are halocarbons that contain hydrogen and fluorine but no chlorine. Sulphur hexafluoride (SF_6), although not a halocarbon, behaves similarly to halocarbons and it is a potent long-lived greenhouse gas. Carbon tetrachloride (CCl_4) and methyl chloroform (CH_3CCl_3) are produced industrially, whereas methyl chloride (CH_3Cl) has natural sources. Although the mole fractions of the halocarbons are relatively low in the atmosphere, they have high global warming potentials. The halocarbons have been shown to account for about 12% of the total increase in radiative forcing due to long-lived greenhouse gases from 1750 to 2010 (WMO, 2011c).

The halocarbons are colourless, odourless and innocuous substances that can be readily gasified and liquefied and have low surface tension. Thus, they were commonly used as refrigerants, propellants and detergents for semiconductors, resulting in a rapid increase in their mole fractions in the atmosphere until the mid-1980s. Halocarbons containing chlorine and bromine led to the depletion of the ozone layer. Since the mid-1990s, the Montreal Protocol on Substances that Deplete the Ozone Layer and its subsequent Adjustments and Amendments have progressively increased the regulation of the production, consumption and trade of ozone-depleting compounds.

The CFCs are destroyed mainly by ultraviolet radiation in the stratosphere, and their lifetimes are generally long (*e.g.*, about 50 years for CFC-11). However, the HCFCs and CH_3CCl_3 , which contain hydrogen, react with hydroxyl radicals (OH) in the troposphere and have relatively short lifetimes (*e.g.*, about 5 years for CH_3CCl_3). As the reaction with OH in the troposphere is a major sink for CH_3CCl_3 , global measurements of CH_3CCl_3 provide an accurate estimate of the global mole fraction of OH (Prinn *et al.*, 2001). Due to substantial decrease of CH_3CCl_3 in the atmosphere the other compounds are considered now to trace OH mole fraction changes.

The Kyoto Protocol to the United Nations Framework Convention on Climate Change (UNFCCC), which entered into force on 16 February

2005, specifies HFCs, PFCs and SF_6 as targets for quantified emission limitation and reduction commitments.

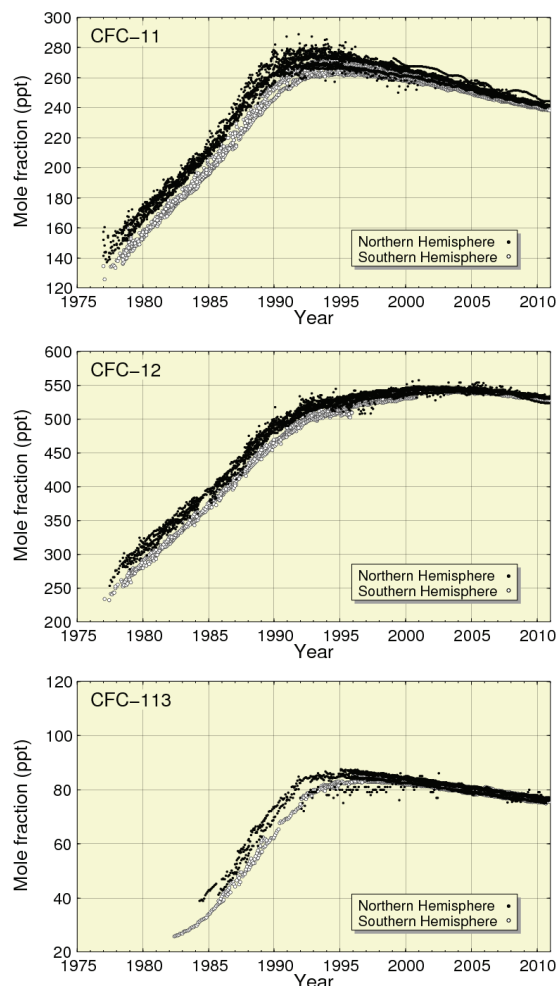


Fig. 6.1 Time series of the monthly mean mole fractions of CFC-11, CFC-12 and CFC-113. Solid circles show mole fractions measured in the Northern Hemisphere and open circles show mole fractions in the Southern Hemisphere.

Annual changes in the levels of halocarbons in the atmosphere

The map at the beginning of this chapter shows observational sites that have submitted data on halocarbons and other halogenated species to the WDCGG. Plates 6.1 and 6.2 show all the monthly mean mole fractions of these gases submitted to the WDCGG. The figures (6.1 – 6.7) in this chapter plot the monthly mean data reported to the WDCGG without spatial averaging. Some discrepancies in the absolute mole fractions were observed for several stations, suggesting that these stations may have

adopted different standard scales. Observational data based on identical standard scales revealed that the differences in the mole fractions between the two hemispheres were large in the 1980s for CFCs, CCl_4 and CH_3CCl_3 but have since narrowed as the emissions have been suppressed and the existing constituents have been mixed across the hemispheres.

Figure 6.1 shows monthly mean mole fractions of CFC-11 (CCl_3F), CFC-12 (CCl_2F_2) and CFC-113 ($\text{CCl}_2\text{FCClF}_2$) over time. The mole fractions of CFC-11 were maximal around 1992 in the Northern Hemisphere, followed by a maximum about one year later in the Southern Hemisphere. The mole fractions of CFC-113 were maximal around 1992 in the Northern Hemisphere and around 1997 in the Southern Hemisphere. The mole fractions of these gases have since been decreasing slowly in both hemispheres. The mole fraction of CFC-12 increased until around 2005 and then started decreasing gradually.

Figure 6.2 shows time series of the monthly mean mole fractions of Halon-1211 (CBrClF_2) and Halon-1301 (CBrF_3). The mole fraction of Halon-1211 has not increased since 2005, whereas the mole fraction of Halon-1301 is increasing.

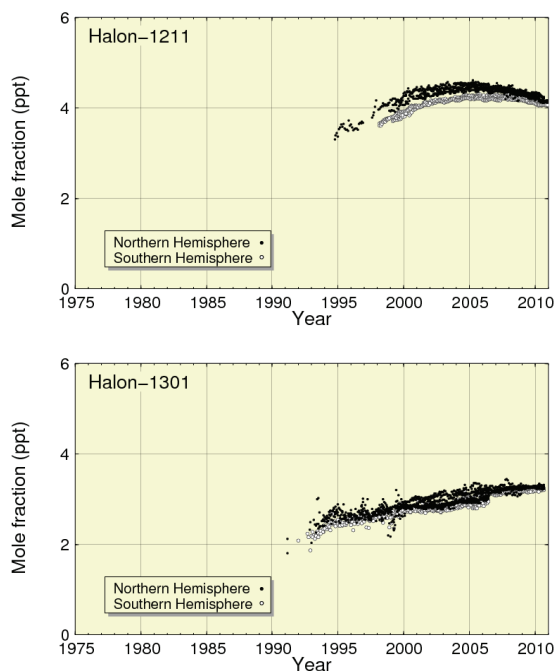


Fig. 6.2 Time series of the monthly mean mole fractions of Halon-1211 and Halon-1301. Solid circles show mole fractions measured in the Northern Hemisphere and open circles show mole fractions in the Southern Hemisphere.

Figure 6.3 shows time series of the mole fractions of HCFC-22 (CHClF_2), HCFC-141b ($\text{CH}_3\text{CCl}_2\text{F}$) and HCFC-142b (CH_3CClF_2). The mole fractions of these gases increased significantly during the last

decade as a result of their continued use as substitutes for CFCs. However, the growth of HCFC-141b decelerated rapidly in the second half of the decade.

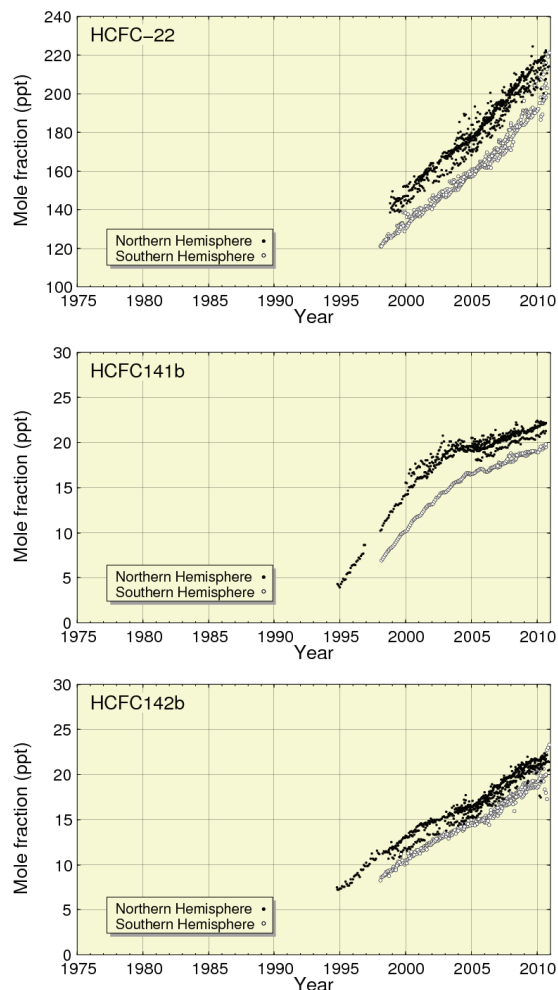


Fig. 6.3 Time series of the monthly mean mole fractions of HCFC-22, HCFC-141b, and HCFC-142b. Solid circles show mole fractions measured in the Northern Hemisphere and open circles show mole fractions in the Southern Hemisphere.

Figure 6.4 shows time series of the mole fractions of CCl_4 and CH_3CCl_3 . The mole fractions of CCl_4 in both hemispheres were at a maximum around 1991. The mole fractions of CH_3CCl_3 were at a maximum around 1992 in the Northern Hemisphere and around 1993 in the Southern Hemisphere. The mole fractions of these gases have since been decreasing.

Figure 6.5 shows time series of the monthly mean mole fractions of HFC-134a (CH_2FCF_3) and HFC-152a (CH_3CHF_2). The mole fractions of HFC-134a and HFC-152a have increased by 4 to 5-fold over the last 10 years. These increases have been larger in the Northern than in the Southern Hemisphere, suggesting that their predominant sources are located in the Northern Hemisphere.

Figure 6.6 shows a time series of the monthly mean mole fractions of methyl chloride (CH_3Cl). The mole fraction of CH_3Cl has remained steady although the signs of the seasonal variation can be noticed in the dataset.

Figure 6.7 shows a time series of the monthly mean mole fractions of SF_6 . The mole fraction of SF_6 in 2010 was double that in the mid-1990s increasing nearly linearly with a rate of 0.24 ppt/year (WMO, 2011c).

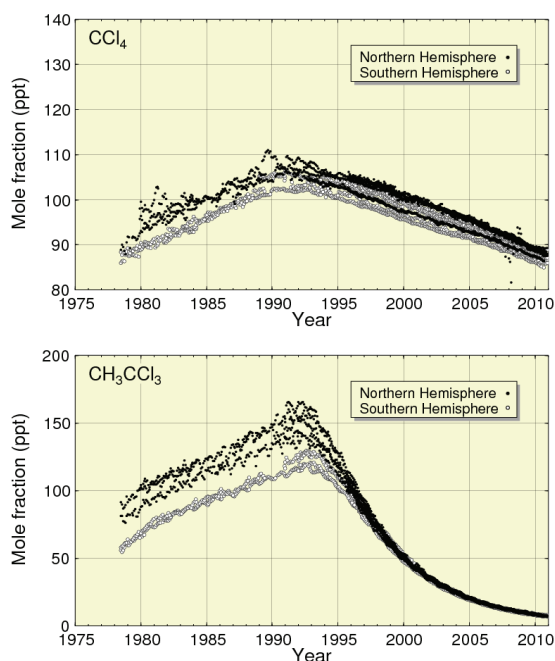


Fig. 6.4 Time series of the monthly mean mole fractions of CCl_4 and CH_3CCl_3 . Solid circles show mole fractions measured in the Northern Hemisphere and open circles show mole fractions in the Southern Hemisphere.

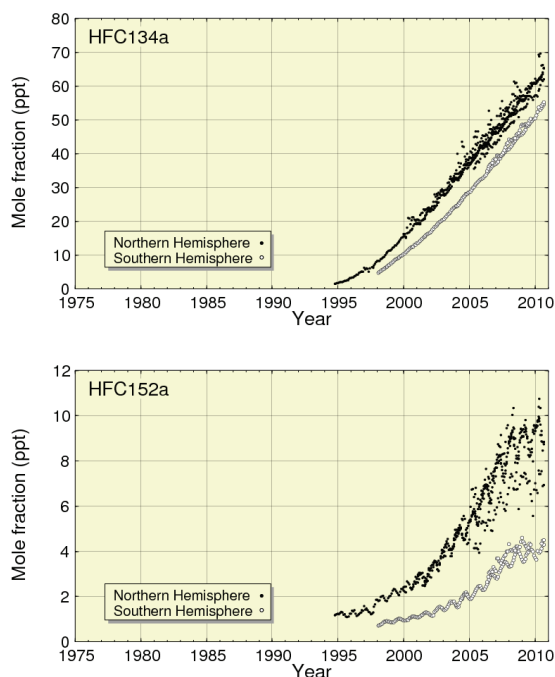


Fig. 6.5 Time series of the monthly mean mole fractions of HFC-134a and HFC-152a. Solid circles show mole fractions measured in the Northern Hemisphere and open circles show mole fractions in the Southern Hemisphere.

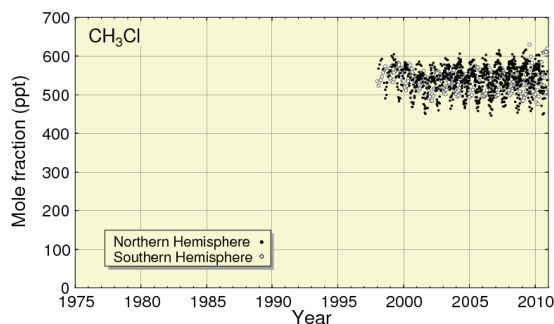


Fig. 6.6 Time series of the monthly mean mole fractions of CH_3Cl . Solid circles show mole fractions measured in the Northern Hemisphere and open circles show mole fractions in the Southern Hemisphere.

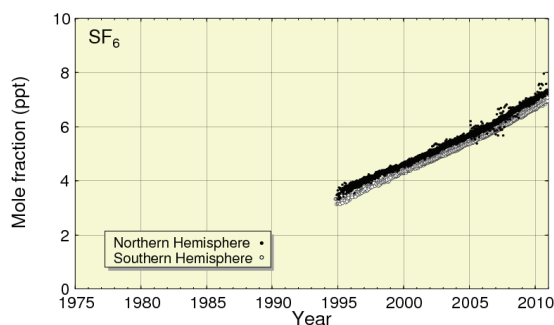
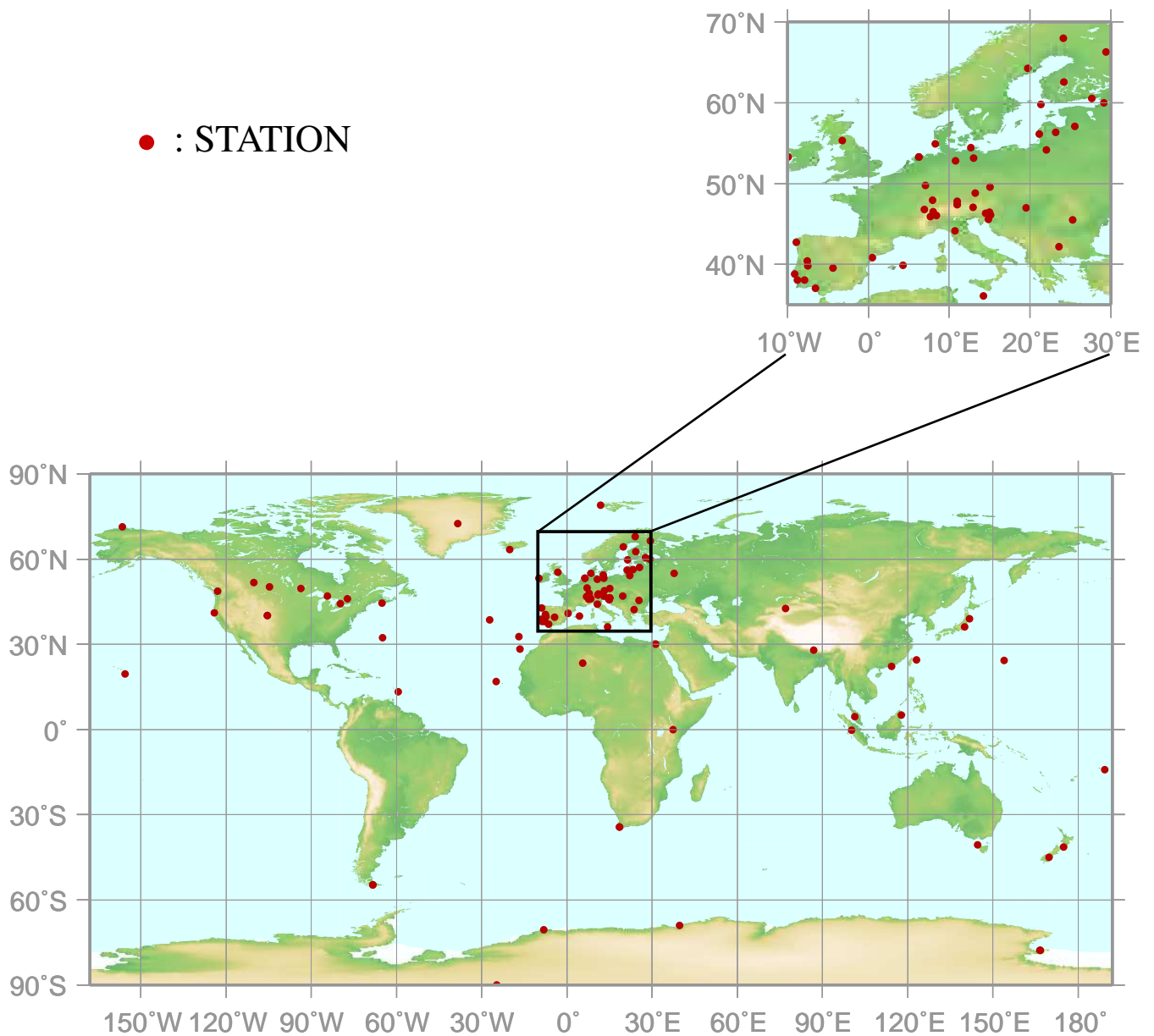


Fig. 6.7 Time series of the monthly mean mole fractions of SF_6 . Solid circles show mole fractions measured in the Northern Hemisphere and open circles show mole fractions in the Southern Hemisphere.

7.

SURFACE OZONE (O₃)

● : STATION



This map shows locations of the stations that have submitted data for monthly mean mole fraction.

O₃ Monthly Data

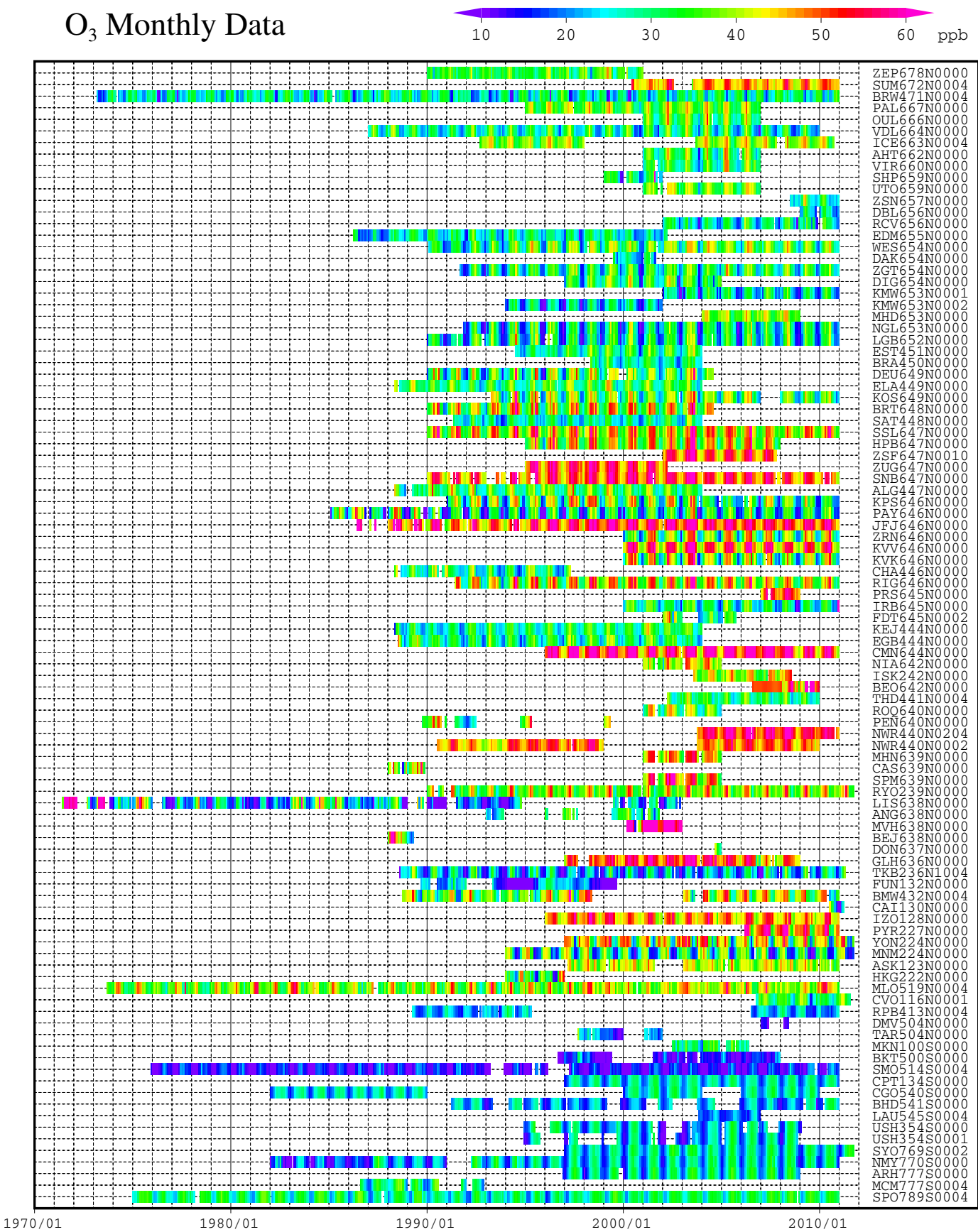


Plate 7.1 Monthly mean O₃ mole fractions that have been reported to the WDCGG. The mole fractions are illustrated in different colors. The sites are listed in order from north to south.

7. SURFACE OZONE (O₃)

Basic information on surface ozone (O₃) with regard to environmental issues

Ozone (O₃) in the atmosphere exists mostly in the stratosphere, with less than 10% in the troposphere. However, O₃ in the troposphere plays an important role in the atmospheric environment through radiative and chemical processes. O₃ absorbs UV radiation in the stratosphere, thus influencing the vertical profile of temperature and circulation in the stratosphere. Moreover, as a greenhouse gas in the troposphere, O₃ absorbs IR radiation. The latter effect is more significant in the upper troposphere, and tropospheric O₃ is the third most important anthropogenic greenhouse gas after CO₂ and CH₄ (Denman *et al.*, 2007; IPCC, 2007). Tropospheric O₃ in the northern extratropics was the greatest contributor to global warming during the 20th century, and increases in tropospheric O₃ from industrialization in developing countries was found to contribute to accelerated warming in the tropics during the latter half of the century (Shindell *et al.*, 2006). Furthermore, by reacting with water vapour in the presence of UV radiation, O₃ produces OH radicals, which control atmospheric mole fractions of many greenhouse gases, such as CH₄, through chemical reactions.

The observational results at high altitudes around 1990, compared with those from the end of the 19th century to the first half of 20th century, show increases in tropospheric O₃ in urban areas (Staehelin *et al.*, 1994). However, ozonesonde measurements in the troposphere show stable or decreasing trends in northern mid-latitudes (Oltmans *et al.*, 2006). There is as yet no consensus on the global trend of tropospheric O₃. Recently an attempt has been done to make a systematic review of the observed trends. It has shown that in most regions of the world — the noteworthy exception being East Asia — surface and free tropospheric ozone concentrations have not risen significantly after the year 2000. Prior to the 1990s almost all records indicate a strong rise, while during the 1990s the picture is very diverse (http://igac.jisao.washington.edu/Newsletter/IGAC_Newsletter_Oct11.pdf).

Tropospheric O₃ originates from flux/mixing from the stratosphere and in-situ photochemical production. O₃ is destroyed in various processes, including chemical reactions with NO, the hydroperoxyl radical (HO₂) and OH, and deposition at the Earth's surface. The lifetime of tropospheric ozone varies from one or a few days in the boundary layer to a few tens of days or even a few months in the free troposphere.

In the troposphere, the mole fractions of O₃ are high in high and mid-latitudes in both hemispheres, and low in the Tropics over the Atlantic (Marenco and Said, 1989) and the Pacific (Tsutsumi *et al.*, 2003) Oceans. The

localised sources of ozone precursors and generally short lifetime of surface O₃ make its distribution spatially non-uniform and time-variant.

Annual variation of surface O₃ mole fraction

The observational sites that have submitted data for surface O₃ to the WDCGG are shown on the map at the beginning of this chapter. The monthly mean mole fractions of O₃ that have been reported from these observational sites are shown in Plate 7.1, with different mole fraction levels illustrated in different colours. Data for the mole fractions of surface O₃ are reported in two different units, *i.e.*, mole fraction (ppb) and weight per volume (μg/m³) at 25°C. The latter is converted to the former using the formula:

$$X_p [\text{ppb}] = (R \times T / M / P_0) \times 10 \times X_g [\mu\text{g}/\text{m}^3]$$

where R is the molar gas constant (8.31451 [J/K/mol]),

T is the absolute temperature reported from each station,

M is the molecular weight of O₃ (47.9982), and

P₀ is the standard pressure (1013.25 [hPa]).

If temperature is not reported in the data the units are converted using 25 °C.

The mole fraction of surface O₃ was found to vary from station to station, though many of these stations are located in Europe. Moreover, the seasonal and interannual variations were found to be relatively large at most stations, making it difficult to identify a global long-term trend in the mole fraction of surface O₃.

The seasonal cycles of monthly mean mole fraction of surface O₃ averaged for each 30° latitudinal zone are shown in Figure 7.1. The latitudinal mean mole fractions were found to be elevated in spring in most latitudinal zones. However, several patterns of seasonal-diurnal cycles were observed at different locations, including a pronounced spring maximum, a spring maximum at night and a summer maximum during the day, a wide spring-summer maximum, and a pronounced winter maximum (Tarasova *et al.*, 2007).

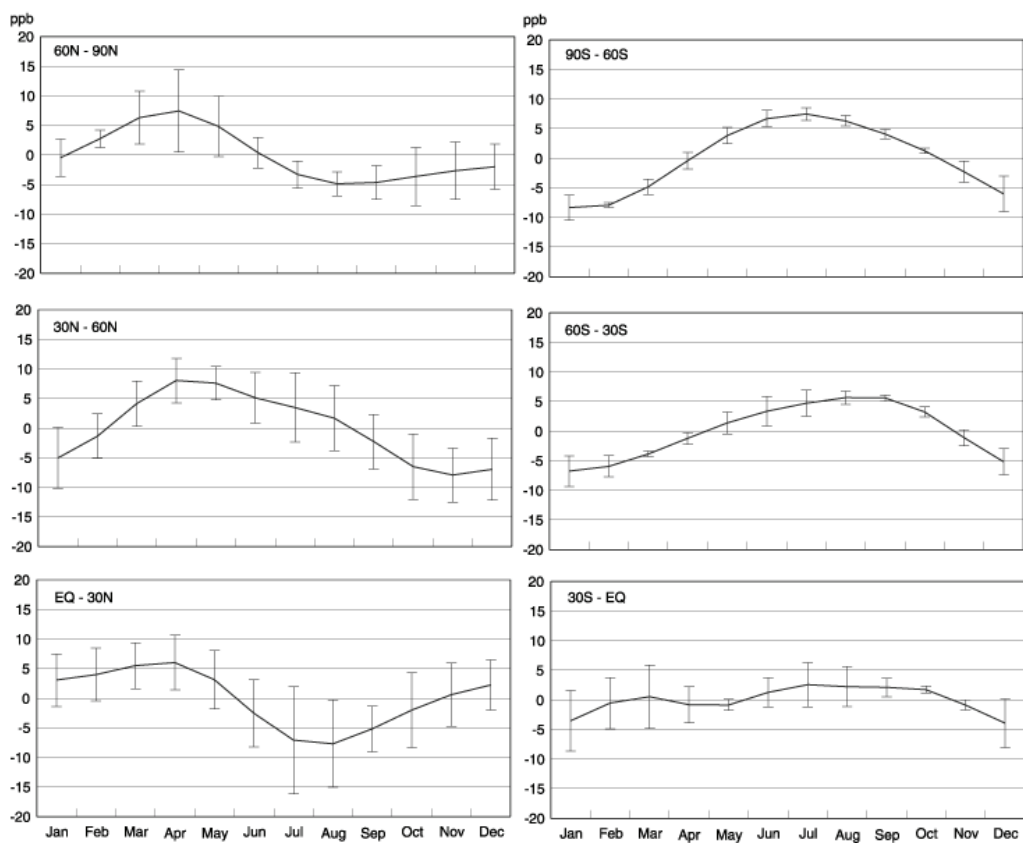
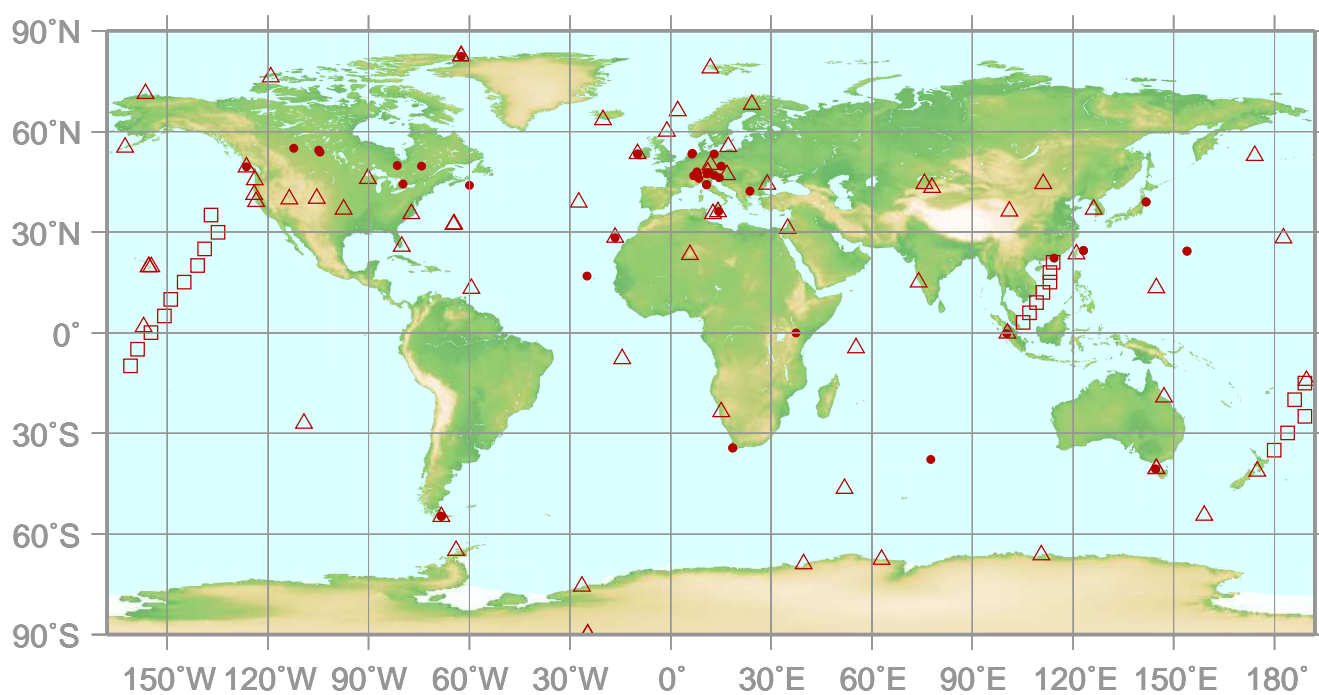


Fig. 7.1 Average seasonal cycles in the mole fraction of O_3 for each 30° latitudinal zone obtained from the seasonal cycle of each station. The standard deviation from the difference of the seasonal cycle for each station within the latitudinal zone is indicated by vertical error bars.

8.

CARBON MONOXIDE (CO)

- : CONTINUOUS STATION
- △ : FLASK STATION
- : FLASK MOBILE (SHIP)



This map shows locations of the stations that have submitted data for monthly mean mole fraction.

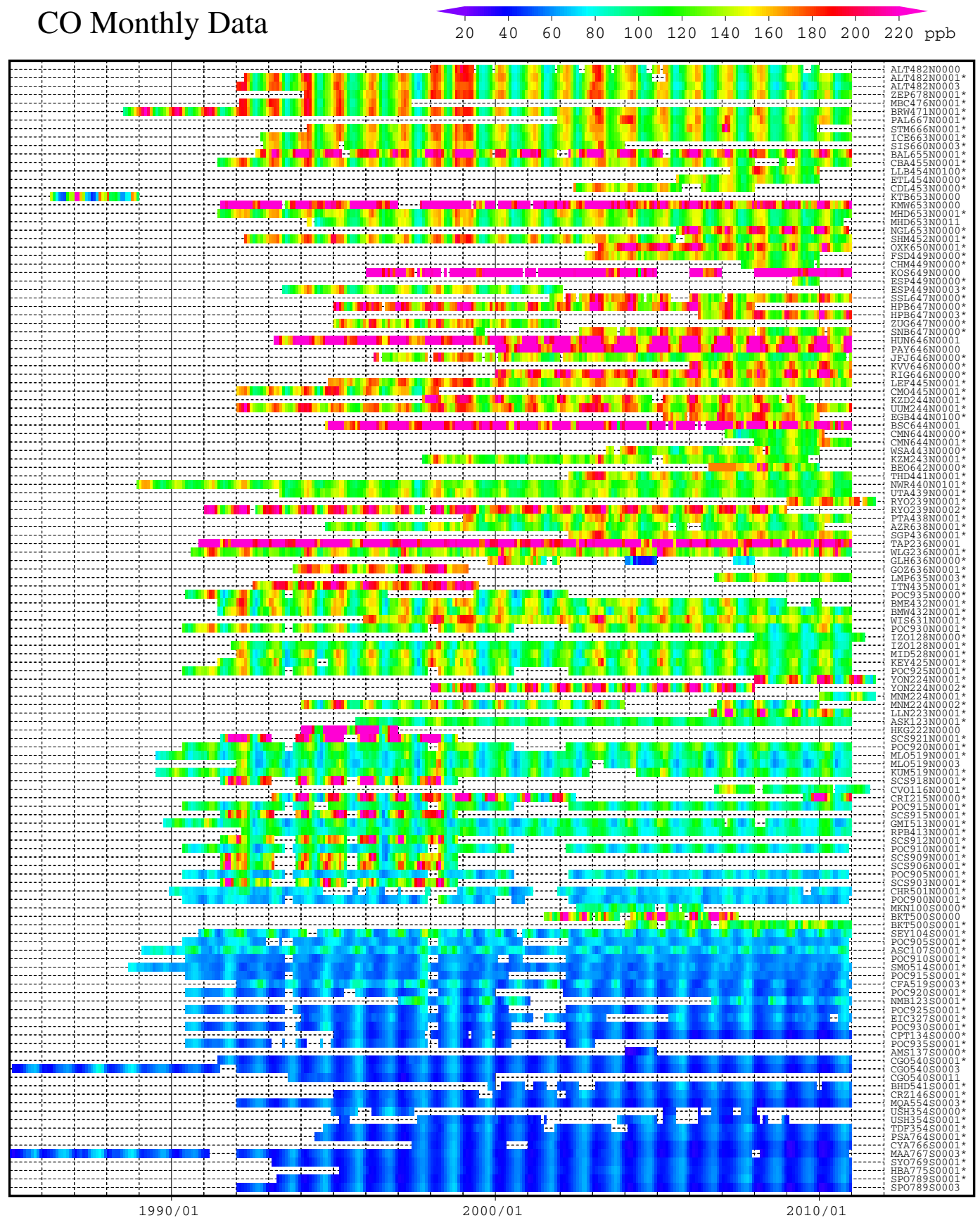
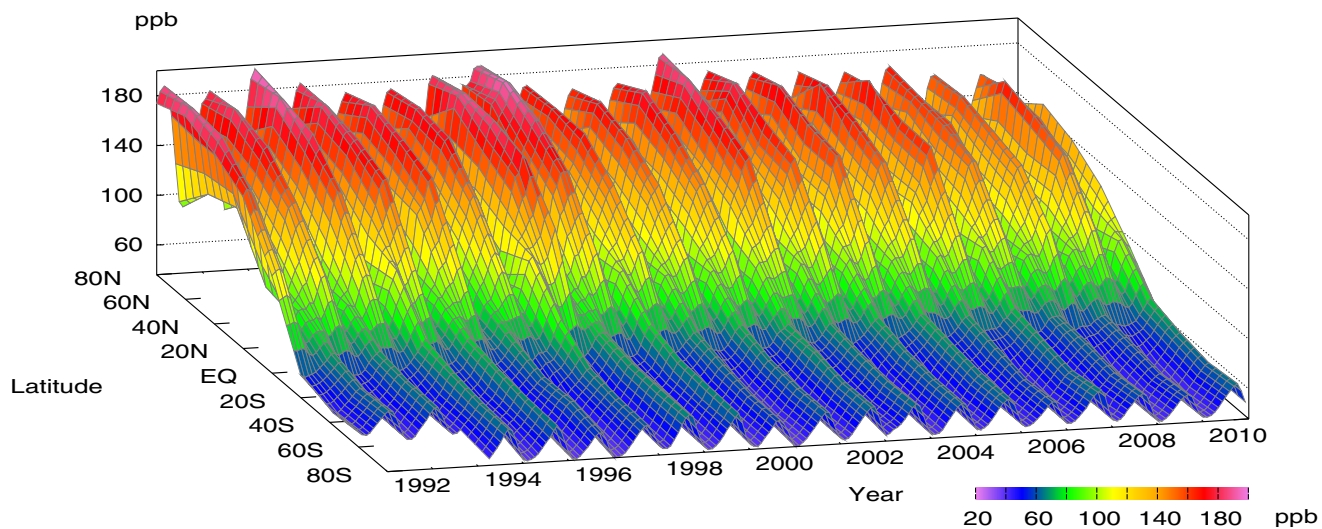
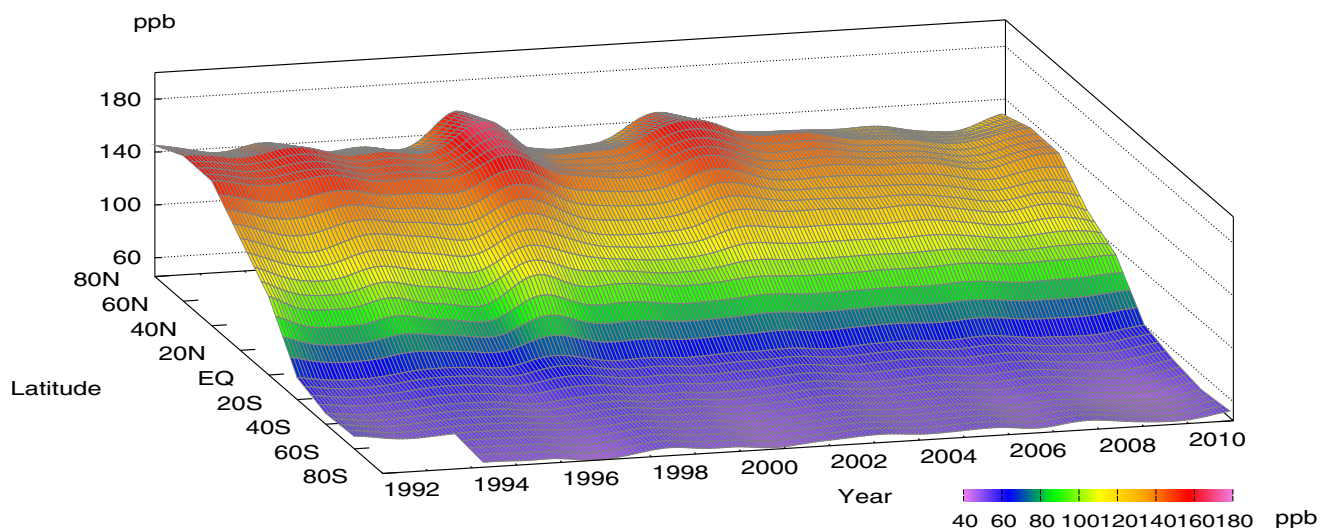


Plate 8.1 Monthly mean CO mole fractions that have been reported to the WDCGG. The mole fractions are illustrated in different colors. The sites are listed in order from north to south. The data from the sites with an asterisk at the end of the station index are used for the analysis shown in Plate 8.2. (see Chapter 2)

CO mole fraction



CO deseasonalized mole fraction



CO growth rate

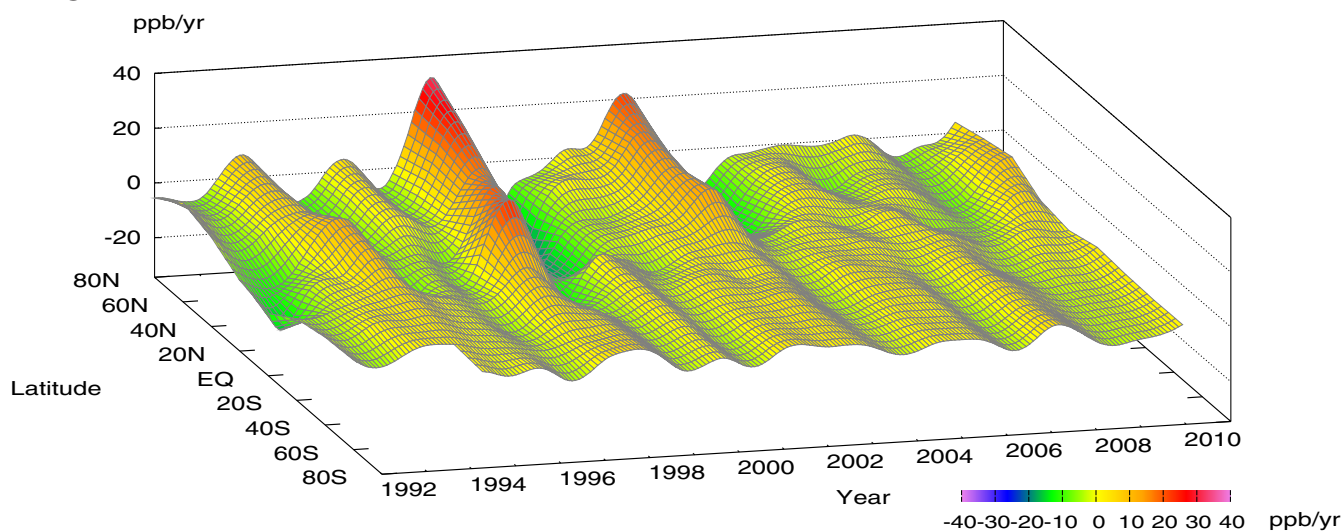


Plate 8.2 Variation of zonally averaged monthly mean CO mole fractions (top), deseasonalized long-term trends (middle), and growth rates (bottom). The zonally averaged mole fractions are calculated for each 20° zone. The deseasonalized trends and growth rates are derived as described in Chapter 2.

8. CARBON MONOXIDE (CO)

Basic information on CO with regard to environmental issues

Carbon monoxide (CO) is not a greenhouse gas; it absorbs hardly any infrared radiation from the Earth. However, CO influences the oxidation capacity of the atmosphere through its interaction with hydroxyl radicals (OH), which react with methane, halocarbons and tropospheric ozone. CO has been monitored due to its indirect influence on greenhouse gases through such reactions.

Sources of atmospheric CO include fossil fuel combustion and biomass burning, along with the oxidation of methane and non-methane hydrocarbons (NMHC). Major sinks include reactions with OH and surface deposition; the reaction of CO and OH accounts for all of the chemical loss of CO in the troposphere (Seinfeld and Pandis, 1998). CO has a relatively long atmospheric lifetime, ranging from 10 days in summer in the tropics to more than a year over the polar regions in winter. Thus, unlike CO₂, anthropogenic CO emissions do not lead to CO accumulation in the atmosphere. Furthermore, the uneven distribution of sources causes large spatial and temporal variations in the CO mole fraction.

Measurements of trapped air in ice cores have shown that the pre-industrial CO mole fraction over central Antarctica during the last two millennia was about 50 ppb and the CO level increased to 110 ppb by 1950 in Greenland (Haan and Raynaud, 1998). Beginning in 1950, the CO mole fraction increased at a rate of 1% per year but started to decrease in the late 1980s (WMO, 1999). Between 1991 and 2001, the global average mole fraction of CO decreased at an annual rate of about 0.5 ppb, excluding temporal enhancements from large biomass burning events (Novelli *et al.*, 2003).

Annual variation of CO mole fraction in the atmosphere

The monthly mean mole fractions of CO that have been reported from fixed stations and some ships to the WDCGG are shown in Plate 8.1, in which different mole fraction levels are plotted in different colours. The observational sites that supplied data for this analysis are shown on the map at the beginning of this chapter.

Latitudinally averaged mole fractions of CO in the atmosphere, together with their deseasonalized mole fractions and growth rates, are shown in Plate 8.2 as three-dimensional representations.

Data for the mole fractions of CO are reported in various units, *i.e.*, ppb, µg/m³-25°C, µg/m³-20°C and mg/m³-25°C. Units other than ppb were converted to ppb using the formulas:

$$X_p \text{ [ppb]} = (R \times T / M / P_0) \times 10 \times X_g \text{ [}\mu\text{g/m}^3\text{]}$$

$$X_p \text{ [ppb]} = (R \times T / M / P_0) \times 10^4 \times X_g \text{ [mg/m}^3\text{]}$$

where R is the molar gas constant (8.31451 [J/K/mol]),

T is the absolute temperature reported from each station,

M is the molecular weight of CO (28.0101), and

P₀ is the standard pressure (1013.25 [hPa]).

If temperature is not reported in the data the units are converted using 25 °C.

Plate 8.2 shows that the seasonal variations of CO were larger in the Northern Hemisphere and smaller in the Southern Hemisphere, and that the deseasonalized mole fractions were the highest in northern mid-latitudes and the lowest in the Southern Hemisphere, having a large latitudinal gradient from northern mid- to southern low latitudes. This is likely due to the presence of numerous CO anthropogenic sources in the northern mid-latitudes, combined with the destruction of CO in the tropics, where OH radicals are abundant.

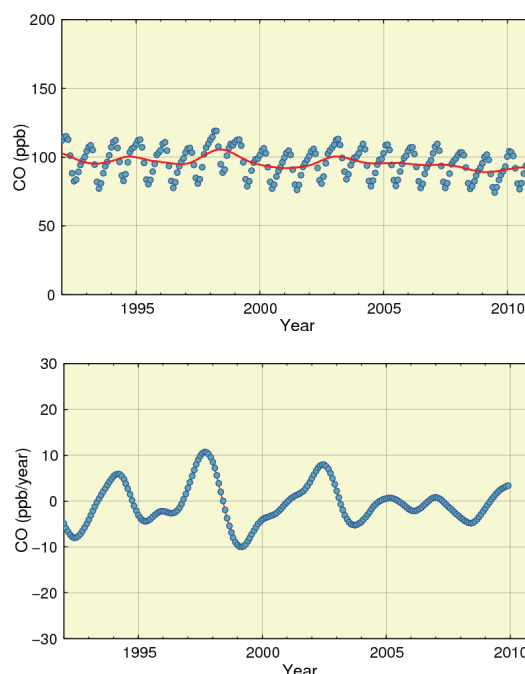


Fig. 8.1 Global monthly mean mole fraction of CO from 1992 to 2010, including deseasonalized long-term trend in red line (top) and annual growth rate (bottom).

Figure 8.1 shows global monthly mean CO mole fractions and their growth rates. Growth rates were high in 1993/1994, 1997/1998 and 2002, and low in 1992 and 1998/1999. The global annual mean mole fraction was about 93 ppb in 2010, which was calculated irrespective of the difference in observation scales.

Figure 8.2 shows monthly mean mole fractions of CO for each 30° latitudinal zone. Seasonal variations were observed in both hemispheres, with mole fractions being higher in winter. Amplitudes of the seasonal cycle were larger in the Northern Hemisphere than in the Southern Hemisphere.

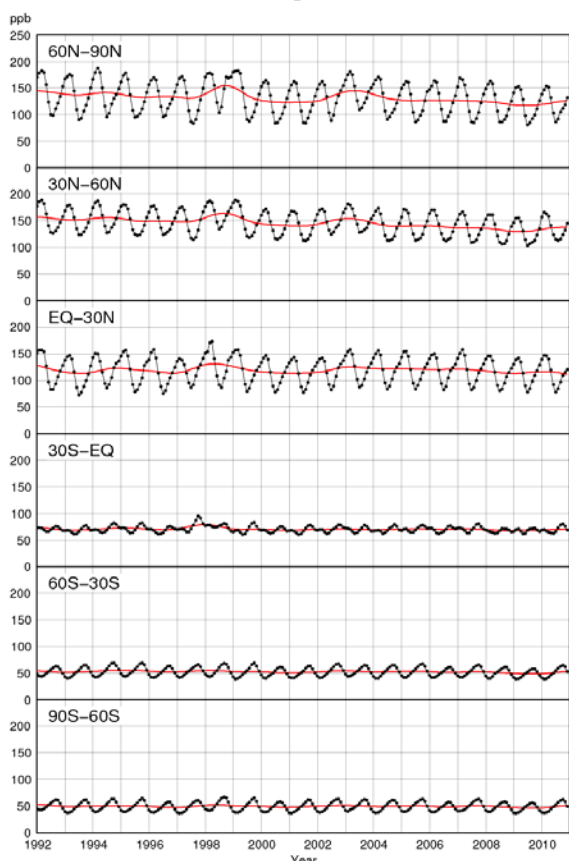


Fig. 8.2 Monthly mean mole fractions of CO from 1992 to 2010 for each 30° latitudinal zone (dots) and their deseasonalized long-term trends (red lines).

Figure 8.3 summarizes deseasonalized long-term trends for each 30° latitudinal zone and their growth rates. The CO mole fractions were highest in northern mid-latitudes. There was a decline in CO mole fractions around 1992, almost coinciding with the decrease in the growth rate of CH₄ mole fractions, most likely due to variations in their common sinks (OH). The enhanced stratospheric ozone depletion due to increased volcanic aerosols following the eruption of Mount Pinatubo in 1991 may have increased atmospheric OH radicals, which react with both CO and CH₄ (Dlugokencky *et al.*, 1996).

Increases in CO mole fractions were observed from 1997 to 1998 in northern latitudes and in southern low latitudes. These increases were attributed to large biomass burning events in Indonesia in late 1997 and in Siberia in the summer and autumn of 1998 (Novelli *et al.*, 1998).

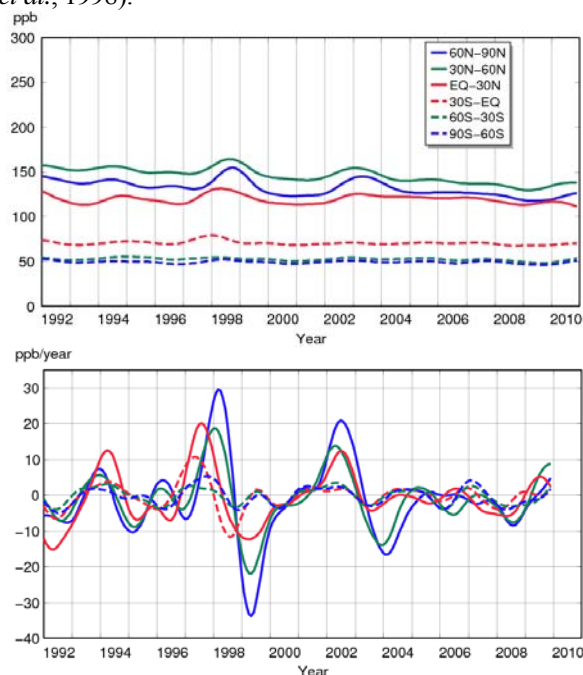


Fig. 8.3 Deseasonalized long-term trends of CO for each 30° latitudinal zone (top) and their growth rates (bottom).

The CO mole fractions returned to normal after 1999, but the growth rates in the Northern Hemisphere increased substantially again in 2002. The latter may have been due to large biomass burning. Large-scale boreal forest fires occurred in Siberia and North America from 2002 to 2003. Strong forest fires also occurred in Russia in summer 2010 which can be seen in the bottom panel of Figure 8.3.

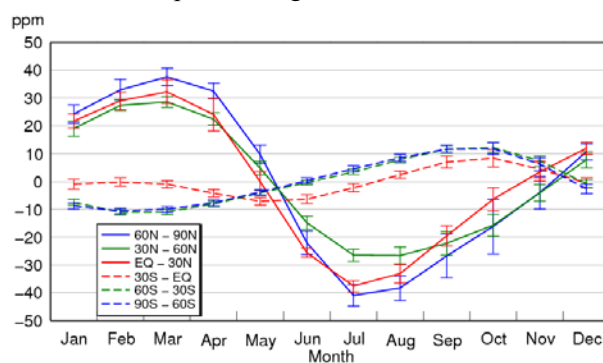


Fig. 8.4 Average seasonal cycles in the mole fraction of CO for each 30° latitudinal zone obtained by subtracting long-term trends from the zonal mean time series. The standard deviation is indicated by vertical error bars.

Seasonal cycle of CO mole fraction in the atmosphere

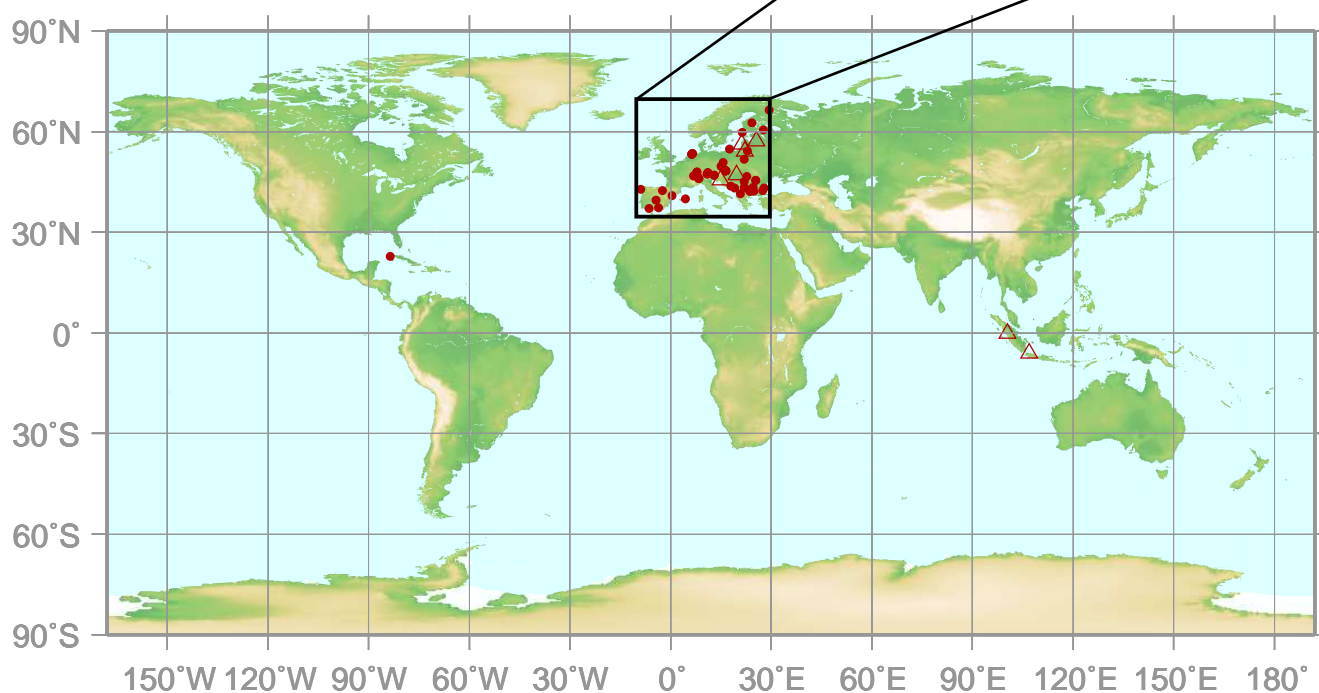
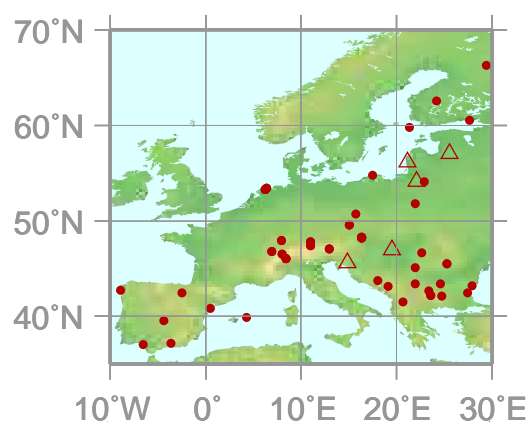
Figure 8.4 shows average seasonal cycles in the mole fraction of CO for each 30° latitudinal zone. The seasonal cycle was driven mainly by seasonal variations in OH abundance as a CO sink. Additional factors include emission and oxidation from CO sources and large-scale transport of CO, despite a relatively weak seasonality in emission and oxidation compared with OH abundance. This seasonality and a short lifetime of about a few months resulted in a sharp decrease in early summer followed by a relatively slow increase in autumn. The levelling-off in the beginning of the year seen in the southern low latitudes may be attributed to the transport of CO from the Northern Hemisphere.

9.

NITROGEN MONOXIDE (NO) AND NITROGEN DIOXIDE (NO₂)

● : CONTINUOUS STATION

△ : FILTER STATION



This map shows locations of the stations that have submitted data for monthly mean mole fraction.

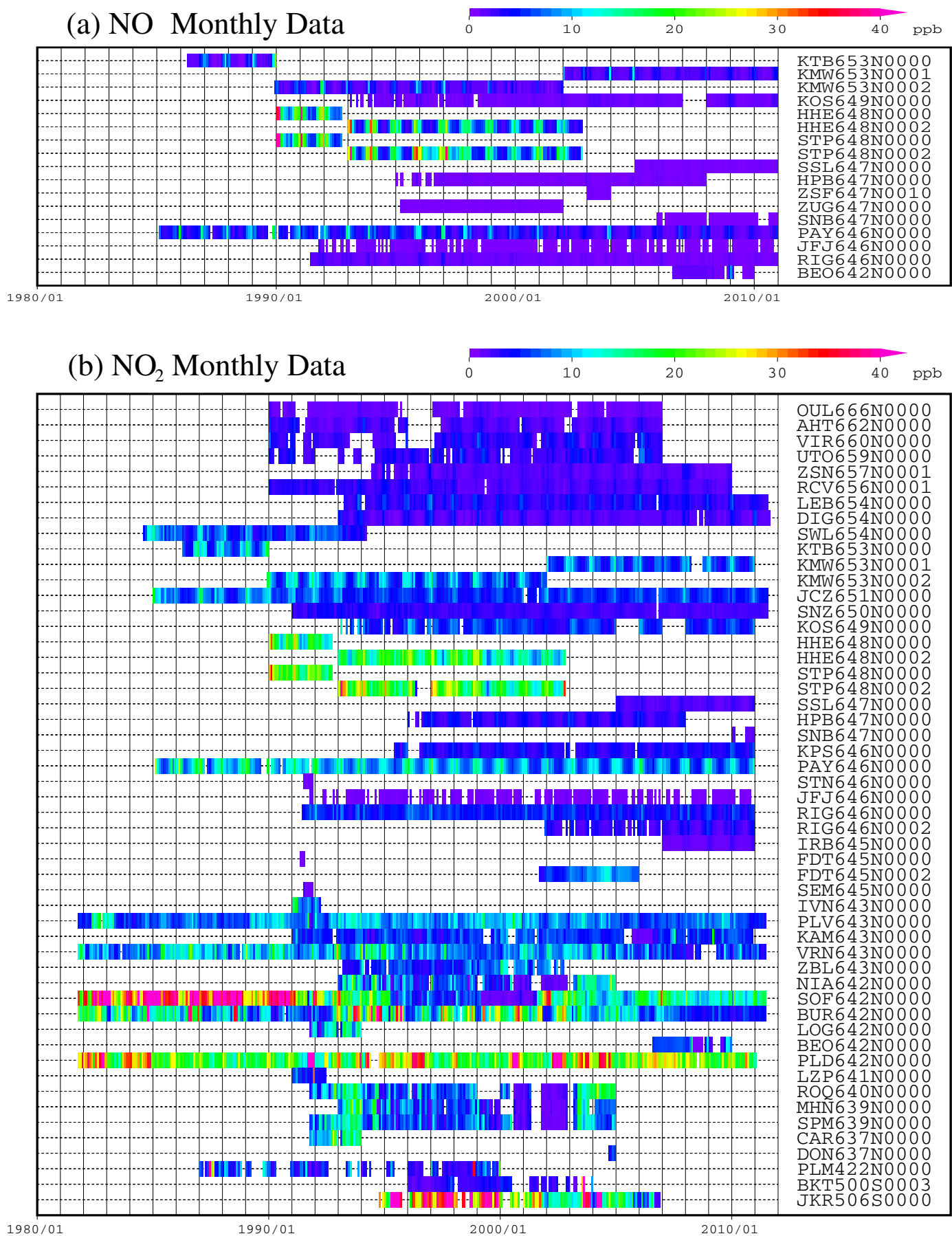


Plate 9.1 Monthly mean (a) NO and (b) NO₂ mole fractions that have been reported to the WDCGG. The mole fractions are illustrated in different colors. The sites are listed in order from north to south.

9. NITROGEN MONOXIDE (NO) AND NITROGEN DIOXIDE (NO₂)

Basic information on NO and NO₂ with regard to environmental issues

Nitrogen oxides (NO_x, *i.e.*, NO and NO₂) are not greenhouse gases. Nevertheless, these compounds have a central regulatory role in the free radical and oxidising photochemistry of the troposphere. This photochemistry regulates the lifetime of methane and the production of tropospheric O₃ and secondary aerosols, all of which have important roles in the natural and anthropogenic greenhouse effect. The O₃ produced in the atmosphere as a result of the nitrogen oxides presence can affect vegetation growth and human health.

Sources of NO_x include energy production, transport, lightning, soils and biomass burning (Reis et al., 2009). They constitute major causes of acid rain and deposition. The dominant sink of NO_x in the atmosphere is its conversion into nitric acid (HNO₃) and peroxyacetylnitrate (PAN), which are eventually removed by dry or wet deposition. In some cases, NO_x is removed from the atmosphere directly by dry deposition. NO_x abundance varies in both space and time because of their short lifetimes and uneven source distribution. Some regional assessments are done based on satellite information to clarify such variations and trends.

Annual variation of NO and NO₂ mole fractions in the atmosphere

The observation stations that have submitted data for NO and NO₂ to the WDCGG are shown on the map at the beginning of this chapter. Most of these stations are located in Europe.

The monthly mean mole fractions of NO and NO₂ reported to the WDCGG are shown in Plate 9.1, in which different mole fraction levels are plotted in different colours. Data for NO_x are reported in various units, *i.e.*, ppb, µg/m³-25°C, µg/m³-20°C, µgN/m³-25°C and mg/m³-25°C. Units other than ppb were converted to ppb using the formulas:

$$\begin{aligned}X_p [\text{ppb}] &= (R \times T / M / P_0) \times 10 \times X_g [\mu\text{g}/\text{m}^3] \\X_p [\text{ppb}] &= (R \times T / M / P_0) \times 10^4 \times X_g [\text{mg}/\text{m}^3] \\X_p [\text{ppb}] &= (R \times T / M_N / P_0) \times 10 \times X_g [\mu\text{gN}/\text{m}^3]\end{aligned}$$

where R is the molar gas constant (8.31451 [J/K/mol]),

T is the absolute temperature reported from each station,

M is the molecular weight of NO (30.00614) or NO₂ (46.00554),

M_N is the atomic weight of N (14.00674), and

P₀ is the standard pressure (1013.25 [hPa]).

If temperature is not reported in the data the units are converted using 25 °C.

The distributions of NO and NO₂ are spatially non-uniform and variable over time. Due to the high temporal variability in the mole fraction of NO₂ at each observation site, it was difficult to identify a long-term trend. A number of stations located in southern Europe showed higher mole fractions, and some stations reported increased NO₂ in winter.

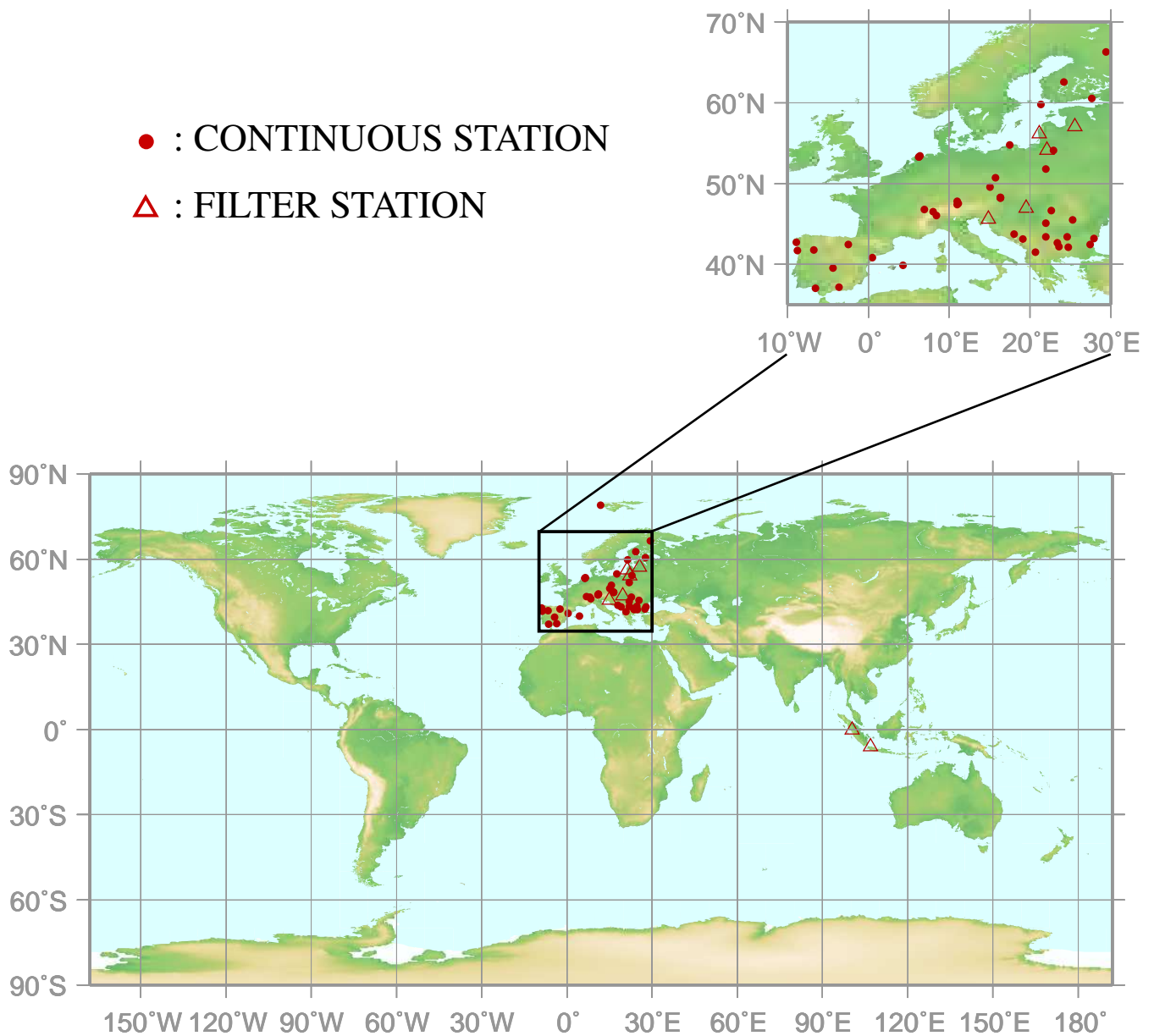
As there are few observational sites for NO, it was difficult to identify whether the global average NO mole fraction increases or decreases.

10.

SULPHUR DIOXIDE

(SO₂)

● : CONTINUOUS STATION
△ : FILTER STATION



This map shows locations of the stations that have submitted data for monthly mean mole fraction.

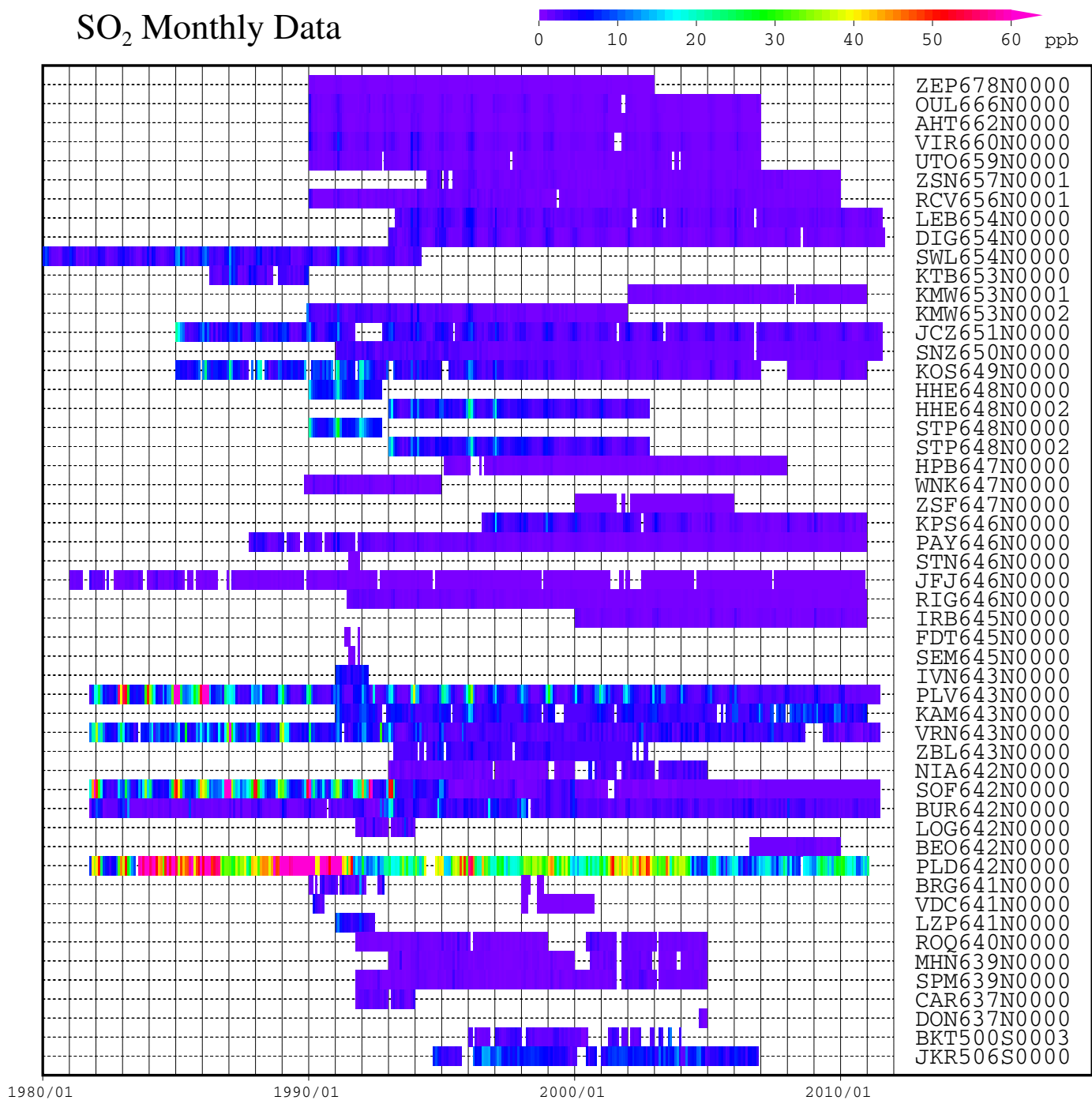


Plate 10.1 Monthly mean SO₂ mole fractions that have been reported to the WDCGG. The mole fractions are illustrated in different colors. The sites are listed in order from north to south.

10. SULPHUR DIOXIDE (SO₂)

Basic information on SO₂ with regard to environmental issues

Sulphur dioxide (SO₂) is not a greenhouse gas, but it is a precursor of atmospheric sulphuric acid (H₂SO₄) and sulphate aerosol. SO₂ is oxidised by hydroxyl radicals (OH) to form sulphuric acid, which then becomes aerosols through photochemical gas-to-particle conversion. While SO₂ reacts much more slowly with OH than does NO₂, SO₂ dissolves readily in suspended liquid droplets in the atmosphere. The global sulphur cycle affects atmospheric chemistry, including tropospheric ozone (Berglen *et al.*, 2004).

Sources of SO₂ include fossil fuel combustion by industry, biomass burning, volcanic release and the oxidation of dimethylsulphide (DMS) from the oceans (IPCC, 2007). Major SO₂ sinks are oxidation by OH and deposition onto wet surfaces. Anthropogenic SO₂ has caused acid rain and deposition throughout the industrial era. The mole fractions of SO₂ have shown large variations in both space and time because of the short lifetime and uneven anthropogenic source distribution of SO₂.

Annual variation of SO₂ mole fraction in the atmosphere

The observational sites that have submitted data for SO₂ to the WDCGG are shown on the map at the beginning of this chapter. Most of these stations are located in Europe.

The monthly mean mole fractions of SO₂ that have been reported to the WDCGG are shown in Plate 10.1, with different mole fraction levels illustrated in different colours. Data for SO₂ are reported in various units, *i.e.*, ppb, µg/m³, mg/m³ and µgS/m³. Units other than ppb were converted to ppb using the formulas:

$$\begin{aligned}X_p [\text{ppb}] &= (R \times T / M / P_0) \times 10 \times X_g [\mu\text{g}/\text{m}^3] \\X_p [\text{ppb}] &= (R \times T / M / P_0) \times 10^4 \times X_g [\text{mg}/\text{m}^3] \\X_p [\text{ppb}] &= (R \times T / M_s / P_0) \times 10 \times X_g [\mu\text{gS}/\text{m}^3]\end{aligned}$$

where R is the molar gas constant (8.31451 [J/K/mol]),

T is the absolute temperature reported from each station,

M is the molecular weight of SO₂ (64.0648),

M_s is the atomic weight of S (32.066), and

P₀ is the standard pressure (1013.25 [hPa]).

Although some stations in southern Europe have reported higher mole fractions, it has been difficult to identify an increasing or decreasing trend for SO₂.

REFERENCES

References

- Angert A., S. Biraud, C. Bonfils, W. Buermann, I. Fung, CO₂ seasonality indicates origins of post-Pinatubo sink, *Geophys. Res. Lett.*, **31**, L11103, doi:10.1029/2004GL019760, 2004.
- Bekki, S., K. S. Law, and J. A. Pyle, Effects of ozone depletion on atmospheric CH₄ and CO concentrations, *Nature*, **371**, 595–597, 1994.
- Berglen, T. F., T. K. Berntsen, I. S. A. Isaksen, and J. K. Sundet, A global model of the coupled sulfur/oxidant chemistry in the troposphere: The sulfur cycle, *J. Geophys. Res.*, **109**, D19310, doi:10.1029/2003JD003948, 2004.
- Boden, T.A., G. Marland, and R.J. Andres. 2011. Global, Regional, and National Fossil-Fuel CO₂ Emissions. Carbon Dioxide Information Analysis Center, Oak Ridge National Laboratory, U.S. Department of Energy, Oak Ridge, Tenn., U.S.A. doi 10.3334/CDIAC/00001_V2011
- Cleveland, W. S., S. J. Devlin, Locally weighted regression: an approach to regression analysis by local fitting, *J. Amer. Statist. Assn.*, **83**, 596–610, 1988.
- Conway, T. J., P. P. Tans, L. S. Waterman, K. W. Thoning, D. R. Kitzis, K. A. Masarie, and N. Zhang, Evidence for interannual variability of the carbon cycle from the National Oceanic and Atmospheric Administration/Climate Monitoring and Diagnostics Laboratory global air sampling network, *J. Geophys. Res.*, **99**, 22831–22855, 1994.
- Denman, K. L., G. Brasseur, A. Chidthaisong, P. Ciais, P. M. Cox, R. E. Dickinson, D. Hauglustaine, C. Heinze, E. Holland, D. Jacob, U. Lohmann, S. Ramachandran, P. L. da Silva Dias, S. C. Wofsy and X. Zhang, 2007: Couplings Between Changes in the Climate System and Biogeochemistry. In: Climate Change 2007: The Physical Science Basis. Contribution of Working Group I to the Fourth Assessment Report of the Intergovernmental Panel on Climate Change [Solomon, S., D. Qin, M. Manning, Z. Chen, M. Marquis, K. B. Averyt, M. Tignor and H. L. Miller (eds.)]. Cambridge University Press, Cambridge, United Kingdom and New York, NY, USA.
- Dlugokencky, E. J., L. P. Steele, P. M. Lang, and K. A. Masarie, The growth rate and distribution of atmospheric methane, *J. Geophys. Res.*, **99**, 17021–17043, 1994.
- Dlugokencky, E. J., E. G. Dutton, P. C. Novelli, P. P. Tans, K. A. Masarie, K. O. Lantz, and S. Mardronich, Changes in CH₄ and CO growth rates after the eruption of Mt. Pinatubo and their link with changes in tropical tropospheric UV flux, *Geophys. Res. Lett.*, **23**, 2761–2764, 1996.
- Dlugokencky, E. J., B. P. Walter, K. A. Masarie, P. M. Lang and E. S. Kasischke, Measurements of an anomalous global methane increase during 1998, *Geophys. Res. Lett.*, **28**, 499–502, 2001.
- Dlugokencky, E. J., L. Bruhwiler, J. W. C. White, L. K. Emmons, P. C. Novelli, S. A. Montzka, K. A. Masarie, P. M. Lang, A. M. Crotwell, J. B. Miller, and L. V. Gatti Observational constraints on recent increases in the atmospheric CH₄ burden, *Geophys. Res. Lett.*, **36**, L18803, 2009.
- Duchon, C. E., Lanczos filtering in one and two dimensions, *J. Appl. Meteor.*, **18**, 1016–1022, 1979.
- Etherridge, D. M., L. P. Steele, R. J. Francey, and R. L. Langenfelds, Atmospheric methane between 1000 A.D. and present: Evidence of anthropogenic emissions and climatic variability, *J. Geophys. Res.*, **103**, 15979–15993, 1998.
- Francey, R. J., P. P. Tans, C. E. Allison, I. G. Enting, J. W. C. White, and M. Troler, Changes in oceanic and terrestrial carbon uptake since 1982, *Nature*, **373**, 326–330, 1995.
- Gu, L., D. D. Baldocchi, S. C. Wofsy, J. W. Munger, J. J. Michalsky, S. P. Urbanski, and T. A. Bonden, Response of a deciduous forest to the Mount Pinatubo eruption enhanced photosynthesis, *Science*, **299**, 2035–2038, 2003.
- Haan, D. and D. Raynaud, Ice core record of CO variations during the last two millennia: atmospheric implications and chemical interactions within the Greenland ice, *Tellus*, **50B**, 253–262, 1998.
- Hansen, J., A. Lacis, R. Ruedy, and M. Sato, Potential Clim. Impact of Mount-Pinatubo Eruption, *Geophys. Res. Lett.*, **19(2)**, 215–218, 1992.
- Heimann, M. and M. Reichstein, Terrestrial ecosystem carbon dynamics and climate feedbacks, *Nature*, **451**, 289–292, 2008.
- IPCC, Climate Change 2007: The Physical Science Basis. Contribution of Working Group I to the Fourth Assessment Report of the Intergovernmental Panel on Climate Change [Solomon, S., D. Qin, M. Manning, Z. Chen, M. Marquis, K. B. Averyt, M. Tignor and H. L. Miller (eds.)]. Cambridge University Press, Cambridge, United Kingdom and New York, NY, USA, 2007.
- Keeling, C. D., R. B. Bacastow, A. F. Carter, S. C. Piper, T. P. Whorf, M. Heimann, W. G. Mook, and H. Roeloffzen, A three-dimensional model of atmospheric CO₂ transport based on observed winds: 1. Analysis of observational data, in aspects of climate variability in the Pacific and the Western Americas, edited by D. H. Peterson, *Geophysical Monograph* **55**, 165–236, American Geophysical Union, Washington, D.C., 1989.

- Keeling, C. D., T. P. Whorf, M. Wahlen, and J. van der Plicht, Interannual extremes in the rate of rise of atmospheric carbon dioxide since 1980, *Nature*, **375**, 666–670, 1995.
- Lambert, G., P. Monfray, B. Ardouin, G. Bonsang,, A. Gaudry, V. Kazan and G. Polian, Year-to-year changes in atmospheric CO₂, *Tellus*, **47B**, 35–55, 1995.
- Manning, A. C., and R. F. Keeling, Global oceanic and land biotic carbon sinks from the Scripps atmospheric oxygen flask sampling network, *Tellus*, **58B**, 95–116, 2006.
- Marenco, A., and F. Said: Meridional and vertical ozone distribution in the background troposphere from Scientific aircraft measurements during the STRATOZ III experiment. *Atmos. Env.*, **23**, 201–214, 1989.
- Matsueda, H., S. Taguchi, H.Y. Inoue, and M. Ishii, A large impact of tropical biomass burning on CO and CO₂ in the upper troposphere. *Science in China (Series C)*, **45**, 116–125, 2002.
- Morimoto, S., S. Aoki, T. Nakazawa, and T. Yamanouchi, Temporal variations of the carbon isotopic ratio of atmospheric methane observed at Ny Alesund, Svalbard from 1996 to 2004, *Geophys. Res. Lett.*, **33**, L01807, doi:10.1029/2005GL024648, 2006.
- Nakazawa, T., K. Miyashita, S. Aoki, and M. Tanaka, Temporal and spatial variations of upper tropospheric and lower stratospheric carbon dioxide, *Tellus*, **43B**, 106–117, 1991.
- Nakazawa, T., S. Morimoto, S. Aoki and M. Tanaka, Time and space variations of the carbon isotopic ratio of tropospheric carbon dioxide over Japan, *Tellus*, **45B**, 258–274, 1993.
- Nakazawa, T., S. Morimoto, S. Aoki and M. Tanaka, Temporal and spatial variations of the carbon isotopic ratio of atmospheric carbon dioxide in the western Pacific region, *J. Geophys. Res.*, **102**, 1271–1285, 1997.
- Nevison, C. D. N. M. Mahowald, S. C. Doney, I. D. Lima, G. R. van der Werf, J. T. Randerson, D. F. Baker, P. Kasibhatla, and G. A. McKinley, Contribution of ocean, fossil fuel, land biosphere, and biomass burning carbon fluxes to seasonal and interannual variability in atmospheric CO₂, *J. Geophys. Res.*, **113**, doi:10.1029/2007JG000408, 2008.
- Novelli, P. C., K. A. Masarie, and P. M. Lang, Distributions and recent changes of carbon monoxide in the lower troposphere, *J. Geophys. Res.*, **103**, 19015–19033, 1998.
- Novelli, P. C., K. A. Masarie, P. M. Lang, B. D. Hall, R. C. Myers, and J. W. Elkins, Reanalysis of tropospheric CO trends: Effects of the 1997–1998 wildfires. *J. Geophys. Res.*, **108(D15)**, 4464, doi:10.1029/2002JD003031, 2003.
- Oltmans et al., Long-term changes in tropospheric ozone, *Atmos. Env.*, **40**, 3156–3173, 2006.
- Prinn, R. G., J. Huang, R. F. Weiss, D. M. Cunnold, P. J. Fraser, P. G. Simmonds, A. McCulloch, C. Harth, P. Salameh, S. O'Doherty, R. H. J. Wang, L. Porter and B. R. Miller, Evidence for substantial variations of atmospheric hydroxyl radicals in the past two decades, *Science*, **292**, 1882–1888, 2001.
- Rayner, P. J., I. G. Enting, R. J. Francey and R. Langenfelds, Reconstructing the recent carbon cycle from atmospheric CO₂, $\delta^{13}\text{C}$ and O₂/N₂ observations, *Tellus*, **51B**, 213–232, 1999.
- Ravishankara A.R., J. S. Daniel, R. W. Portmann, Nitrous Oxide (N₂O): the dominant ozone-depleting substance emitted in the 21st century, *Science*, vol. 326, p. 123–125, 2009
- Reis, S., R. W. Pinder, M. Zhang, G. Lijie, and M. A. Sutton, Reactive nitrogen in atmospheric emission inventories, *Atmos. Chem. Phys.*, **9**, 7657–7677, 2009.
- Rigby, M., R. G. Prinn, P. J. Fraser, P. G. Simmonds, R. L. Langenfelds, J. Huang, D. M. Cunnold, L. P. Steele, P. B. Krummel, R. F. Weiss, S. O'Doherty, P. K. Salameh, H. J. Wang, C. M. Harth, J. Mühle, and L. W. Porter, Renewed growth of atmospheric methane, *Geophys. Res. Lett.*, **35**, L22805, doi:10.1029/2008GL036037, 2008.
- Seinfeld, J. H., and S. N. Pandis, Atmospheric Chemistry and Physics: From Air Pollution to Climate Change, *John Wiley & Sons, Inc., New York*, 1326 pp., 1998.
- Shindell, D., G. Faluvegi, A. Lacis, J. Hansen, R. Ruedy, and E. Aguilar, Role of tropospheric ozone increases in 20th-century climate change, *J. Geophys. Res.*, **111**, D08302, doi:10.1029/2005JD006348, 2006.
- Solomon, S., D. Qin, M. Manning, R.B. Alley, T. Berntsen, N.L. Bindoff, Z. Chen, A. Chidthaisong, J.M. Gregory, G.C. Hegerl, M. Heimann, B. Hewitson, B.J. Hoskins, F. Joos, J. Jouzel, V. Kattsov, U. Lohmann, T. Matsuno, M. Molina, N. Nicholls, J. Overpeck, G. Raga, V. Ramaswamy, J. Ren, M. Rusticucci, R. Somerville, T.F. Stocker, P. Whetton, R.A. Wood and D. Wratt, Technical Summary. In: Climate Change 2007: The Physical Science Basis. Contribution of Working Group I to the Fourth Assessment Report of the Intergovernmental Panel on Climate Change [Solomon, S., D. Qin, M. Manning, Z. Chen, M. Marquis, K.B. Averyt, M. Tignor and H.L. Miller (eds.)]. Cambridge University Press, Cambridge, United Kingdom and New York, NY, USA., 2007.
- Solomon, S., G-K. Plattner, R. Knutti and P. Friedlingstein, Irreversible climate change due to carbon dioxide emissions, *Proc Natl Acad Sci USA*, **106**, 1704–1709, doi: 10.1073/pnas.0812721106, 2009.

- Staehelin, J., J. Thudium, R. Buehler, A. Voltz-Thomas, and W. Graber, Trends in surface ozone concentrations at Arosa (Switzerland), *Atmos. Env.*, **28**, 75–87, 1994.
- Stenchikov, G., A. Robock, V. Ramaswamy, M. D. Schwarzkopf, K. Hamilton, and S. Ramachandran, Arctic Oscillation response to the 1991 Mount Pinatubo eruption: Effects of volcanic aerosols and ozone depletion, *J. Geophys. Res.*, **107(D24)**, 4803, doi:10.1029/2002JD002090, 2002.
- Tarasova, O. A., C. A. M. Brenninkmeijer, P. Jöckel, A. M. Zvyagintsev, and G. I. Kuznetsov: A climatology of surface ozone in the extra tropics: cluster analysis of observations and model results. *Atmos. Chem. Phys.*, **7**, 6099–6117, 2007.
- Tsutsumi, Y., Y. Makino, and J. B. Jensen: Vertical and latitudinal distributions of tropospheric ozone over the western Pacific: Case studies from the PACE aircraft missions. *J. Geophys. Res.*, **108(D8)**, 4251, doi:10.1029/2001JD001374, 2003.
- Thoning, K. W., P. P. Tans, and W. D. Komhyr, Atmospheric carbon dioxide at Mauna Loa observatory, 2. Analysis of the NOAA GMCC data, 1974–1985, *J. Geophys. Res.*, **94**, 8549–8565, 1989.
- WMO, Scientific assessment of ozone depletion: 1998. WMO global ozone research and monitoring project—Report No. 44, World Meteorological Organization, Geneva, 1999.
- WMO, World Data Centre for Greenhouse Gases (WDCGG) Data Summary, WDCGG No. 22, 84pp, 2000.
- WMO, Global Atmospheric Watch (GAW) Strategic Plan: 2008–2015, GAW Report No. 172, WMO TD No. 1384, 2007a.
- WMO, World Data Centre for Greenhouse Gases Data Submission and Dissemination Guide, GAW Report No. 174, WMO TD No. 1416, 2007b.
- WMO, Technical Report of Global Analysis Method for Major Greenhouse Gases by the World Data Center for Greenhouse Gases, GAW Report No. 184, WMO/TD - No. 1473, 2009a.
- WMO, Revision of the World Data Centre for Greenhouse Gases Data Submission and Dissemination Guide, GAW Report No. 188, WMO/TD - No. 1507, 2009b.
(http://www.wmo.int/pages/prog/arep/gaw/documents/GAW_188_web_20100128.pdf, accessed 1 Mar. 2011)
- WMO, Addendum for the Period 2012–2015 to the WMO Global Atmosphere Watch (GAW) Strategic Plan 2008–2015, GAW Report No. 197, 2011a.
- WMO, Second Tropospheric Ozone Workshop - Tropospheric Ozone Changes: observations, state of understanding and model performances, GAW Report No. 199, 2011b.
- WMO, WMO Greenhouse Gas Bulletin No. 7, 2011c.
(<http://www.wmo.int/pages/prog/arep/gaw/ghg/GHGbuletin.html>, accessed 24 Nov. 2011)

APPENDICES

CALIBRATION AND STANDARD SCALES

1. Calibration System in the GAW programme

Under the Global Atmosphere Watch (GAW) programme, the World Calibration Centres (WCCs) are responsible for maintaining calibration standards for certain compounds, establishing instrument calibrations and providing training to the stations. A Reference Standard is designated for each variable to be used for all GAW measurements of that variable at

the Central Calibration Laboratories. Table 1 lists the organizations that serve as WCCs and CCLs for GAW [WMO, 2007]. For CFCs and SO₂, no central facilities or quality control systems have so far been established within the GAW program, while central facilities for NO_x have only recently been formulated.

Table 1. Overview of the GAW Central Calibration Laboratories (GAW-CCL, Reference Standard) and World Calibration Centres for greenhouse and other related gases. The World Calibration Centres have assumed global responsibilities, except where indicated (Am, Americas; E/A, Europe and Africa; A/O, Asia and the South-West Pacific)

| Compounds | Central Calibration Laboratory (Host of Primary Standard) | World Calibration Centre |
|--|---|--|
| Carbon Dioxide (CO ₂) | NOAA/ESRL | NOAA/ESRL (round robin) Empa (audits) |
| carbon isotopes | MPI-BGC | |
| Methane (CH ₄) | NOAA/ESRL | Empa (Am, E/A) JMA (A/O) |
| Nitrous Oxide (N ₂ O) | NOAA/ESRL | IMK-IFU |
| Chlorofluorocarbons (CFCs) | | |
| Sulfur Hexafluoride (SF ₆) | ESRL | KRISS&KMA |
| Molecular Hydrogen (H ₂) | MPI-BGC | |
| Surface Ozone (O ₃) | NIST | Empa |
| Carbon Monoxide (CO) | NOAA/ESRL | Empa |
| Volatile Organic Compounds (VOCs) | NPL (8 components) | IMK-IFU |
| Sulphur Dioxide (SO ₂) | | |
| Nitrogen Oxides (NO _x) | | IEK-8 |

2. Carbon Dioxide (CO₂)

In 1995, the National Oceanic and Atmospheric Administration's Earth System Research Laboratory (NOAA/ESRL, formerly CMDL; Climate Monitoring and Diagnostics Laboratory) in Boulder, Colorado, USA, took over the role of the Central Calibration Laboratory (CCL) from the Scripps Institution of Oceanography (SIO) in San Diego, California, USA. Since then, NOAA/ESRL has served as the CCL responsible for the maintenance of the GAW Primary Standard for CO₂. As the World Calibration Centre

(WCC) for CO₂, NOAA/ESRL maintains a high-precision manometric system for absolute calibration of CO₂ as the reference for GAW measurements throughout the world [Zhao *et al.*, 1997]. It has been recommended that the standards of the GAW measurement laboratories be calibrated every two years at the CCL (WMO, 2003).

Under the WMO calibration system, there have been several calibration scales for CO₂, *e.g.*, SIO-based X74, X85, X87, X93 and X2002 scales and the

NOAA/ESRL-based WMO Mole Fraction Scale partially based on previous SIO scales. The NOAA/ESRL and SIO are working to resolve the possible small differences between their scales. The CCL adopted the WMO X2005 scale, reflecting historical manometric calibrations of the CCL's set of cylinders and the possible small differences between SIO and NOAA/ESRL calibrations. The most current WMO Mole Fraction Scale is the WMO-X2007 scale.

To assess the differences in standard scales among measuring laboratories, NOAA/ESRL organizes intercomparisons or Round Robin experiments endorsed by WMO every few years. Many laboratories

participated in the experiments organized in 1991–1992, 1995–1997, 1999–2000, and 2002–2006. Table 2 shows the results of the experiments performed in 2002–2006, in which the mole fractions measured by various laboratories are compared with the mole fractions measured by NOAA/ESRL [Zhou *et al.*, 2009]. In addition, many laboratories compare their standards bilaterally or multilaterally.

Table 3 lists laboratories and sites used in the present issue of the *Data Summary* with standard scales of reported data and history of participation in WMO intercomparison experiments.

Table 2. Round robin results for the mole fraction of carbon dioxide. Differences between the mole fractions measured by various laboratories and the mole fractions measured by NOAA (Laboratory minus NOAA, ppm).

| Laboratory | Analysis Date | Mole fraction Difference (ppm) | | |
|------------------|---------------|--------------------------------|-----------------------|---------------------|
| | | Low 340–350 ppm | Medium 350–360 ppm | High 370–380 ppm |
| Tohoku Univ. | Jan-03 | –0.11 | –0.19 | –0.29 |
| NIES | Apr-03 | –0.10 | –0.15 | –0.14 |
| MRI | Jul-03 | –0.16 | –0.16 | –0.08 |
| AIST | Sep/Dec-03 | –0.11 | –0.22 | –0.29 |
| JMA | Jan-04 | 0.13 | 0.00 | –0.02 |
| KMA | Mar/Jun-04 | –0.44 | –0.12 | –0.08 |
| CMA (WLG) | Jul-04 | –0.05 | –0.19 | –0.10 |
| CMA (BJ) | Aug-04 | –0.03 | –0.20 | 0.02 |
| Scripps (CMM) | Jun-05 | 0.23 | 0.17 | 0.20 |
| Scripps (ECM II) | | 0.10 | 0.02 | 0.02 |
| LSCE | Oct/Nov-05 | –0.05 | –0.11 | –0.09 |
| Monte Cimone | Oct-02 | 0.08 | 0.02 | –0.03 |
| Lampedusa | Nov-02 | 0.05 | –0.15 | –0.26 |
| Plateau Rosa | Dec-02 | –0.02 | 0.00 | –0.05 |
| HMS | Feb-03 | 0.06 | –0.21 | –0.06 |
| EC | May-05 | 0.06 | –0.05 | –0.06 |
| Penn State Univ. | Sep-05 | 0.09 | –0.07 | –0.05 |
| Univ. Heidelberg | Sep/Oct-02 | –0.01 | –0.06 | –0.06 |
| UBA | Oct-02 | 0.05 | –0.11 | –0.21 |
| LSCE | Nov/Dec-02 | 0.10 | 0.03 | 0.05 |
| FMI | Jan-03 | –0.02 | –0.04 | –0.14 |
| Univ. Groningen | Oct/Nov-03 | 0.01 | 0.02 | 0.04 |
| MPI-BGC | Nov/Dec-03 | 0.04 | 0.02 | –0.02 |
| HMS | Mar-04 | –0.19 | –0.36 | –0.59 |
| NIWA | May-05 | –0.08 | –0.08 | –0.09 |
| CSIRO | Sep/Oct-05 | –0.01 | –0.03 | –0.08 |
| Cape Point | Dec-05 | –0.02 | –0.09 | –0.18 |
| NCAR | May/Jun-06 | 0.07 | –0.04 | –0.04 |

Table 3. Status of standard scales and calibration/intercomparison for CO₂ at laboratories.

| Laboratory | WDCGG Filename Code | Calibration Scale | WMO Inter-comparison |
|--------------------|---|--------------------------|-----------------------------|
| AEMET | IZO128N0000 | WMO | 91/92, 96/97, 99/00 |
| Aichi | MKW234N0000 | WMO | |
| AIST | TKY236N0000 | AIST | 96/97, 99/00, 02/06 |
| BoM & CSIRO | CGO540S0000,CGO540S0010 | WMO | |
| CMA | WLG236N0000 | WMO | 96/97, 99/00, 02/06 |
| CNR-ICES & DNA-IAA | JBN762S0000 | WMO | |
| CSIRO | ALT482N0003, CFA519S0003, CGO540S0003, CRI215N0000, CYA766S0001, ESP449N0003, MAA767S0003, MLO519N0003, MQA554S0003, SIS660N0003, SPO789S0003 | WMO | 91/92, 96/97, 99/00, 02/06 |
| EC | ALT482N0000, ALT482N0005, CDL453N0000,CHM449N0000, CSJ451N0000, EGB444N0100 , ESP449N0000, ETL454N0000 , FSD449N0000, LLB454N0100, WSA443N0000, WSA443N0001 | WMO | 91/92, 96/97, 99/00, 02/06 |
| EMA | CAI130N0000 | | |
| Empa | JFJ646N0000 | WMO | |
| ENEA | LMP635N0001 | WMO | 91/92, 96/97, 99/00, 02/06 |
| FMI | PAL667N0000 | WMO | 02/06 |
| HKO | HKG222N0001, HKO222N0001 | WMO | |
| | HKO222N0000 | NIST | |
| HMS | HUN646N0000, KPS646N0000 | WMO | 91/92, 96/97, 99/00, 02/06 |
| IAFMS | CMN644N0000 | WMO | 91/92, 96/97, 02/06 |
| IGP | HUA312S0000 | WMO | |
| IMK-IFU | WNK647N0000, ZUG647N0014 | WMO | 99/00 |
| INRNE | BEO642N0000 | WMO | |
| IOEP | DIG654N0000 | | |
| ITM | ZEP678N0000 | WMO | 96/97, 99/00 |
| JMA | MNM224N0000, RYO239N0000, YON224N0000 | WMO | 91/92, 96/97, 99/00, 02/06 |
| KMA | AMY236N0000 | KRISS | 02/06 |
| KSNU | ISK242N0000 | | |
| KUP | JFJ646N0003 | WMO | |
| LSCE | AMS137S0000, BGU641N0000, FIK635N0000, LPO648N0000, MHD653N0002, PDM642N0000, PUY645N0000 | WMO | 91/92, 96/97, 99/00, 02/06 |
| MGO | BER255N0001, KOT276N0001, KYZ240N0001, STC652N0001, TER669N0001 | WMO | |
| MMD | DMV504N0000 | WMO | |
| MRI | TKB236N0002 | | 91/92, 96/97, 99/00, 02/06 |

| | | | |
|---------------------|---|------|---|
| NIER | GSN233N0103 | WMO | |
| NIES | COI243N0000, HAT224N0000 | NIES | 96/97, 99/00, 02/06 |
| NIMR | GSN233N0001 | WMO | 96/97 |
| NIPR & Tohoku Univ. | SYO769S0000 | | Tohoku Univ.:91/92, 96/97, 99/00, 02/06 |
| NIWA | BHD541S0000 | WMO | 91/92, 96/97, 99/00, 02/06 |
| NMA | FDT645N0002 | | |
| NOAA/ESRL | BRW471N0000, MLO519N0000, SMO514S0000, SPO789S0000, NOAA/ESRL flask network* | WMO | 91/92, 96/97, 99/00, 02/06 |
| Osaka Univ. | SUI234N0000 | | |
| RIVM | KMW653N0000 | NIST | |
| RSE | PRS645N0000 | WMO | 99/00, 02/06 |
| Saitama | DDR236N0000, KIS236N0000, URW235N0000 | WMO | |
| SAWS | CPT134S0000 | WMO | 99/00, 02/06 |
| Shizuoka Univ. | HMM234N0000 | | |
| UBA | BRT648N0000, DEU649N0000, LGB652N0000, NGL653N0000, SNB647N0000, SSL647N0000, SSL647N0002, WES654N0000, ZGT654N0000, ZSF647N0010, ZUG647N0000 | WMO | 91/92, 96/97, 99/00, 02/06 |

* NOAA/ESRL flask network:

ABP312S0001,ALT482N0001,AMS137S0001,ASC107S0001,ASK123N0001,AVI417N0001,AZR638N0001,BAL655N0001,BHD541S0001, BKT500S0001,BME432N0001,BMW432N0001,BRW471N0001,BSC644N0001,CBA455N0001,CGO540S0001,CHR501N0001,CMO445N0001, CRZ146S0001,EIC327S0001,GMI513N0001,GOZ636N0001,HBA775S0001,HPB647N0003,HUN646N0001,ICE663N0001,ITN435N0001, IZO128N0001,KCO204N0001,KEY425N0001,KUM519N0001,KZD244N0001,KZM243N0001,LEF445N0001,LLB454N0001,LLN223N0001, LMP635N0003,MBG476N0001,MEX419N0001,MHD653N0001,MID528N0001,MKN100S0001,MLO519N0001,NMB123S0001,NWR440N0101, OPW448N0001,PAL667N0001,POC900N0001,POC905N0001,POC905S0001,POC910N0001,POC910S0001,POC915N0001,POC915S0001, POC920N0001,POC920S0001,POC925N0001,POC925S0001,POC930N0001,POC930S0001,POC935S0001,PSA764S0001,PTA438N0001, RPB413N0001,SCS903N0001,SCS906N0001,SCS909N0001,SCS912N0001,SCS915N0001,SCS918N0001,SCS921N0001,SEY104S0001, SGP436N0001,SHM452N0001,SMO514S0001,SPO789S0001,STC654N0001,STM666N0001,SUM672N0001,SYO769S0001,TAP236N0001, TDF354S0001,THD441N0001,UTA439N0001,UUM244N0001,WIS631N0001,WLG236N0001,ZEP678N0001

3. Methane (CH₄)

The GAW programmes have established two WCCs for CH₄, the Swiss Federal Laboratory for Materials Testing and Research (Empa), Dübendorf, Switzerland; and the Japan Meteorological Agency (JMA), Tokyo, Japan [WMO, 2007]. In addition, the Central Calibration Laboratory for CH₄ has been established at NOAA/ESRL [Dlugokencky, *et. al.*, 2005; WMO, 2007].

The NOAA04 scale has been designated as the Primary Standard of the GAW programme. This scale results in CH₄ mole fractions that are a factor of 1.0124 higher than the previous NOAA scale [Dlugokencky *et al.*, 2005].

Table 4 summarises the methane standard scales used by laboratories contributing to the WDCGG and lists tentative multiplying conversion factors applied for analysis in this issue of the *Data Summary*. The

standard is the NOAA04 scale, and conversion factors were calculated from the results of comparisons with other laboratories performed bilaterally or multilaterally before the establishment of the GAW Standard.

The former CMDL scale is lower than an absolute gravimetric scale [Aoki *et al.*, 1992] by ~1.5% [Dlugokencky *et al.*, 1994] and lower than the AES (Atmospheric Environment Service, currently EC) scale by a factor of 1.0151 [Worthy *et al.*, 1998]. The former CMDL scale can be converted to the Tohoku University standard by multiplying by 1.0121 [Dlugokencky *et al.*, 2005]. The conversion factors 1.0124 / 1.0151 = 0.9973 and 1.0124 / 1.0121 = 1.0003 have been adopted for comparisons with the NOAA04 scale.

Table 4. Status of the standard scales of CH₄ at laboratories with conversion factors.

| Laboratory | WDCGG Filename Code | Calibration Scale | Conversion Factor |
|------------|---|-------------------|-------------------|
| AEMET | IZO128N0000 | NOAA04 | 1 |
| AGAGE | CGO540S0011, CGO540S0013, CMO445N0011, MHD653N0011, MHD653N0013, RPB413N0000, RPB413N0011, SMO514S0014, SMO514S0016, THD441N0000 | Tohoku Univ. | 1.0003 |
| CHMI | KOS649N0000 | CHMI | 0.9973 |
| CMA | WLG236N0000 | NOAA04 | 1 |
| CSIRO | ALT482N0003, CFA519S0003, CGO540S0003, CRI215N0000, CYA766S0001, ESP449N0003, MAA767S0003, MLO519N0003, MQA554S0003, SIS660N0003, SPO789S0003 | NOAA04 | 1 |
| EC | ALT482N0000, CDL453N0000, CHM449N0000, EGB444N0100, ESP449N0000, ETL454N0000, FSD449N0000, LLB454N0100, WSA443N0000 | NOAA04 | 1 |
| Empa | JFJ646N0000 | NOAA04 | 1 |
| ENEA | LMP635N0001 | NOAA04 | 1 |
| FMI | PAL667N0000 | NOAA04 | |
| ISAC | CMN644N0000 | NOAA04 | 1 |
| JMA | MNM224N0000, RYO239N0000, YON224N0000 | NOAA04 | 1 |
| KMA | AMY236N0000 | KRISS | |
| KSNU | ISK242N0000 | | |
| LSCE | AMS137S0002, BGU641N0000, LPO648N0000, PDM642N0000, PUY645N0001 | NOAA83 | 1.0124 |
| | FIK635N0000, MHD653N0007 | | |
| MGO | TER669N0001 | NOAA04 | 1 |
| MRI | TKB236N0000 | | 0.9973 |
| NIER | GSN233N0103 | NOAA04 | 1 |
| NIES | COI243N0000, HAT224N0000 | NIES | 0.9973 |
| NIMR | GSN233N0001 | SIO X97 | |
| NOAA/ESRL | BRW471N0000, MLO519N0000, NOAA/ESRL flask network* | NOAA04 | 1 |
| | KPA431N0001, LEF445N0001, MCM777S0001, NZL543S0001, POC935S0001, SGI354S0001, SIO432N0001 | NOAA/CMDL | 1.0124 |
| RIVM | KMW653N0000 | NIST | 0.9973 |
| RSE | PRS645N0000 | NOAA04 | 1 |
| SAWS | CPT134S0000 | NOAA04 | 1 |
| UBA | DEU649N0000, NGL653N0000, SSL647N0000, ZGT654N0000, ZSF647N0010, ZUG647N0000 | NOAA04 | 1 |

* NOAA/ESRL flask network:

ABP312S0001,ALT482N0001,AMS137S0001,ASC107S0001,ASK123N0001,AVI417N0001,AZR638N0001,BAL655N0001,BKT500S0001, BME432N0001,BMW432N0001,BRW471N0001,BSC644N0001,CBA455N0001,CGO540S0001,CHR501N0001,CMO445N0001,CRZ146S0001, EIC327S0001,GMI513N0001,GOZ636N0001,HBA775S0001,HPB647N0003,HUN646N0001,ICE663N0001,ITN435N0001,IZO128N0001, KEY425N0001,KUM519N0001,KZD244N0001,KZM243N0001,LLB454N0001,LLN223N0001,LMP635N0003,MBC476N0001,MEX419N0001, MHD653N0001,MID528N0001,MKN100S0001,MLO519N0001,NMB123S0001,NWR440N0101,OPW448N0001,OXK650N0001,PAL667N0001, POC900N0001,POC905N0001,POC905S0001,POC910N0001,POC910S0001,POC915N0001,POC915S0001,POC920N0001,POC920S0001, POC925N0001,POC925S0001,POC930N0001,POC930S0001,PSA764S0001,PTA438N0001,RPB413N0001,SCS903N0001,SCS906N0001, SCS909N0001,SCS912N0001,SCS915N0001,SCS918N0001,SCS921N0001,SEY104S0001,SGP436N0001,SHM452N0001,SMO514S0001, SPO789S0001,STM666N0001,SUM672N0001,SYO769S0001,TAP236N0001,TDF354S0001,THD441N0001,UTA439N0001,UUM244N0001, WIS631N0001,WKT431N0001, WLG236N0001,ZEP678N0001

4. Nitrous Oxide (N₂O)

The Halocarbons and other Atmospheric Trace Species (HATS) Group of NOAA/ESRL maintains a set of standards for N₂O [Hall *et al.*, 2001]. The NOAA-2006 N₂O scale [Hall *et al.*, 2007] has been designated as the Primary Standard of the GAW programme. This group analyses the standards of laboratories, including those of Environment Canada (EC) and the Australian Commonwealth Scientific and Industrial Research Organisation (CSIRO). The Fraunhofer Institut für Atmosphärische Umweltforschung (IFU) in Garmisch-Partenkirchen,

Germany, serves as the GAW WCC.

The SIO-98 scale is essentially equivalent to the NOAA-2006 scale, with an average difference of 0.01% over the range of 299–319 ppb; the NOAA-2000 scale can be converted to the 2006 scale by using the factor 0.99402 [Hall *et al.*, 2007]. A constant ratio of 1.0017 between CSIRO and AGAGE data was used by Huang *et al.* (2008), and a factor of $1 / 1.0017 = 0.9983$ has been used in this report to convert CSIRO scale to the NOAA-2006 scale.

Table 5. Status of the standard scales of N₂O at laboratories.

| Laboratory | WDCGG Filename Code | Calibration Scale | Conversion Factor |
|--------------|---|-------------------|-------------------|
| AEMET | IZO128N0000 | NOAA-2006 | 1 |
| AGAGE | ADR651N0010, CGO540S0011, CGO540S0012, CGO540S0013, CMO445N0010, CMO445N0011, MHD653N0011, MHD653N0013, RPB413N0000, RPB413N0010, RPB413N0011, SMO514S0014, SMO514S0015, SMO514S0016, THD441N0000 | SIO 1998 | 1 |
| CSIRO | ALT482N0003, CFA519S0003, CGO540S0003, CRI215N0000, CYA766S0001, ESP449N0003, MAA767S0003, MLO519N0003, MQA554S0003, SIS660N0003, SPO789S0003 | NOAA-2006 | 1 |
| Empa | JFJ646N0000 | SIO 1998 | 1 |
| ENEA | LMP635N0001 | NOAA-2006 | 1 |
| ISAC | CMN644N0000 | NOAA-2006 | 1 |
| JMA | RYO239N0000 | NOAA-2006 | 1 |
| KMA | AMY236N0000 | KRISS | |
| MRI | MMB243N0000 | | |
| Nagoya Univ. | NGY235N0000 | | |
| NIER | GSN233N0103 | NOAA-2006 | 1 |
| NIES | HAT224N0000 | | |
| NILU | ZEP678N0000 | | |
| NIMR | GSN233N0001 | WMO X97 | |
| NOAA/ESRL | ALT482N0001, BRW471N0001, BRW471N0011, CGO540S0001, KUM519N0001, MLO519N0001, MLO519N0011, NWR440N0001, NWR440N0011, SMO514S0001, SMO514S0011, SPO789S0001, SPO789S0011 | NOAA/CMDL | 0.999402 |

| | | | |
|-----------|---|-----------|----------|
| NOAA/ESRL | ALT482N0004, ALT482N0006, BRW471N0003, BRW471N0005, BRW471N0010, CGO540S0009, CGO540S0014, KUM519N0002, MHD653N0008, MLO519N0005, MLO519N0006, MLO519N0010, NWR440N0003, NWR440N0004, NWR440N0010, PSA764S0000, SMO514S0008, SMO514S0009, SMO514S0010, SPO789S0005, SPO789S0006, SPO789S0010, SUM672N0000, SUM672N0002, THD441N0002 | NOAA-2006 | 1 |
| SAWS | CPT134S0000 | NOAA/CMDL | 0.999402 |
| UBA | SSL647N0000, ZSF647N0010 | SIO 1998 | 1 |

5. Surface Ozone (O₃)

The National Institute of Standards and Technology (NIST) has developed and deployed Standard Reference Photometers (SRPs) in the USA and other countries. The GAW has designated SRP #2 maintained by NIST as the Primary Standard for the GAW programme, making NIST the CCL for O₃. The Swiss Federal Laboratory for Materials Testing and Research (Empa) maintains NIST SRP #15 as the reference and is the GAW WCC for surface ozone

[Hofer *et al.*, 1998]. The traceability and uncertainty of O₃ within the GAW network were reported by Klausen *et al.*, (2003). Regional Calibration Centres have been established at the Solar and Ozone Observatory, Hradec Kralove, Czech Republic, and Observatorio Central Buenos Aires, Argentina [WMO, 2007]. The former maintains SRP #17 directly purchased from NIST.

Table 6. Status of surface ozone standard scales at laboratories

| Laboratory | WDCGG Filename Code | Calibration Scale | Audit Empa-WCC |
|-------------|--|----------------------|--------------------|
| AEMET | IZO128N0000 | WMO (NIST & Empa) | 96, 98, 00, 04 |
| | DON637N0000, MHN639N0000, NIA642N0000, ROQ640N0000, SPM639N0000 | NPL (U. K.) | |
| AQRB | ALG447N0000, BRA450N0000, CHA446N0000, EGB444N0000, ELA449N0000, EST451N0000, KEJ444N0000, SAT448N0000 | | |
| AWI | NMY770S0000 | | |
| BMKG & Empa | BKT500S0000 | WMO (NIST & Empa) | 99, 01, 04, 07, 08 |
| BoM & CSIRO | CGO540S0000 | WMO (NIST & Empa) | 02 |
| CHMI | KOS649N0000 | WMO (NIST & Empa) | |
| DEFRA | EDM655N0000 | | |
| DWD | HPB647N0000 | WMO (NIST & Empa) | 97, 06 |
| EARS | IRB645N0000, KVK646N0000, KVV646N0000, ZRN646N0000 | WMO (NIST & Empa) | |
| EMA | CAI130N0000 | | |

| | | | |
|-------------|--|-----------------------------|----------------------------------|
| Empa | JFJ646N0000, PAY646N0000, RIG646N0000 | WMO (NIST & Empa) | Jungfrauoch: 99, 06 |
| Empa & KMD | MKN100S0000 | WMO (NIST & Empa) | |
| FMI | AHT662N0000, OUL666N0000, PAL667N0000, UTO659N0000, VIR660N0000 | | Pallas-Sammaltunturi: 97, 03, 07 |
| HMS | KPS646N0000 | WMO (NIST & Empa) | |
| IM | ANG638N0000, BEJ638N0000, CAS639N0000, FUN132N0000, LIS638N0000, MVH638N0000, PEN640N0000 | | |
| INRNE | BEO642N0000 | WMO (NIST & Empa) | |
| IOEP | DIG654N0000 | WMO (NIST & Empa) | |
| ISAC | CMN644N0000, PYR227N0000 | WMO (NIST & Empa) | |
| IVL | VDL664N0000 | Stockholm Univ. (Sweden) | |
| JMA | MNM224N0000, RYO239N0000, SYO769S0002, TKB236N1004, YON224N0000 | WMO (NIST & Empa) | Ryori: 05 |
| KSNU | ISK242N0000 | | |
| LEGMA | DBL656N0000, RCV656N0000, ZSN657N0000 | WMO (NIST & Empa) | |
| MMD | DMV504N0000, TAR504N0000 | | |
| NILU | ZEP678N0000 | WMO (NIST & Empa) | 97, 01, 05 |
| NIWA | BHD541S0000 | WMO (NIST & Empa) | |
| NMA | FDT645N0002 | | |
| NOAA/ESRL | ARH777S0000, BMW432N0004, BRW471N0004, ICE663N0004, LAU545S0004, MCM777S0004, MLO519N0004, NWR440N0002, NWR440N0204, RPB413N0004, SMO514S0004, SPO789S0004, SUM672N0004, THD441N0004 | WMO (NIST & Empa) | Mauna Loa: 03 Barrow: 08 |
| NUI | MHD653N0000 | WMO (NIST & Empa) | 96, 98, 02, 05 |
| ONM | ASK123N0000 | WMO (NIST & Empa) | 03, 07 |
| PolyU | HKG222N0000 | | |
| RIVM | KMW653N0001, KMW653N0002 | | |
| Roshydromet | DAK654N0000, SHP659N0000 | | |
| RSE | PRS645N0000 | | |
| SAWS | CPT134S0000 | WMO (NIST & Empa) | 97, 98, 02, 06 |

| | | | |
|-------------|--|----------------------|--|
| SMN | USH354S0000,USH354S0001 | WMO (NIST & Empa) | 98, 03 |
| UBA | BRT648N0000, DEU649N0000, LGB652N0000, NGL653N0000, SNB647N0000, SSL647N0000, WES654N0000, ZGT654N0000, ZSF647N0010, ZUG647N0000 | WMO (NIST & Empa) | Zugspitze: 96, 97, 01 Sonnblick: 98 Zugspitze/Schneefern erhaus: 06 |
| Univ. Malta | GLH636N0000 | UMEG | |
| Univ. York | CVO116N0001 | NPL | |

6. Carbon Monoxide (CO)

The Swiss Federal Laboratory for Materials Testing and Research (Empa) serves as the WCC under GAW based on its secondary standards calibrated against the

standard at NOAA/ESRL designated as the Primary Standard for GAW.

Table 7. Status of carbon monoxide standard scales at laboratories

| Laboratory | WDCGG Filename Code | Calibration Scale | Audit Empa-WCC |
|-------------|---|--------------------------------|------------------------|
| AEMET | IZO128N0000 | WMO 2004 (NOAA/ESRL & Empa) | |
| AGAGE | CGO540S0011, MHD653N0011 | CSIRO | |
| BMKG & Empa | BKT500S0000 | WMO 2000 (NOAA/ESRL & Empa) | |
| CHMI | KOS649N0000 | CHMI | |
| CSIRO | ALT482N0003, CFA519S0003, CGO540S0003, CRI215N0000, CYA766S0001, ESP449N0003, MAA767S0003, MLO519N0003, MQA554S0003, SIS660N0003, SPO789S0003 | CSIRO | Cape Grim: 02 |
| DWD | HPB647N0000 | WMO (NOAA/ESRL & Empa) | 06 |
| EARS | KVV646N0000 | CHMI | |
| EC | ALT482N0000,CDL453N0000, CHM449N0000, EGB444N0100, ESP449N0000, ETL454N0000, FSD449N0000, LLB454N0100, WSA443N0000 | WMO (NOAA/ESRL & Empa) | |
| Empa | JFJ646N0000, PAY646N0000, RIG646N0000 | WMO 2000 (NOAA/ESRL & Empa) | Jungfraujoch: 99,06 |
| Empa & KMD | MKN100S0000 | WMO 2000 (NOAA/ESRL & Empa) | |
| INRNE | BEO642N0000 | WMO (NOAA/ESRL & Empa) | |
| ISAC | CMN644N0000, CMN644N0001 | WMO 2004 (NOAA/ESRL & Empa) | |
| JMA | MNM224N0001,RYO239N0001, YON224N0001 | JMA | |
| | MNM224N0002, RYO239N0002, YON224N0002 | WMO 2000 (NOAA/ESRL) | Ryori:05 |
| LSCE | AMS137S0000 | WMO 2004 (NOAA/ESRL & Empa) | |

| | | | |
|-------------|---|--------------------------------|--------------------------------|
| NOAA/ESRL | NOAA/ESRL flask network* | WMO (NOAA/ESRL & Empa) | Mauna Loa: 03 Barrow: 08 |
| PolyU | HKG222N0000 | | |
| RIVM | KMW653N0000, KTB653N0000 | | |
| SAWS | CPT134S0000 | WMO (NOAA/CMDL) | 98, 02, 06 |
| SMN | USH354S0000, USH354S0001 | WMO (NOAA/ESRL & Empa) | 98, 03 |
| UBA | NGL653N0000, SNB647N0000, SSL647N0000, ZUG647N0000 | WMO (NOAA/CMDL) | Zugspitze: 01 Sonnblick: 98 |
| Univ. Malta | GLH636N0000 | | |
| Univ. York | CVO116N0001 | WMO 2000 (NOAA/ESRL & Empa) | |

NOAA/ESRL flask network:

ALT482N0001,ASC107S0001,ASK123N0001,AZR638N0001,BAL655N0001,BHD541S0001,BKT500S0001,BME432N0001,BMW432N0001, BRW471N0001,BSC644N0001,CBA455N0001,CGO540S0001,CHR501N0001,CMO445N0001,CRZ146S0001,EIC327S0001,GMI513N0001, GOZ636N0001,HBA775S0001,HPB647N0003,HUN646N0001,ICE663N0001,ITN435N0001,IZO128N0001,KEY425N0001,KUM519N0001, KZD244N0001,KZM243N0001,LEF445N0001,LLN223N0001,LMP635N0003,MB476N0001,MHD653N0001,MID528N0001,MLO519N0001, NMB123S0001,NWR440N0101,OXK650N0001,PAL667N0001,POC900N0001,POC905N0001,POC905S0001,POC910N0001,POC910S0001, POC915N0001,POC915S0001,POC920N0001,POC920S0001,POC925N0001,POC925S0001,POC930N0001,POC930S0001,POC935N0000, POC935S0001,PSA764S0001,PTA438N0001,RPB413N0001,SCS903N0001,SCS906N0001,SCS909N0001,SCS912N0001,SCS915N0001, SCS918N0001,SCS921N0001,SEY104S0001,SGP436N0001,SHM452N0001,SMO514S0001,SPO789S0001,STM666N0001,SYO769S0001, TAP236N0001,TDF354S0001,THD441N0001,UTA439N0001,UUM244N0001,WIS631N0001,WLG236N0001,ZEP678N0001

References

- Aoki, S., T. Nakazawa, S. Murayama and S. Kawaguchi, Measurements of atmospheric methane at the Japanese Antarctic station, Syowa, *Tellus, Ser. B*, **44**, 273–281, 1992.
- CMDL, Climate Monitoring and Diagnostics Laboratory Summary Report No.26 2000-2001, 2002.
- Cunnold, D. M., L. P. Steele, P. J. Fraser, P. G. Simmonds, R. G. Prinn, R. F. Weiss, L. W. Porter, S. O'Doherty, R. L. Langenfelds, P. B. Krummel, H. J. Wang, L. Emmons, X. X. Tie, and E. J. Dlugokencky, In situ measurements of atmospheric methane at GAGE/AGAGE sites during 1985–2000 and resulting source inferences, *J. Geophys. Res.*, **107(D14)**, 10.1029/2001JD001226, 2002.
- Dlugokencky, E. J., L. P. Steele, P. M. Lang, and K. A. Masarie, The growth rate and distribution of atmospheric methane, *J. Geophys. Res.*, **99**, 17021-17043, 1994.
- Dlugokencky, E. J., R. C. Myers, P. M. Lang, K. A. Masarie, A. M. Crotwell, K. W. Thoning, B. D. Hall, J. W. Elkins, and L. P. Steele, Conversion of NOAA atmospheric dry air CH₄ mole fractions to a gravimetrically prepared standard scale, *J. Geophys. Res.*, **110**, D18306, doi: 10.1029/2005JD006035, 2005.
- Hall, B. D. (ed.), J. W. Elkins, J. H. Butler, S. A. Montzka, T. M. Thompson, L. Del Negro, G. S. Dutton, D. F. Hurst, D. B. King, E. S. Kline, L. Lock, D. Mactaggart, D. Mondeel, F. L. Moore, J. D. Nance, E. A. Ray, and P. A. Romashkin, Halocarbons and Other Atmospheric Gases, Section 5 in Climate Monitoring and Diagnostics Laboratory, Summary Report N. 25, 1998–1999, R. S. Schnell, D. B. King, R. M. Rosson (eds.), NOAA-CMDL, Boulder, CO., USA, 2001.
- Hall, B. D., G. S. Dutton, and J. W. Elkins, The NOAA nitrous oxide standard scale for atmospheric observations, *J. Geophys. Res.*, **112**, D09305, doi:10.1029/2006JD007954, 2007.
- Hofer, P., B. Buchmann and A. Herzog, Traceability, Uncertainty and Assessment Criteria of Surface Ozone Measurements, *EMPA-WCC Report* 98/5, 20 pp, 1998.
- Huang, J., A. Golombek, R. Prinn, R. Weiss, P. Fraser, P. Simmonds, E. J. Dlugokencky, B. Hall, J. Elkins, P. Steele, R. Langenfelds, P. Krummel, G. Dutton, and L. Porter, Estimation of regional emissions of nitrous oxide from 1997 to 2005 using multinetowrk measurements, a chemical transport model, and an inverse method, *J. Geophys. Res.*, **113**, D17313, doi:10.1029/2007JD009381, 2008.
- Klausen, J., C. Zellweger, B. Buchmann, and P. Hofer, Uncertainty and bias of surface ozone measurements at selected Global Atmosphere Watch sites, *J. Geophys. Res.*, **108(D19)**, 4622,

doi:10.1029/2003JD003710, 2003.

WMO, Report of the Eleventh WMO/IAEA Meeting of Experts on Carbon Dioxide Concentration and Related Tracer Measurement Techniques, Global Atmosphere Watch Report Series No.148, 2003.

WMO, WMO Global Atmosphere Watch (GAW) Strategic Plan: 2008–2015, WMO/GAW Report No. 172, 104pp, 2007.

Worthy, D. E. J., I. Levin, N. B. A. Trivett, A. J. Kuhlmann, J. F. Hopper and M. K. Ernst, Seven years of continuous methane observations at a remote boreal site in Ontario, Canada, *J. Geophys. Res.*, **103**, 15995–16007,

1998.

Zhao, C. L., P. P. Tans, and K. W. Thoning, A high precision manometric system for absolute calibrations of CO₂ in dry air, *J. Geophys. Res.*, **102**, 5885–5894, 1997.

Zhou, L. X., D. Kitzis, P. P. Tans, “Report of the fourth WMO round-robin reference gas intercomparison, 2002–2007” in the report of the 14th WMO/IAEA meeting of experts on carbon dioxide, other greenhouse gases and related tracers measurement techniques, Helsinki, Finland, 10–13 September 2007, edited by T. Laurila, WMO/GAW Report No. 186, 2009

LIST OF ABBREVIATIONS IN THE CALIBRATION AND STANDARD SCALES

| | |
|-----------------|---|
| AEMET | Agencia Estatal de Meteorología (Spain) |
| AGAGE | Advanced Global Atmospheric Gases Experiment |
| Aichi | Aichi Prefecture (Japan) |
| AIST | National Institute of Advanced Industrial Science and Technology (Japan) |
| AQRB | Air Quality Research Branch, Meteorological Service of Canada (Canada) |
| AWI | Alfred Wegener Institute for Polar and Marine Research (Germany) |
| BMKG | Agency for Meteorology, Climatology and Geophysics (Indonesia) |
| BoM | Commonwealth Bureau of Meteorology (Australia) |
| CHMI | Czech Hydrometeorological Institute (Czech Republic) |
| CMA | China Meteorological Administration (China) |
| CNR-ICES | International Center for Earth Sciences, Consiglio Nazionale delle Ricerche (Italy) |
| CSIRO | Commonwealth Scientific and Industrial Research Organisation (Australia) |
| DEFRA | Department for Environment, Food and Rural Affairs (United Kingdom) |
| DNA-IAA | Dirección Nacional del Antártico-Instituto Antártico Argentino (Argentina) |
| DWD | Deutscher Wetterdienst (German Meteorological Service, Germany) |
| EARS | Environmental Agency of the Republic of Slovenia |
| EC | Environment Canada (Canada) |
| EMA | Egyptian Meteorological Authority (Egypt) |
| Empa | Swiss Federal Laboratories for Material Testing and Research (Switzerland) |
| ENEA | Italian National Agency for New Technology, Energy and the Environment (Italy) |
| FMI | Finnish Meteorological Institute |
| GAGE | Global Atmospheric Gases Experiment |
| GAW | Global Atmosphere Watch (WMO) |
| HATS | Halocarbons and other Atmospheric Trace Species Group, NOAA/ESRL |
| HKO | Hong Kong Observatory (Hong Kong, China) |
| HMS | Hungarian Meteorological Service (Hungary) |
| IAFMS | Italian Air Force Meteorological Service (Italy) |
| IEK-8 | Institute for Energy and Climate Research: Troposphere (IEK-8), Research Center Juelich GmbH (Germany) |
| IGP | Instituto Geofísico del Perú (Peru) |
| IM | Instituto de Meteorologia (Portugal) |
| IMK-IFU | Institut für Meteorologie und Klimatologie, Atmosphärische Umweltforschung, Forschungszentrum Karlsruhe (Germany) |
| INMH | National Meteorological Administration (Romania) |
| INRNE | Institute for Nuclear Research and Nuclear Energy (Bulgaria) |
| IOEP | Institute of Environmental Protection (Poland) |
| ISAC | Istituto di Scienze dell'Atmosfera e del Clima, Consiglio Nazionale delle Ricerche (Italy) |
| ITM | Department of Applied Environmental Science, Stockholm University, (Sweden) |
| IVL | Swedish Environmental Research Institute, Göteborg (Sweden) |
| JMA | Japan Meteorological Agency (Japan) |
| KMA | Korea Meteorological Administration (Republic of Korea) |
| KMD | Kenya Meteorological Department (Kenya) |
| KRISS | Korea Research Institute of Standards and Science (Republic of Korea) |
| KSNU | Kyrgyz State National University (Kyrgyzstan) |
| KUP | Physics Institute, Climate and Environmental Physics, University of Bern |

| | |
|-----------------------|--|
| | (Switzerland) |
| LEGMA | Latvian Environment, Geology and Meteorology Agency (Latvia) |
| LSCE | Laboratoire des Sciences du Climat et de l'Environnement (France) |
| MGO | Main Geophysical Observatory, Roshydromet (Russian Federation) |
| MPI-BGC | Max-Planck Institute (MPI) for Biogeochemistry in Jena (Germany) |
| MMD | Malaysian Meteorological Department |
| MRI | Meteorological Research Institute, JMA (Japan) |
| Nagoya Univ. | Nagoya University (Japan) |
| NIER | National Institute of Environmental Research (Republic of Korea) |
| NIES | National Institute for Environmental Studies (Japan) |
| NILU | Norwegian Institute for Air Research (Norway) |
| NIMR | National Institute of Meteorological Research, KMA (Republic of Korea) |
| NIPR | National Institute of Polar Research (Japan) |
| NIST | National Institute of Standards and Technology (USA) |
| NIWA | National Institute of Water & Atmospheric Research (New Zealand) |
| NMA | National Meteorological Administration (Romania) |
| NOAA/ESRL | Earth System Research Laboratory, NOAA (USA) |
| NPL | National Physical Laboratory (United Kingdom) |
| NUI | National University of Ireland, Galway (Ireland) |
| ONM | Office National de la Météorologie (Algeria) |
| Osaka Univ. | Osaka University (Japan) |
| PolyU | Hong Kong Polytechnic University (Hong Kong, China) |
| RIVM | National Institute for Health and Environment (Netherlands) |
| Roshydromet | Federal Service for Hydrometeorology and Environmental Monitoring (Russian Federation) |
| RSE | Ricerca sul Sistema Elettrico (Italy) |
| Saitama | Saitama Prefecture (Japan) |
| SAWS | South African Weather Service (South Africa) |
| Shizuoka Univ. | Shizuoka University (Japan) |
| SMN | Servicio Meteorológico Nacional (Argentina) |
| Tohoku Univ. | Tohoku University (Japan) |
| UBA | Umweltbundesamt (Germany) |
| Univ. Malta | University of Malta (Malta) |
| Univ. York | University of York (United Kingdom of Great Britain and Northern Ireland) |
| WDCGG | World Data Centre for Greenhouse Gases, operated by JMA, Japan (WMO) |
| WMO | World Meteorological Organization |

LIST OF OBSERVING STATIONS

| Station | Country/Territory | Index Number | Latitude (° ') | Location Longitude (° ') | Altitude (m) | Parameter |
|------------------------|--|--------------|-------------------|--------------------------------|-----------------|---|
| REGION I (Africa) | | | | | | |
| Amsterdam Island | France | AMS137S00 | 37 47 S | 77 31 E | 55 | CH ₄ , CO, CO ₂ , VOCs |
| Amsterdam Island | France | AMS137S00 | 37 47 S | 77 31 E | 55 | CH ₄ , CO ₂ |
| Ascension Island | United Kingdom of Great Britain and Northern Ireland | ASC107S00 | 7 55 S | 14 25 W | 54 | ¹³ CH ₄ , ¹³ CO ₂ , C ¹⁸ O ₂ , CH ₄ , CO, CO ₂ , H ₂ , VOCs |
| Assekrem | Algeria | ASK123N00 | 23 16 N | 5 37 E | 2710 | O ₃ |
| Assekrem | Algeria | ASK123N00 | 23 16 N | 5 37 E | 2710 | ¹³ CO ₂ , C ¹⁸ O ₂ , CH ₄ , CO, CO ₂ , H ₂ , VOCs |
| Cairo | Egypt | CAI130N00 | 30 04 N | 31 16 E | 35 | CO ₂ , O ₃ |
| Cape Point | South Africa | CPT134S00 | 34 21 S | 18 28 E | 230 | CH ₄ , CO, CO ₂ , N ₂ O, O ₃ |
| Cape Point | South Africa | CPT134S00 | 34 21 S | 18 28 E | 230 | CH ₄ , CO ₂ |
| Cape Verde Observatory | Cape Verde | CVO116N00 | 16 50 N | 24 52 W | 10 | CO, NO _x , O ₃ , VOCs |
| Crozet | France | CRZ146S00 | 46 27 S | 51 51 E | 120 | ¹³ CO ₂ , C ¹⁸ O ₂ , CH ₄ , CO, CO ₂ , H ₂ , VOCs |
| Funchal | Portugal | FUN132N00 | 32 38 N | 16 52 W | 58 | O ₃ |
| Gobabeb | Namibia | NMB123S00 | 23 34 S | 15 01 E | 461 | ¹³ CO ₂ , C ¹⁸ O ₂ , CH ₄ , CO, CO ₂ |
| Izaña (Tenerife) | Spain | IZO128N00 | 28 18 N | 16 30 W | 2367 | CH ₄ , CO, CO ₂ , N ₂ O, O ₃ , SF ₆ |
| Izaña (Tenerife) | Spain | IZO128N00 | 28 18 N | 16 30 W | 2367 | ¹³ CO ₂ , C ¹⁸ O ₂ , CH ₄ , CO, CO ₂ , H ₂ , VOCs |
| Mahe Island | Seychelles | SEY104S00 | 4 40 S | 55 10 E | 7 | ¹³ CO ₂ , C ¹⁸ O ₂ , CH ₄ , CO, CO ₂ , H ₂ , VOCs |
| Mt. Kenya | Kenya | MKN100S00 | 0 03 S | 37 17 E | 3678 | CO, O ₃ |
| Mt. Kenya | Kenya | MKN100S00 | 0 03 S | 37 17 E | 3678 | ¹³ CO ₂ , C ¹⁸ O ₂ , CH ₄ , CO ₂ , VOCs |
| REGION II (Asia) | | | | | | |
| Anmyeon-do | Republic of Korea | AMY236N00 | 36 31 N | 126 19 E | 47 | CFCs, CH ₄ , CO ₂ , N ₂ O |
| Bering Island | Russian Federation | BER255N00 | 55 12 N | 165 58 E | 13 | CO ₂ |
| Cape Ochi-ishi | Japan | COI243N00 | 43 08 N | 145 30 E | 45 | CH ₄ , CO ₂ |
| Cape Rama | India | CRI215N00 | 15 04 N | 73 49 E | 60 | ¹³ CO ₂ , CH ₄ , CO, CO ₂ , H ₂ , N ₂ O |
| Everest - Pyramid | Nepal | PYR227N00 | 27 57 N | 86 48 E | 5079 | O ₃ |
| Gosan | Republic of Korea | GSN233N00 | 33 16 N | 126 10 E | 72 | CFCs, CH ₄ , CO ₂ , N ₂ O |
| Gosan | Republic of Korea | GSN233N01 | 33 10 N | 126 05 E | 72 | CFCs, CH ₄ , CO ₂ , N ₂ O |
| Hamamatsu | Japan | HMM234N00 | 34 43 N | 137 43 E | 35 | CO ₂ |
| Hateruma | Japan | HAT224N00 | 24 03 N | 123 47 E | 10 | CH ₄ , CO ₂ , N ₂ O |
| Hok Tsui | Hong Kong, China | HKG222N00 | 22 12 N | 114 15 E | 60 | CO ₂ |
| Hok Tsui | Hong Kong, China | HKG222N00 | 22 12 N | 114 15 E | 60 | CO, O ₃ |
| Issyk-Kul | Kyrgyzstan | ISK242N00 | 42 37 N | 76 58 E | 1640 | CH ₄ , CO ₂ , O ₃ |
| Kaashidhoo | Maldives | KCO204N00 | 4 58 N | 73 28 E | 1 | ¹³ CO ₂ , CH ₄ , CO ₂ |
| King's Park | Hong Kong, China | HKO222N00 | 22 18 N | 114 10 E | 65 | CO ₂ |
| Kisai | Japan | KIS236N00 | 36 04 N | 139 33 E | 13 | CO ₂ |
| Kotelny Island | Russian Federation | KOT276N00 | 76 00 N | 137 52 E | 5 | CO ₂ |
| Kyzylcha | Uzbekistan | KYZ240N00 | 40 52 N | 66 09 E | 340 | CO ₂ |
| Lulin | China | LLN223N00 | 23 28 N | 120 52 E | 2867 | ¹³ CO ₂ , C ¹⁸ O ₂ , CH ₄ , CO, CO ₂ |
| Memambetsu | Japan | MMB243N00 | 43 55 N | 144 11 E | 32.9 | N ₂ O |
| Mikawa-Ichinomiya | Japan | MKW234N00 | 34 51 N | 137 25 E | 50 | CO ₂ |
| Minamitorishima | Japan | MNM224N00 | 24 16 N | 153 58 E | 8 | CH ₄ , CO, CO ₂ , O ₃ |
| Mt. Dodaira | Japan | DDR236N00 | 36 00 N | 139 10 E | 840 | CO ₂ |
| Mt. Waliguan | China | WLG236N00 | 36 16 N | 100 54 E | 3810 | CH ₄ , CO ₂ |
| Mt. Waliguan | China | WLG236N00 | 36 16 N | 100 54 E | 3810 | ¹³ CH ₄ , ¹³ CO ₂ , C ¹⁸ O ₂ , CH ₄ , CO, CO ₂ , H ₂ |

LIST OF OBSERVING STATIONS (continued)

| Station | Country/Territory | Index Number | Location | | Altitude (m) | Parameter |
|--|-------------------|--------------|-------------------|--------------------|-----------------|--|
| | | | Latitude (° ') | Longitude (° ') | | |
| Nagoya | Japan | NGY235N00 | 35 08 N | 136 58 E | 35 | N ₂ O |
| Plateau Assy | Kazakhstan | KZM243N00 | 43 15 N | 77 52 E | 2519 | ¹³ CO ₂ , C ¹⁸ O ₂ , CH ₄ , CO, CO ₂ , H ₂ |
| Ryori | Japan | RYO239N00 | 39 01 N | 141 49 E | 260 | CCl ₄ , CFCs, CH ₃ CCl ₃ , CH ₄ , CO, CO ₂ , N ₂ O, O ₃ |
| Sary Taukum | Kazakhstan | KZD244N00 | 44 27 N | 75 34 E | 412 | ¹³ CO ₂ , C ¹⁸ O ₂ , CH ₄ , CO, CO ₂ , H ₂ |
| Shangdianzi | China | SDZ240N00 | 40 38 N | 117 06 E | 287 | CH ₄ , CO ₂ |
| Ship between Ishigaki Island and Hateruma Island | Japan | SIH224N00 | 24 07 N | 123 49 E | 5 | CO ₂ |
| South China Sea (03N) | N/A | SCS903N00 | 3 00 N | 105 00 E | 15 | ¹³ CO ₂ , C ¹⁸ O ₂ , CH ₄ , CO, CO ₂ , H ₂ |
| South China Sea (06N) | N/A | SCS906N00 | 6 00 N | 107 00 E | 15 | ¹³ CO ₂ , C ¹⁸ O ₂ , CH ₄ , CO, CO ₂ , H ₂ |
| South China Sea (09N) | N/A | SCS909N00 | 9 00 N | 109 00 E | 15 | ¹³ CO ₂ , C ¹⁸ O ₂ , CH ₄ , CO, CO ₂ , H ₂ |
| South China Sea (12N) | N/A | SCS912N00 | 12 00 N | 111 00 E | 15 | ¹³ CO ₂ , C ¹⁸ O ₂ , CH ₄ , CO, CO ₂ , H ₂ |
| South China Sea (15N) | N/A | SCS915N00 | 15 00 N | 113 00 E | 15 | ¹³ CO ₂ , C ¹⁸ O ₂ , CH ₄ , CO, CO ₂ , H ₂ |
| South China Sea (18N) | N/A | SCS918N00 | 18 00 N | 113 00 E | 15 | ¹³ CO ₂ , C ¹⁸ O ₂ , CH ₄ , CO, CO ₂ , H ₂ |
| South China Sea (21N) | N/A | SCS921N00 | 21 00 N | 114 00 E | 15 | ¹³ CO ₂ , C ¹⁸ O ₂ , CH ₄ , CO, CO ₂ , H ₂ |
| Suita | Japan | SUI234N00 | 34 49 N | 135 31 E | 63 | CO ₂ |
| Tae-ahn Peninsula | Republic of Korea | TAP236N00 | 36 43 N | 126 07 E | 20 | ¹³ CH ₄ , ¹³ CO ₂ , C ¹⁸ O ₂ , CH ₄ , CO, CO ₂ , H ₂ , VOCs |
| Takayama | Japan | TKY236N00 | 36 08 N | 137 25 E | 1420 | CO ₂ |
| Tsukuba | Japan | TKB236N00 | 36 02 N | 140 07 E | 26 | CH ₄ , CO ₂ |
| Tsukuba | Japan | TKB236N10 | 36 02 N | 140 07 E | 25 | O ₃ |
| Ulaan Uul | Mongolia | UUM244N00 | 44 27 N | 111 04 E | 914 | ¹³ CO ₂ , C ¹⁸ O ₂ , CH ₄ , CO, CO ₂ , H ₂ |
| Urawa | Japan | URW235N00 | 35 52 N | 139 35 E | 10 | CO ₂ |
| Yonagunijima | Japan | YON224N00 | 24 28 N | 123 01 E | 30 | CH ₄ , CO, CO ₂ , O ₃ |

REGION III (South America)

| | | | | | | |
|------------------|--|-----------|---------|----------|------|---|
| Arembepe | Brazil | ABP312S00 | 12 46 S | 38 10 W | 0 | CH ₄ , CO, CO ₂ , N ₂ O |
| Arembepe | Brazil | ABP312S00 | 12 46 S | 38 10 W | 0 | O ₃ |
| Arembepe | Brazil | ABP312S00 | 12 46 S | 38 10 W | 0 | ¹³ CO ₂ , C ¹⁸ O ₂ , CH ₄ , CO ₂ , VOCs |
| Bird Island | United Kingdom of Great Britain and Northern Ireland | SGI354S00 | 54 00 S | 38 02 W | 30 | CH ₄ , CO ₂ |
| Easter Island | Chile | EIC327S00 | 27 07 S | 109 27 W | 50 | ¹³ CO ₂ , C ¹⁸ O ₂ , CH ₄ , CO, CO ₂ , H ₂ , VOCs |
| Huancayo | Peru | HUA312S00 | 12 04 S | 75 31 W | 3313 | CO ₂ |
| Tierra del Fuego | Argentina | TDF354S00 | 54 52 S | 68 28 W | 20 | ¹³ CO ₂ , C ¹⁸ O ₂ , C ₂ Cl ₄ , CBrClF ₂ , CFCs, CH ₂ Cl ₂ , CH ₃ Br, CH ₃ CCl ₃ , CH ₃ Cl, CH ₄ , CO, CO ₂ , H ₂ , HCFCs, HFCs, VOCs |
| Ushuaia | Argentina | USH354S00 | 54 49 S | 68 17 W | 18 | CO, O ₃ |

REGION IV (North and Central America)

| | | | | | | |
|-------|--------|-----------|---------|---------|-----|---|
| Alert | Canada | ALT482N00 | 82 27 N | 62 31 W | 210 | ¹³ CO ₂ , CH ₄ , CO, CO ₂ , H ₂ , N ₂ O |
| Alert | Canada | ALT482N00 | 82 27 N | 62 31 W | 210 | CH ₄ , CO, CO ₂ , N ₂ O, SF ₆ |

LIST OF OBSERVING STATIONS (continued)

| Station | Country/Territory | Index Number | Location | | Altitude (m) | Parameter |
|----------------------------|-----------------------------|--------------|-------------------|--------------------|-----------------|--|
| | | | Latitude (° ') | Longitude (° ') | | |
| Alert | Canada | ALT482N00 | 82 27 N | 62 31 W | 210 | ¹³ CH ₄ , ¹³ CO ₂ , C ¹⁸ O ₂ , C ₂ Cl ₄ , CBrClF ₂ , CBrF ₃ , CCl ₄ , CFCs, CH ₂ Cl ₂ , CH ₃ Br, CH ₃ CCl ₃ , CH ₃ Cl, CH ₄ , CO, CO ₂ , H ₂ , HCFCs, HFCs, N ₂ O, SF ₆ , VOCs |
| Algoma | Canada | ALG447N00 | 47 01 N | 84 22 W | 411 | O ₃ |
| Argyle | United States of America | AMT445N00 | 45 01 N | 68 40 W | 50 | ¹³ CO ₂ , C ¹⁸ O ₂ , CH ₄ , VOCs |
| Barrow | United States of America | BRW471N00 | 71 19 N | 156 35 W | 11 | ¹³ CH ₄ , ¹³ CO ₂ , C ¹⁸ O ₂ , C ₂ Cl ₄ , CBrClF ₂ , CBrF ₃ , CCl ₄ , CFCs, CH ₂ Cl ₂ , CH ₃ Br, CH ₃ CCl ₃ , CH ₃ Cl, CH ₄ , CO, CO ₂ , H ₂ , HCFCs, HFCs, N ₂ O, O ₃ , SF ₆ , VOCs |
| Bratt's Lake | Canada | BRA450N00 | 50 12 N | 104 42 W | 595 | O ₃ |
| Candle Lake | Canada | CDL453N00 | 53 52 N | 104 39 W | 489 | CH ₄ , CO, CO ₂ |
| Cape Meares | United States of America | CMO445N00 | 45 28 N | 123 58 W | 30 | CCl ₄ , CFCs, CH ₃ CCl ₃ , CH ₄ , N ₂ O |
| Cape Meares | United States of America | CMO445N00 | 45 28 N | 123 58 W | 30 | ¹³ CO ₂ , C ¹⁸ O ₂ , CH ₄ , CO, CO ₂ , H ₂ |
| Cape St. James | Canada | CSJ451N00 | 51 55 N | 131 01 W | 89 | CO ₂ |
| Chalk River | Canada | CHA446N00 | 46 04 N | 77 24 W | 184 | O ₃ |
| Chapais | Canada | CPS449N00 | 49 49 N | 74 58 W | 381 | O ₃ |
| Chibougamau | Canada | CHM449N00 | 49 40 N | 74 20 W | 393 | CH ₄ , CO, CO ₂ |
| Churchill | Canada | CHL458N00 | 58 45 N | 94 04 W | 35 | ¹³ CO ₂ , C ¹⁸ O ₂ |
| Cold Bay | United States of America | CBA455N00 | 55 12 N | 162 43 W | 25 | ¹³ CH ₄ , ¹³ CO ₂ , C ¹⁸ O ₂ , CH ₄ , CO, CO ₂ , H ₂ , VOCs |
| East Trout Lake | Canada | ETL454N00 | 54 21 N | 104 59 W | 492 | CH ₄ , CO, CO ₂ |
| Egbert | Canada | EGB444N00 | 44 13 N | 79 46 W | 253 | O ₃ |
| Egbert | Canada | EGB444N01 | 44 13 N | 79 46 W | 253 | CH ₄ , CO, CO ₂ , VOCs |
| Estevan Point | Canada | ESP449N00 | 49 22 N | 126 32 W | 39 | ¹³ CO ₂ , CH ₄ , CO, CO ₂ , H ₂ , N ₂ O |
| Estevan Point | Canada | ESP449N00 | 49 22 N | 126 32 W | 39 | ¹³ CO ₂ , C ¹⁸ O ₂ , CH ₄ , CO, CO ₂ , N ₂ O, SF ₆ |
| Esther | Canada | EST451N00 | 51 40 N | 110 12 W | 707 | O ₃ |
| Experimental Lakes Area | Canada | ELA449N00 | 49 40 N | 93 43 W | 369 | O ₃ |
| Fraserdale | Canada | FSD449N00 | 49 52 N | 81 34 W | 210 | CH ₄ , CO, CO ₂ |
| Grifton | United States of America | ITN435N00 | 35 21 N | 77 22 W | 505 | ¹³ CO ₂ , C ¹⁸ O ₂ , CCl ₄ , CFCs, CH ₄ , CO, CO ₂ , H ₂ , N ₂ O, SF ₆ |
| Harvard Forest | United States of America | HFM442N00 | 42 53 N | 72 17 W | 340 | C ₂ Cl ₄ , CBrClF ₂ , CCl ₄ , CFCs, CH ₂ Cl ₂ , CH ₃ Br, CH ₃ CCl ₃ , CH ₃ Cl, HCFCs, HFCs, N ₂ O, SF ₆ |
| Kejimikujik | Canada | KEJ444N00 | 44 25 N | 65 12 W | 127 | O ₃ |
| Key Biscayne | United States of America | KEY425N00 | 25 40 N | 80 12 W | 3 | ¹³ CO ₂ , C ¹⁸ O ₂ , CH ₄ , CO, CO ₂ , H ₂ , VOCs |
| Kitt Peak | United States of America | KPA431N00 | 31 58 N | 111 35 W | 2083 | CH ₄ |
| La Jolla | United States of America | SIO432N00 | 32 49 N | 117 16 W | 14 | CH ₄ |
| La Palma | Cuba | PLM422N00 | 22 45 N | 83 31 W | 47 | NO ₂ |
| Lac La Biche | Canada | LLB454N00 | 54 57 N | 112 27 W | 540 | CH ₄ , CO ₂ , VOCs |
| Lac La Biche (Alberta) | Canada | LLB454N01 | 54 57 N | 112 27 W | 540 | CH ₄ , CO, CO ₂ |
| Longwoods | Canada | LON442N00 | 42 52 N | 81 28 W | 239 | O ₃ |

LIST OF OBSERVING STATIONS (continued)

| Station | Country/Territory | Index Number | Location | | Altitude (m) | Parameter |
|--|--|--------------|-------------------|--------------------|-----------------|--|
| | | | Latitude (° ') | Longitude (° ') | | |
| Mex High Altitude Global Climate Observation Center, Mexico | Mexico | MEX419N00 | 19 58 N | 97 10 W | 4560 | CH ₄ , CO ₂ , VOCs |
| Moody | United States of America | WKT431N00 | 31 19 N | 97 19 W | 708 | ¹³ CO ₂ , C ¹⁸ O ₂ , CH ₄ |
| Mould Bay | Canada | MBC476N00 | 76 15 N | 119 19 W | 58 | ¹³ CO ₂ , C ¹⁸ O ₂ , CH ₄ , CO, CO ₂ , H ₂ |
| Niwot Ridge (C-1) | United States of America | NWR440N00 | 40 02 N | 105 32 W | 3021 | C ₂ Cl ₄ , CBrClF ₂ , CBrF ₃ , CCl ₄ , CFCs, CH ₂ Cl ₂ , CH ₃ Br, CH ₃ CCl ₃ , CH ₃ Cl, HCFCs, HFCs, N ₂ O, O ₃ , SF ₆ |
| Niwot Ridge (Saddle) | United States of America | NWR440N02 | 40 03 N | 105 35 W | 3528 | O ₃ |
| Niwot Ridge (T-van) | United States of America | NWR440N01 | 40 03 N | 105 35 W | 3523 | ¹³ CH ₄ , ¹³ CO ₂ , C ¹⁸ O ₂ , CH ₄ , CO, CO ₂ , H ₂ |
| Olympic Peninsula | United States of America | OPW448N00 | 48 15 N | 124 25 W | 488 | CH ₄ , CO ₂ , H ₂ |
| Pacific Ocean (15N) | N/A | POC915N00 | 15 00 N | 145 00 W | 10 | ¹³ CO ₂ , C ¹⁸ O ₂ , CH ₄ , CO, CO ₂ , H ₂ |
| Pacific Ocean (20N) | N/A | POC920N00 | 20 00 N | 141 00 W | 10 | ¹³ CO ₂ , C ¹⁸ O ₂ , CH ₄ , CO, CO ₂ , H ₂ |
| Pacific Ocean (25N) | N/A | POC925N00 | 25 00 N | 139 00 W | 10 | ¹³ CO ₂ , C ¹⁸ O ₂ , CH ₄ , CO, CO ₂ , H ₂ |
| Pacific Ocean (30N) | N/A | POC930N00 | 30 00 N | 135 00 W | 10 | ¹³ CO ₂ , C ¹⁸ O ₂ , CH ₄ , CO, CO ₂ , H ₂ |
| Pacific Ocean (35N) | N/A | POC935N00 | 35 00 N | 137 00 W | 10 | ¹³ CO ₂ , C ¹⁸ O ₂ , CO, H ₂ |
| Pacific Ocean (40N) | N/A | POC940N00 | 40 00 N | 136 00 W | 10 | ¹³ CO ₂ , H ₂ |
| Pacific Ocean (45N) | N/A | POC945N00 | 45 00 N | 131 00 W | 10 | ¹³ CO ₂ , H ₂ |
| Park Falls | United States of America | LEF445N00 | 45 55 N | 90 16 W | 868 | ¹³ CO ₂ , C ¹⁸ O ₂ , C ₂ Cl ₄ , CBrClF ₂ , CCl ₄ , CFCs, CH ₂ Cl ₂ , CH ₃ Br, CH ₃ CCl ₃ , CH ₃ Cl, CH ₄ , CO, CO ₂ , H ₂ , HCFCs, HFCs, N ₂ O, SF ₆ , VOCs |
| Point Arena | United States of America | PTA438N00 | 38 57 N | 123 43 W | 17 | ¹³ CO ₂ , C ¹⁸ O ₂ , CH ₄ , CO, CO ₂ |
| Ragged Point | Barbados | RPB413N00 | 13 10 N | 59 25 W | 45 | C ₂ Cl ₄ , C ₂ HCl ₃ , CBrClF ₂ , CBrF ₃ , CCl ₄ , CFCs, CH ₂ Cl ₂ , CH ₃ Br, CH ₃ CCl ₃ , CH ₃ Cl, CH ₄ , CHCl ₃ , HCFCs, HFCs, N ₂ O, PFCs, SF ₆ , SO ₂ F ₂ |
| Ragged Point | Barbados | RPB413N00 | 13 10 N | 59 25 W | 45 | ¹³ CO ₂ , C ¹⁸ O ₂ , CH ₄ , CO, CO ₂ , H ₂ , O ₃ |
| Sable Island | Canada | WSA443N00 | 43 55 N | 60 01 W | 5 | CH ₄ , CO, CO ₂ , N ₂ O, SF ₆ |
| Saturna | Canada | SAT448N00 | 48 46 N | 123 07 W | 178 | O ₃ |
| Shemya Island | United States of America | SHM452N00 | 52 43 N | 174 04 E | 40 | ¹³ CO ₂ , C ¹⁸ O ₂ , CH ₄ , CO, CO ₂ , H ₂ , VOCs |
| Southern Great Plains | United States of America | SGP436N00 | 36 46 N | 97 30 W | 314 | ¹³ CO ₂ , C ¹⁸ O ₂ , CH ₄ , CO, CO ₂ , N ₂ O, SF ₆ , VOCs |
| St. Croix | United States of America | AVI417N00 | 17 45 N | 64 45 W | 3 | CH ₄ , CO ₂ |
| St. David's Head | United Kingdom of Great Britain and Northern Ireland | BME432N00 | 32 22 N | 64 39 W | 30 | ¹³ CO ₂ , C ¹⁸ O ₂ , CH ₄ , CO, CO ₂ , H ₂ |
| Sutton | Canada | SUT445N00 | 45 04 N | 72 40 W | 243 | O ₃ |

LIST OF OBSERVING STATIONS (continued)

| Station | Country/Territory | Index Number | Location | | Altitude (m) | Parameter |
|--------------------------------------|--|--------------|-------------------|--------------------|-----------------|--|
| | | | Latitude (° ') | Longitude (° ') | | |
| Trinidad Head | United States of America | THD441N00 | 41 02 N | 124 09 W | 120 | C ₂ Cl ₄ , C ₂ HCl ₃ , CBrClF ₂ , CBrF ₃ , CCl ₄ , CFCs, CH ₂ Cl ₂ , CH ₃ Br, CH ₃ CCl ₃ , CH ₃ Cl, CH ₄ , CHCl ₃ , HCFCs, HFCs, N ₂ O, PFCs, SF ₆ , SO ₂ F ₂ |
| Trinidad Head | United States of America | THD441N00 | 41 02 N | 124 09 W | 120 | ¹³ CO ₂ , C ¹⁸ O ₂ , C ₂ Cl ₄ , CBrClF ₂ , CCl ₄ , CFCs, CH ₂ Cl ₂ , CH ₃ Br, CH ₃ CCl ₃ , CH ₃ Cl, CH ₄ , CO, CO ₂ , HCFCs, HFCs, N ₂ O, O ₃ , SF ₆ , VOCs |
| Tudor Hill | United Kingdom of Great Britain and Northern Ireland | BMW432N00 | 32 16 N | 64 52 W | 30 | ¹³ CO ₂ , C ¹⁸ O ₂ , CH ₄ , CO, CO ₂ , H ₂ , O ₃ , VOCs |
| Wendover | United States of America | UTA439N00 | 39 52 N | 113 43 W | 1320 | ¹³ CO ₂ , C ¹⁸ O ₂ , CH ₄ , CO, CO ₂ , H ₂ , VOCs |
| West Branch | United States of America | WBI441N00 | 41 43 N | 91 21 W | 241.7 | ¹³ CO ₂ , C ¹⁸ O ₂ |
| REGION V (South-West Pacific) | | | | | | |
| Baring Head | New Zealand | BHD541S00 | 41 24 S | 174 52 E | 85 | ¹³ CH ₄ , ¹⁴ CO ₂ , CH ₄ , CO, CO ₂ , N ₂ O, O ₃ , VOCs |
| Baring Head | New Zealand | BHD541S00 | 41 24 S | 174 52 E | 85 | ¹³ CO ₂ , C ¹⁸ O ₂ , CH ₄ , CO, CO ₂ |
| Bukit Koto Tabang | Indonesia | BKT500S00 | 0 12 S | 100 19 E | 864.5 | NO ₂ , SO ₂ |
| Bukit Koto Tabang | Indonesia | BKT500S00 | 0 12 S | 100 19 E | 864.5 | CO, O ₃ |
| Bukit Koto Tabang | Indonesia | BKT500S00 | 0 12 S | 100 19 E | 864.5 | ¹³ CO ₂ , C ¹⁸ O ₂ , CH ₄ , CO, CO ₂ , H ₂ , N ₂ O, SF ₆ , VOCs |
| Cape Ferguson | Australia | CFA519S00 | 19 16 S | 147 03 E | 2 | ¹³ CO ₂ , CH ₄ , CO, CO ₂ , H ₂ , N ₂ O |
| Cape Grim | Australia | CGO540S00 | 40 40 S | 144 40 E | 94 | ¹³ CO ₂ , CH ₄ , CO, CO ₂ , H ₂ , N ₂ O |
| Cape Grim | Australia | CGO540S00 | 40 40 S | 144 40 E | 94 | C ₂ Cl ₄ , C ₂ HCl ₃ , CBrClF ₂ , CBrF ₃ , CCl ₄ , CFCs, CH ₂ Cl ₂ , CH ₃ Br, CH ₃ CCl ₃ , CH ₃ Cl, CH ₄ , CHCl ₃ , CO, H ₂ , HCFCs, HFCs, N ₂ O, PFCs, SF ₆ , SO ₂ F ₂ |
| Cape Grim | Australia | CGO540S00 | 40 40 S | 144 40 E | 94 | CO ₂ , O ₃ |
| Cape Grim | Australia | CGO540S00 | 40 40 S | 144 40 E | 94 | ¹³ CH ₄ , ¹³ CO ₂ , C ¹⁸ O ₂ , C ₂ Cl ₄ , CBrClF ₂ , CBrF ₃ , CCl ₄ , CFCs, CH ₂ Cl ₂ , CH ₃ Br, CH ₃ CCl ₃ , CH ₃ Cl, CH ₄ , CO, CO ₂ , H ₂ , HCFCs, HFCs, N ₂ O, SF ₆ , VOCs |
| Cape Kumukahi | United States of America | KUM519N00 | 19 31 N | 154 49 W | 3 | ¹³ CH ₄ , ¹³ CO ₂ , C ¹⁸ O ₂ , C ₂ Cl ₄ , CBrClF ₂ , CBrF ₃ , CCl ₄ , CFCs, CH ₂ Cl ₂ , CH ₃ Br, CH ₃ CCl ₃ , CH ₃ Cl, CH ₄ , CO, CO ₂ , H ₂ , HCFCs, HFCs, N ₂ O, SF ₆ , VOCs |
| Christmas Island | Kiribati | CHR501N00 | 1 42 N | 157 10 W | 3 | ¹³ CO ₂ , C ¹⁸ O ₂ , CH ₄ , CO, CO ₂ , H ₂ |
| Danum Valley GAW | Malaysia | DMV504N00 | 4 58 N | 117 49 E | 426 | CO ₂ , O ₃ |
| Baseline Station Guam | United States of America | GMI513N00 | 13 25 N | 144 46 E | 2 | ¹³ CO ₂ , C ¹⁸ O ₂ , CH ₄ , CO, CO ₂ , H ₂ , VOCs |
| Jakarta | Indonesia | JKR506S00 | 6 10 S | 106 49 E | 7 | NO ₂ , SO ₂ |
| Kaitorete Spit | New Zealand | NZL543S00 | 43 49 S | 172 37 E | 3 | CH ₄ |
| Lauder | New Zealand | LAU545S00 | 45 01 S | 169 40 E | 370 | O ₃ |
| Macquarie Island | Australia | MQA554S00 | 54 28 S | 158 58 E | 12 | ¹³ CO ₂ , CH ₄ , CO, CO ₂ , H ₂ , N ₂ O |

LIST OF OBSERVING STATIONS (continued)

| Station | Country/Territory | Index Number | Location | | Altitude (m) | Parameter |
|---------------------------|--------------------------|--------------|-------------------|--------------------|-----------------|---|
| | | | Latitude (° ') | Longitude (° ') | | |
| Mauna Loa | United States of America | MLO519N00 | 19 32 N | 155 34 W | 3397 | ¹³ CO ₂ , CH ₄ , CO, CO ₂ , H ₂ , N ₂ O |
| Mauna Loa | United States of America | MLO519N00 | 19 32 N | 155 34 W | 3397 | ¹³ CH ₄ , ¹³ CO ₂ , C ¹⁸ O ₂ , C ₂ Cl ₄ , CBrClF ₂ , CBrF ₃ , CCl ₄ , CFCs, CH ₂ Cl ₂ , CH ₃ Br, CH ₃ CCl ₃ , CH ₃ Cl, CH ₄ , CO, CO ₂ , H ₂ , HCFCs, HFCs, N ₂ O, O ₃ , SF ₆ , VOCs |
| Pacific Ocean (00N) | N/A | POC900N00 | 0 00 N | 155 00 W | 10 | ¹³ CO ₂ , C ¹⁸ O ₂ , CH ₄ , CO, CO ₂ , H ₂ |
| Pacific Ocean (05N) | N/A | POC905N00 | 5 00 N | 151 00 W | 10 | ¹³ CO ₂ , C ¹⁸ O ₂ , CH ₄ , CO, CO ₂ , H ₂ |
| Pacific Ocean (05S) | N/A | POC905S00 | 5 00 S | 159 00 W | 10 | ¹³ CO ₂ , C ¹⁸ O ₂ , CH ₄ , CO, CO ₂ , H ₂ |
| Pacific Ocean (10N) | N/A | POC910N00 | 10 00 N | 149 00 W | 10 | ¹³ CO ₂ , C ¹⁸ O ₂ , CH ₄ , CO, CO ₂ , H ₂ |
| Pacific Ocean (10S) | N/A | POC910S00 | 10 00 S | 161 00 W | 10 | ¹³ CO ₂ , C ¹⁸ O ₂ , CH ₄ , CO, CO ₂ , H ₂ |
| Pacific Ocean (15S) | N/A | POC915S00 | 15 00 S | 171 00 W | 10 | ¹³ CO ₂ , C ¹⁸ O ₂ , CH ₄ , CO, CO ₂ , H ₂ |
| Pacific Ocean (20S) | N/A | POC920S00 | 20 00 S | 174 00 W | 10 | ¹³ CO ₂ , C ¹⁸ O ₂ , CH ₄ , CO, CO ₂ , H ₂ |
| Pacific Ocean (25S) | N/A | POC925S00 | 25 00 S | 171 00 W | 10 | ¹³ CO ₂ , C ¹⁸ O ₂ , CH ₄ , CO, CO ₂ , H ₂ |
| Pacific Ocean (30S) | N/A | POC930S00 | 30 00 S | 176 00 W | 10 | ¹³ CO ₂ , C ¹⁸ O ₂ , CH ₄ , CO, CO ₂ , H ₂ |
| Pacific Ocean (35S) | N/A | POC935S00 | 35 00 S | 180 00 E | 10 | ¹³ CO ₂ , C ¹⁸ O ₂ , CH ₄ , CO, CO ₂ , H ₂ |
| Sand Island | United States of America | MID528N00 | 28 11 N | 177 22 W | 7.7 | ¹³ CO ₂ , C ¹⁸ O ₂ , CH ₄ , CO, CO ₂ , H ₂ , VOCs |
| Tanah Rata | Malaysia | TAR504N00 | 4 28 N | 101 22 E | 1545 | O ₃ |
| Tutuila (Cape Matatula) | United States of America | SMO514S00 | 14 14 S | 170 34 W | 42 | C ₂ Cl ₄ , C ₂ HCl ₃ , CBrClF ₂ , CBrF ₃ , CCl ₄ , CFCs, CH ₂ Cl ₂ , CH ₃ Br, CH ₃ CCl ₃ , CH ₃ Cl, CH ₄ , CHCl ₃ , HCFCs, HFCs, N ₂ O, PFCs, SF ₆ , SO ₂ F ₂ |
| Tutuila (Cape Matatula) | United States of America | SMO514S00 | 14 14 S | 170 34 W | 42 | ¹³ CH ₄ , ¹³ CO ₂ , C ¹⁸ O ₂ , C ₂ Cl ₄ , CBrClF ₂ , CBrF ₃ , CCl ₄ , CFCs, CH ₂ Cl ₂ , CH ₃ Br, CH ₃ CCl ₃ , CH ₃ Cl, CH ₄ , CO, CO ₂ , H ₂ , HCFCs, HFCs, N ₂ O, O ₃ , SF ₆ , VOCs |
| REGION VI (Europe) | | | | | | |
| Ähtäri | Finland | AHT662N00 | 62 34 N | 24 11 E | 180 | NO ₂ , O ₃ , SO ₂ |
| Adrigole | Ireland | ADR651N00 | 51 40 N | 9 43 W | 50 | CCl ₄ , CFCs, CH ₃ CCl ₃ , N ₂ O |
| Angra do Heroismo | Portugal | ANG638N00 | 38 40 N | 27 13 W | 74 | O ₃ |
| BEO Moussala | Bulgaria | BEO642N00 | 42 10 N | 23 35 E | 2925 | CO, CO ₂ , NO, NO ₂ , NO _x , O ₃ , SO ₂ |
| Baltic Sea | Poland | BAL655N00 | 55 21 N | 17 13 E | 28 | ¹³ CO ₂ , C ¹⁸ O ₂ , CH ₄ , CO, CO ₂ , H ₂ , VOCs |
| Begur | Spain | BGU641N00 | 41 58 N | 3 13 E | 13 | CH ₄ , CO ₂ |
| Beja | Portugal | BEJ638N00 | 38 01 N | 7 52 W | 246 | O ₃ |
| Black Sea | Romania | BSC644N00 | 44 10 N | 28 40 E | 3 | ¹³ CO ₂ , C ¹⁸ O ₂ , CH ₄ , CO, CO ₂ , H ₂ , VOCs |
| Bragança | Portugal | BRG641N00 | 41 47 N | 6 43 W | 690 | SO ₂ |
| Brotjacklriegel | Germany | BRT648N00 | 48 49 N | 13 13 E | 1016 | VOCs |
| Brotjacklriegel | Germany | BRT648N00 | 48 49 N | 13 13 E | 1016 | CO ₂ , O ₃ |
| Burgas | Bulgaria | BUR642N00 | 42 28 N | 27 28 E | 16 | NO ₂ , SO ₂ |
| Campisabalos | Spain | CAM641N00 | 41 16 N | 3 08 W | 1360 | VOCs |
| Castelo Branco | Portugal | CAS639N00 | 39 49 N | 7 28 W | 386 | O ₃ |
| Danki | Russian Federation | DAK654N00 | 54 53 N | 37 47 E | 140 | O ₃ |
| Deuselbach | Germany | DEU649N00 | 49 46 N | 7 02 E | 480 | CH ₄ , CO ₂ , O ₃ |

LIST OF OBSERVING STATIONS (continued)

| Station | Country/Territory | Index Number | Location | | Altitude (m) | Parameter |
|--------------------|--|--------------|-------------------|--------------------|-----------------|---|
| | | | Latitude (° ') | Longitude (° ') | | |
| Doñana | Spain | DON637N00 | 37 02 N | 6 32 W | 5 | NO ₂ , O ₃ , SO ₂ |
| Dobele | Latvia | DBL656N00 | 56 22 N | 23 11 E | 42 | O ₃ |
| Donon | France | DNN648N00 | 48 30 N | 7 07 E | 775 | VOCs |
| Dwejra Point | Malta | GOZ636N00 | 36 02 N | 14 10 E | 30 | ¹³ CO ₂ , C ¹⁸ O ₂ , CH ₄ , CO, CO ₂ , H ₂ |
| Eskdalemuir | United Kingdom of Great Britain and Northern Ireland | EDM655N00 | 55 19 N | 3 12 W | 242 | O ₃ |
| Finokalia | Greece | FIK635N00 | 35 20 N | 25 40 E | 150 | CH ₄ , CO ₂ |
| Fundata | Romania | FDT645N00 | 45 28 N | 25 18 E | 1383.5 | CO ₂ , NO ₂ , O ₃ |
| Fundata | Romania | FDT645N00 | 45 28 N | 25 18 E | 1383.5 | NO ₂ , SO ₂ |
| Giordan Lighthouse | Malta | GLH636N00 | 36 04 N | 14 13 E | 167 | CO, O ₃ |
| Hegyhatsal | Hungary | HUN646N00 | 46 57 N | 16 38 E | 248 | CO ₂ |
| Hegyhatsal | Hungary | HUN646N00 | 46 57 N | 16 38 E | 248 | ¹³ CO ₂ , C ¹⁸ O ₂ , CH ₄ , CO, CO ₂ , H ₂ |
| Heimaey | Iceland | ICE663N00 | 63 23 N | 20 16 W | 100 | ¹³ CO ₂ , C ¹⁸ O ₂ , CH ₄ , CO, CO ₂ , H ₂ , O ₃ , VOCs |
| Hohe Warte | Austria | HHE648N00 | 48 15 N | 16 22 E | 202 | NO, NO ₂ , SO ₂ |
| Hohe Warte | Austria | HHE648N00 | 48 15 N | 16 22 E | 202 | NO, NO ₂ , SO ₂ |
| Hohenpeissenberg | Germany | HPB647N00 | 47 47 N | 11 01 E | 985 | ²²² Rn, CO, H ₂ O ₂ , NO, NO ₂ , NO _x , , NO _y , O ₃ , PAN, ROOH, SO ₂ , VOCs |
| Hohenpeissenberg | Germany | HPB647N00 | 47 47 N | 11 01 E | 985 | ¹³ CO ₂ , C ¹⁸ O ₂ , CH ₄ , CO, CO ₂ , VOCs |
| Ile Grande | France | LPO648N00 | 48 48 N | 3 35 W | 10 | CH ₄ , CO ₂ |
| Iskrba | Slovenia | IRB645N00 | 45 34 N | 14 52 E | 520 | NO ₂ , O ₃ , SO ₂ |
| Ivan Sedlo | Bosnia and Herzegovina | IVN643N00 | 43 46 N | 18 01 E | 970 | NO ₂ , SO ₂ |
| Jarczew | Poland | JCZ651N00 | 51 49 N | 21 58 E | 180 | NO ₂ , SO ₂ |
| Jungfraujoch | Switzerland | JFJ646N00 | 46 32 N | 7 59 E | 3580 | CO ₂ |
| Jungfraujoch | Switzerland | JFJ646N00 | 46 32 N | 7 59 E | 3580 | CH ₄ , CO, CO ₂ , N ₂ O, NO, NO ₂ , NO _x , NO _y , O ₃ , PAN, SF ₆ , SO ₂ |
| Jungfraujoch | Switzerland | JFJ646N00 | 46 32 N | 7 59 E | 3580 | C ₂ Cl ₄ , C ₂ HCl ₃ , CBrClF ₂ , CBrF ₃ , CFCs, CH ₂ Cl ₂ , CH ₃ Br, CH ₃ CCl ₃ , CH ₃ Cl, CHCl ₃ , HCFCs, HFCs, PFCs, SF ₆ , SO ₂ F ₂ |
| K-pusztá | Hungary | KPS646N00 | 46 58 N | 19 33 E | 125 | CO ₂ , NO ₂ , O ₃ , SO ₂ |
| Kamenicki Vis | Serbia | KAM643N00 | 43 23 N | 21 56 E | 813 | NO ₂ , SO ₂ |
| Kloosterburen | Netherlands (the) | KTb653N00 | 53 23 N | 6 25 E | 0 | CO, NO, NO ₂ , NO _x , SO ₂ |
| Kollumerwaard | Netherlands (the) | KMW653N00 | 53 19 N | 6 16 E | 0 | CH ₄ , CO, CO ₂ , NO, NO ₂ , NO _x , O ₃ , SO ₂ |
| Kosetice | Czech Republic | KOS649N00 | 49 34 N | 15 04 E | 534 | VOCs |
| Kosetice | Czech Republic | KOS649N00 | 49 34 N | 15 04 E | 534 | CH ₄ , CO, NO, NO ₂ , O ₃ , SO ₂ |
| Kovk | Slovenia | KVK646N00 | 46 07 N | 15 05 E | 600 | O ₃ |
| Krvavec | Slovenia | KVV646N00 | 46 17 N | 14 31 E | 1720 | CO, O ₃ |
| La Cartuja | Spain | CAR637N00 | 37 12 N | 3 36 W | 720 | NO ₂ , SO ₂ |
| La Tardiere | France | LAT646N00 | 46 38 N | 0 45 W | 133 | VOCs |
| Lampedusa | Italy | LMP635N00 | 35 31 N | 12 37 E | 45 | CBrClF ₂ , CBrF ₃ , CCl ₄ , CFCs, CH ₂ Br ₂ , CH ₂ Cl ₂ , CH ₃ Br, CH ₃ CCl ₃ , CH ₃ Cl, CH ₃ I, CH ₄ , CHCl ₃ , CO ₂ , HCFCs, HFCs, N ₂ O, SF ₆ |
| Lampedusa | Italy | LMP635N00 | 35 31 N | 12 37 E | 45 | ¹³ CO ₂ , C ¹⁸ O ₂ , CH ₄ , CO, CO ₂ |
| Lazaropole | The former Yugoslav Republic of Macedonia | LZP641N00 | 41 31 N | 20 41 E | 1320 | NO ₂ , SO ₂ |

LIST OF OBSERVING STATIONS (continued)

| Station | Country/Territory | Index Number | Location | | Altitude (m) | Parameter |
|-----------------------------|--------------------------|--------------|-------------------|--------------------|-----------------|--|
| | | | Latitude (° ') | Longitude (° ') | | |
| Leba | Poland | LEB654N00 | 54 45 N | 17 31 E | 2 | NO ₂ , SO ₂ |
| Lisboa / Gago Coutinho | Portugal | LIS638N00 | 38 46 N | 9 07 W | 105 | O ₃ |
| Logroño | Spain | LOG642N00 | 42 27 N | 2 30 W | 370 | NO ₂ , SO ₂ |
| Mace Head | Ireland | MHD653N00 | 53 19 N | 9 54 W | 8 | O ₃ |
| Mace Head | Ireland | MHD653N00 | 53 19 N | 9 54 W | 8 | CH ₄ , CO ₂ |
| Mace Head | Ireland | MHD653N00 | 53 19 N | 9 54 W | 8 | C ₂ Cl ₄ , C ₂ HCl ₃ , CBrClF ₂ , CBrF ₃ , CCl ₄ , CFCs, CH ₂ Cl ₂ , CH ₃ Br, CH ₃ CCl ₃ , CH ₃ Cl, CH ₄ , CHCl ₃ , CO, H ₂ , HCFCs, HFCs, N ₂ O, PFCs, SF ₆ , SO ₂ F ₂ |
| Mace Head | Ireland | MHD653N00 | 53 19 N | 9 54 W | 8 | ¹³ CH ₄ , ¹³ CO ₂ , C ¹⁸ O ₂ , C ₂ Cl ₄ , CBrClF ₂ , CBrF ₃ , CCl ₄ , CFCs, CH ₂ Cl ₂ , CH ₃ Br, CH ₃ CCl ₃ , CH ₃ Cl, CH ₄ , CO, CO ₂ , H ₂ , HCFCs, HFCs, N ₂ O, SF ₆ , VOCs |
| Mahón | Spain | MHN639N00 | 39 52 N | 4 19 E | 78 | NO ₂ , O ₃ , SO ₂ |
| Monte Cimone | Italy | CMN644N00 | 44 10 N | 10 41 E | 2165 | CH ₄ , CO, H ₂ , N ₂ O, O ₃ , SF ₆ |
| Monte Cimone | Italy | CMN644N00 | 44 10 N | 10 41 E | 2165 | CO ₂ |
| Monte Velho | Portugal | MVH638N00 | 38 04 N | 8 48 W | 43 | O ₃ |
| Neuglobsow | Germany | NGL653N00 | 53 10 N | 13 01 E | 65 | CH ₄ , CO, CO ₂ , O ₃ |
| Noia | Spain | NIA642N00 | 42 43 N | 8 55 W | 685 | NO ₂ , O ₃ , SO ₂ |
| Ocean Station "M" | Norway | STM666N00 | 66 00 N | 2 00 E | 5 | ¹³ CO ₂ , C ¹⁸ O ₂ , CH ₄ , CO, CO ₂ , H ₂ |
| Ocean Station Charlie | Russian Federation | STC652N00 | 52 45 N | 35 30 W | 5 | CO ₂ |
| Ocean Station Charlie | United States of America | STC654N00 | 54 00 N | 35 00 W | 6 | CO ₂ |
| Ochsenkopf | Germany | OXK650N00 | 50 01 N | 11 48 E | 1185 | ¹³ CO ₂ , C ¹⁸ O ₂ , CH ₄ , CO, CO ₂ , VOCs |
| Oulanka | Finland | OUL666N00 | 66 19 N | 29 23 E | 310 | NO ₂ , O ₃ , SO ₂ |
| Pallas-Sammaltunturi | Finland | PAL667N00 | 67 58 N | 24 07 E | 560 | VOCs |
| Pallas-Sammaltunturi | Finland | PAL667N00 | 67 58 N | 24 07 E | 560 | CH ₄ , CO ₂ , O ₃ |
| Pallas-Sammaltunturi | Finland | PAL667N00 | 67 58 N | 24 07 E | 560 | ¹³ CO ₂ , C ¹⁸ O ₂ , CBrF ₃ , CH ₄ , CO, CO ₂ , VOCs |
| Payerne | Switzerland | PAY646N00 | 46 49 N | 6 57 E | 490 | CO, NO, NO ₂ , NO _x , O ₃ , SO ₂ |
| Penhas Douradas | Portugal | PEN640N00 | 40 25 N | 7 32 W | 1380 | O ₃ |
| Peyrusse Vieille | France | PVI643N00 | 43 37 N | 0 10 E | 200 | VOCs |
| Pic du Midi | France | PDM642N00 | 42 56 N | 0 08 E | 2877 | CO, O ₃ |
| Pic du Midi | France | PDM642N00 | 42 56 N | 0 08 E | 2877 | CH ₄ , CO ₂ |
| Plateau Rosa | Italy | PRS645N00 | 45 55 N | 7 42 E | 3480 | CH ₄ , CO ₂ , O ₃ |
| Pleven | Bulgaria | PLV643N00 | 43 25 N | 24 36 E | 64 | NO ₂ , SO ₂ |
| Plovdiv | Bulgaria | PLD642N00 | 42 07 N | 24 45 E | 179 | NO ₂ , SO ₂ |
| Puszcza Borecka/Diabla Gora | Poland | DIG654N00 | 54 08 N | 22 04 E | 157 | CO ₂ , NO ₂ , O ₃ , SO ₂ |
| Puy de Dome | France | PUY645N00 | 45 46 N | 2 57 E | 1465 | CH ₄ , CO ₂ |
| Rigi | Switzerland | RIG646N00 | 46 04 N | 8 26 E | 1031 | CO, NO, NO ₂ , NO _x , O ₃ , SO ₂ , VOCs |
| Roquetes | Spain | ROQ640N00 | 40 49 N | 0 28 E | 50 | NO ₂ , O ₃ , SO ₂ |
| Rucava | Latvia | RCV656N00 | 56 09 N | 21 10 E | 18 | NO ₂ , O ₃ , SO ₂ |
| San Pablo de los Montes | Spain | SPM639N00 | 39 32 N | 4 20 W | 917 | NO ₂ , O ₃ , SO ₂ |
| Schauinsland | Germany | SSL647N00 | 47 55 N | 7 55 E | 1205 | CH ₄ , CO, CO ₂ , N ₂ O, NO, NO ₂ , O ₃ , PAN, SF ₆ |
| Schmuecke | Germany | SCH650N00 | 50 38 N | 10 46 E | 937 | VOCs |
| Sede Boker | Israel | WIS631N00 | 31 07 N | 34 52 E | 400 | ¹³ CO ₂ , C ¹⁸ O ₂ , CH ₄ , CO, CO ₂ , H ₂ |

LIST OF OBSERVING STATIONS (continued)

| Station | Country/Territory | Index Number | Location | | Altitude (m) | Parameter |
|---------------------------------|--|--------------|-------------------|--------------------|-----------------|--|
| | | | Latitude (° ') | Longitude (° ') | | |
| Semenic | Romania | SEM645N00 | 45 07 N | 21 58 E | 1432 | NO ₂ , SO ₂ |
| Shepelevo | Russian Federation | SHP659N00 | 59 58 N | 29 07 E | 4 | O ₃ |
| Shetland | United Kingdom of Great Britain and Northern Ireland | SIS660N00 | 60 04 N | 1 15 W | 30 | ¹³ CO ₂ , CH ₄ , CO, CO ₂ , H ₂ , N ₂ O |
| Site J | Denmark | GRL666N00 | 66 30 N | 46 12 W | 2030 | CH ₄ |
| Sniezka | Poland | SNZ650N00 | 50 43 N | 15 43 E | 1603 | NO ₂ , SO ₂ |
| Sofia | Bulgaria | SOF642N00 | 42 38 N | 23 22 E | 586 | NO ₂ , SO ₂ |
| Sonnblick | Austria | SNB647N00 | 47 02 N | 12 56 E | 3106 | CO, CO ₂ , NO, NO ₂ , NO _y , O ₃ |
| Stîna de Vale | Romania | STN646N00 | 46 40 N | 22 37 E | 1116 | NO ₂ , SO ₂ |
| Starina | Slovakia | STA649N00 | 49 02 N | 22 16 E | 345 | VOCs |
| Stephansplatz | Austria | STP648N00 | 48 13 N | 16 22 E | 171 | NO, NO ₂ , SO ₂ |
| Stephansplatz | Austria | STP648N00 | 48 13 N | 16 22 E | 171 | NO, NO ₂ , SO ₂ |
| Summit | Denmark | SUM672N00 | 72 34 N | 38 28 W | 3238 | ¹³ CO ₂ , C ¹⁸ O ₂ , CBrClF ₂ , CCl ₄ , CFCs, CH ₂ Cl ₂ , CH ₃ Br, CH ₃ CCl ₃ , CH ₃ Cl, CH ₄ , CO ₂ , HCFCs, HFCs, N ₂ O, O ₃ , SF ₆ , VOCs |
| Suwalki | Poland | SWL654N00 | 54 07 N | 22 56 E | 184 | NO ₂ , SO ₂ |
| Terceira Island | Portugal | AZR638N00 | 38 46 N | 27 22 W | 40 | ¹³ CH ₄ , ¹³ CO ₂ , C ¹⁸ O ₂ , CH ₄ , CO, CO ₂ , H ₂ , VOCs |
| Teriberka | Russian Federation | TER669N00 | 69 12 N | 35 06 E | 40 | CH ₄ , CO ₂ |
| Utö | Finland | UTO659N00 | 59 46 N | 21 22 E | 7 | VOCs |
| Utö | Finland | UTO659N00 | 59 46 N | 21 22 E | 7 | NO ₂ , O ₃ , SO ₂ |
| Varna | Bulgaria | VRN643N00 | 43 12 N | 27 55 E | 41 | NO ₂ , SO ₂ |
| Viana do Castelo | Portugal | VDC641N00 | 41 42 N | 8 48 W | 16 | SO ₂ |
| Vindeln | Sweden | VDL664N00 | 64 15 N | 19 46 E | 271 | O ₃ |
| Virolahti | Finland | VIR660N00 | 60 31 N | 27 40 E | 4 | NO ₂ , O ₃ , SO ₂ |
| Waldhof | Germany | LGB652N00 | 52 47 N | 10 46 E | 74 | VOCs |
| Waldhof | Germany | LGB652N00 | 52 47 N | 10 46 E | 74 | CO ₂ , O ₃ |
| Wank Peak | Germany | WNK647N00 | 47 31 N | 11 09 E | 1780 | CO ₂ , NO _x , SO ₂ |
| Westerland | Germany | WES654N00 | 54 55 N | 8 19 E | 12 | CO ₂ , O ₃ |
| Zabljak | Montenegro | ZBL643N00 | 43 08 N | 19 07 E | 1450 | NO ₂ , SO ₂ |
| Zavodnje | Slovenia | ZRN646N00 | 46 25 N | 15 00 E | 770 | O ₃ |
| Zeppelinfjellet (Ny-Alesund) | Norway | ZEP678N00 | 78 54 N | 11 52 E | 475 | CCl ₄ , CFCs, CH ₃ CCl ₃ , N ₂ O, O ₃ , SO ₂ |
| Zeppelinfjellet (Ny-Alesund) | Norway | ZEP678N00 | 78 54 N | 11 52 E | 475 | CO ₂ |
| Zeppelinfjellet (Ny-Alesund) | Norway | ZEP678N00 | 78 54 N | 11 52 E | 475 | C ₂ Cl ₄ , C ₂ HCl ₃ , CBrClF ₂ , CBrF ₃ , CH ₂ Cl ₂ , CH ₃ Br, CH ₃ CCl ₃ , CH ₃ Cl, CHCl ₃ , HCFCs, HFCs |
| Zeppelinfjellet (Ny-Alesund) | Norway | ZEP678N00 | 78 54 N | 11 52 E | 475 | ¹³ CH ₄ , ¹³ CO ₂ , C ¹⁸ O ₂ , CH ₄ , CO, CO ₂ , H ₂ , VOCs |
| Zingst | Germany | ZGT654N00 | 54 25 N | 12 43 E | 1 | VOCs |
| Zingst | Germany | ZGT654N00 | 54 25 N | 12 43 E | 1 | CH ₄ , CO ₂ , O ₃ |
| Zoseni | Latvia | ZSN657N00 | 57 04 N | 25 32 E | 182 | NO ₂ , O ₃ , SO ₂ |
| Zugspitze | Germany | ZUG647N00 | 47 25 N | 10 58 E | 2960 | CO ₂ |
| Zugspitze | Germany | ZUG647N00 | 47 25 N | 10 58 E | 2960 | CH ₄ , CO, CO ₂ , NO, NO _x , NO _y , O ₃ |
| Zugspitze / Schneefernerhaus | Germany | ZSF647N00 | 47 25 N | 10 58 E | 2656 | SO ₂ |
| Zugspitze / Schneefernerhaus | Germany | ZSF647N00 | 47 25 N | 10 58 E | 2656 | CH ₄ , CO, CO ₂ , N ₂ O, NO, NO ₂ , NO _y , O ₃ , PAN, SF ₆ |

LIST OF OBSERVING STATIONS (continued)

| Station | Country/Territory | Index Number | Latitude (° ') | Location Longitude (° ') | Altitude (m) | Parameter |
|--|--|--------------|-------------------|--------------------------------|-----------------|--|
| ANTARCTICA | | | | | | |
| Arrival Heights | New Zealand | ARH777S00 | 77 47 S | 166 40 E | 184 | ¹³ CH ₄ , CH ₄ , CO, N ₂ O |
| Arrival Heights | New Zealand | ARH777S00 | 77 47 S | 166 40 E | 184 | O ₃ |
| Casey Station | Australia | CYA766S00 | 66 16 S | 110 31 E | 60 | ¹³ CO ₂ , CH ₄ , CO, CO ₂ , H ₂ , N ₂ O |
| Halley Bay | United Kingdom of Great Britain and Northern Ireland | HBA775S00 | 75 34 S | 26 30 W | 33 | ¹³ CO ₂ , C ¹⁸ O ₂ , CH ₄ , CO, CO ₂ , H ₂ , VOCs |
| Jubany | Argentina | JBN762S00 | 62 13 S | 58 40 W | 15 | CO ₂ |
| Mawson | Australia | MAA767S00 | 67 37 S | 62 52 E | 32 | ¹³ CO ₂ , CH ₄ , CO, CO ₂ , H ₂ , N ₂ O |
| McMurdo Station | United States of America | MCM777S00 | 77 49 S | 166 34 E | 11 | CH ₄ , O ₃ |
| Mizuho | Japan | MZH770S00 | 70 42 S | 44 17 E | 2230 | CH ₄ |
| Neumayer | Germany | NMY770S00 | 70 39 S | 8 15 W | 42 | O ₃ |
| Palmer Station | United States of America | PSA764S00 | 64 55 S | 64 00 W | 10 | ¹³ CO ₂ , C ¹⁸ O ₂ , C ₂ Cl ₄ , CBrClF ₂ , CCl ₄ , CFCs, CH ₂ Cl ₂ , CH ₃ Br, CH ₃ CCl ₃ , CH ₃ Cl, CH ₄ , CO, CO ₂ , H ₂ , HCFCs, HFCs, N ₂ O, SF ₆ , VOCs |
| South Pole | United States of America | SPO789S00 | 89 58 S | 24 48 W | 2810 | ¹³ CO ₂ , CH ₄ , CO, CO ₂ , H ₂ , N ₂ O |
| South Pole | United States of America | SPO789S00 | 89 58 S | 24 48 W | 2810 | ¹³ CH ₄ , ¹³ CO ₂ , C ¹⁸ O ₂ , C ₂ Cl ₄ , CBrClF ₂ , CBrF ₃ , CCl ₄ , CFCs, CH ₂ Cl ₂ , CH ₃ Br, CH ₃ CCl ₃ , CH ₃ Cl, CH ₄ , CO, CO ₂ , H ₂ , HCFCs, HFCs, N ₂ O, O ₃ , SF ₆ , VOCs |
| Syowa Station | Japan | SYO769S00 | 69 00 S | 39 34 E | 16 | CO ₂ |
| Syowa Station | Japan | SYO769S00 | 69 00 S | 39 34 E | 16 | ¹³ CO ₂ , C ¹⁸ O ₂ , CH ₄ , CO, CO ₂ , H ₂ , VOCs |
| Syowa Station | Japan | SYO769S00 | 69 00 S | 39 34 E | 16 | O ₃ |
| MOBILE STATION | | | | | | |
| Aircraft (over Bass Strait and Cape Grim) | Australia | AIA999900 | | | | ¹³ CO ₂ , CH ₄ , CO, CO ₂ , H ₂ , N ₂ O |
| Aircraft Observation of Atmospheric trace gases by JMA | Japan | AOA999900 | | | | CH ₄ , CO, CO ₂ , N ₂ O |
| Aircraft: Orleans | France | ORL999900 | | | 150 | CH ₄ , CO ₂ |
| Akademik Korolev, R/V | United States of America | AKD999900 | | | | CH ₄ |
| Alligator liberty, M/V | Japan | ALG999900 | | | | CO ₂ |
| Atlantic Ocean | United States of America | AOC9XXX00 | | | 10 | CH ₄ , CO ₂ |
| BACPAC 99 | United States of America | BAC999900 | | | | CCl ₄ , CFCs, CH ₃ Br, CH ₃ CCl ₃ , CH ₃ Cl, HCFCs |
| BLAST1 | United States of America | BLA999900 | | | | CCl ₄ , CFCs, CH ₃ Br, CH ₃ CCl ₃ , CH ₃ Cl, HCFCs |
| BLAST2 | United States of America | BLA999901 | | | | CCl ₄ , CFCs, CH ₃ Br, CH ₃ CCl ₃ , CH ₃ Cl, HCFCs |
| BLAST3 | United States of America | BLA999902 | | | | CCl ₄ , CFCs, CH ₃ Br, CH ₃ CCl ₃ , CH ₃ Cl, HCFCs |

LIST OF OBSERVING STATIONS (continued)

| Station | Country/Territory | Index Number | Location | | | Parameter |
|--|--------------------------|--------------|-------------------|--------------------|-----------------|---|
| | | | Latitude (° ') | Longitude (° ') | Altitude (m) | |
| CLIVAR 01 | United States of America | CLI999900 | | | | CCl ₄ , CFCs, CH ₃ Br, CH ₃ CCl ₃ , CH ₃ Cl, HCFCs |
| Comprehensive Observation Network for TRace gases by AIrLiner (CONTRAIL) | Japan | EOM999900 | | | | CH ₄ , CO ₂ |
| Discoverer 1983 & 1984, R/V | United States of America | DIS999900 | | | | CH ₄ |
| Discoverer 1985, R/V | United States of America | DSC999900 | | | | CH ₄ |
| Drake Passage | United States of America | DRP999900 | | | | ¹³ CO ₂ , C ¹⁸ O ₂ , CH ₄ , CO ₂ |
| Gas Change Experiment | United States of America | GAS999900 | | | | CCl ₄ , CFCs, CH ₃ Br, CH ₃ CCl ₃ , CH ₃ Cl, HCFCs |
| HATS Ocean Projects | United States of America | HOP999900 | | | | HFCs |
| INSTAC-I (International Strato/Tropospheric Air Chemistry Project) | Japan | INS999900 | | | | ¹³ CO ₂ , CH ₄ , CO ₂ |
| John Biscoe, R/V | United States of America | JBS999900 | | | | CH ₄ |
| Keifu Maru, R/V | Japan | KEF999900 | | | | CO ₂ |
| Kofu Maru, R/V | Japan | KOF999900 | | | | CO ₂ |
| Korolev, R/V | United States of America | KOR999900 | | | | CH ₄ |
| Long Lines Expedition, R/V | United States of America | LLE999900 | | | | CH ₄ |
| MRI Research, 1978-1986, R/V | Japan | MRI999900 | | | | CH ₄ |
| MRI Research, Hakuho Maru, R/V | Japan | HKH999900 | | | | CO ₂ |
| MRI Research, Kaiyo Maru, R/V | Japan | KIY999900 | | | | CO ₂ |
| MRI Research, Mirai, R/V | Japan | MMR999900 | | | | CO ₂ |
| MRI Research, Natushima, R/V | Japan | NTU999900 | | | | CO ₂ |
| MRI Research, Ryofu Maru, R/V | Japan | RFM999900 | | | | CO ₂ |
| MRI Research, Wellington Maru, R/V | Japan | WLT999900 | | | | CO ₂ |
| Mexico Naval H-02, R/V | United States of America | MXN999900 | | | | CH ₄ |
| NOPACCS - Hakurei Maru - | Japan | HAK999900 | | | | TIC |
| Observation of Atmospheric Chemistry Over Japan | Japan | OAJ999900 | | | | CFCs, N ₂ O |
| Oceanographer, R/V | United States of America | OCE999900 | | | | CH ₄ |
| PHASE I-04 | United States of America | PHA999900 | | | | CCl ₄ , CFCs, CH ₃ Br, CH ₃ CCl ₃ , CH ₃ Cl, HCFCs |
| Pacific Ocean | New Zealand | BSL999900 | | | | ¹³ CH ₄ , CH ₄ , VOCs |

LIST OF OBSERVING STATIONS (continued)

| Station | Country/Territory | Index Number | Location | | Altitude (m) | Parameter |
|---|--------------------------|--------------|-------------------|--------------------|-----------------|--|
| | | | Latitude (° ') | Longitude (° ') | | |
| Pacific Ocean | United States of America | POC9XXX00 | | | 10 | ¹³ CO ₂ , C ¹⁸ O ₂ , CH ₄ , CO, CO ₂ , H ₂ |
| Pacific-Atlantic Ocean | United States of America | PAO999900 | | | | CH ₄ |
| Polar Star, R/V | United States of America | PLS999900 | | | | CH ₄ |
| Ryofu Maru, R/V | Japan | RYF999900 | | | | CFCs, CH ₄ , CO ₂ , N ₂ O, TIC |
| Santarem | Brazil | SAN999900 | | | | CH ₄ , CO, CO ₂ , N ₂ O, SF ₆ |
| South China Sea | United States of America | SCS9XXX00 | | | 15 | ¹³ CO ₂ , C ¹⁸ O ₂ , CH ₄ , CO, CO ₂ , H ₂ |
| Soyo Maru, R/V | Japan | SOY999900 | | | | CO ₂ |
| Surveyor, R/V | United States of America | SUR999900 | | | | CH ₄ |
| The Observation of Atmospheric Methane Over Japan | Japan | OAM999900 | | | | CH ₄ |
| The Observation of Atmospheric Sulfur Hexafluoride Over Japan | Japan | OAS999900 | | | | SF ₆ |
| WEST COSMIC - Hakurei Maru No.2 - | Japan | HAK999901 | | | | TIC |
| Wakataka-Maru | Japan | WAK999900 | | | | CO ₂ |
| Western Pacific | United States of America | WPC9XXX00 | | | 10 | ¹³ CH ₄ , ¹³ CO ₂ , C ¹⁸ O ₂ , CH ₄ , CO ₂ |
| northern and western Pacific | Japan | NWP999900 | | | | N ₂ O |

LIST OF CONTRIBUTORS

| Station Country/Territory | Name | Address |
|---|---|--|
| REGION I (Africa) | | |
| Izaña (Tenerife) (Spain) | Angel J. Gomez-Pelaez Carlos Marrero | Izana Atmospheric Research Center, Meteorological State Agency of Spain (AEMET) C/ La Marina, 20, Planta 6. Apartado 880. 38071 Santa Cruz de Tenerife, Spain |
| Cape Point (South Africa) | Ernst Günther Brunke | South African Weather Service (Climate Division) SAWS, c/o CSIR (Environmentek), P.O. Box 320, Stellenbosch 7599, South Africa |
| Cairo (Egypt) | Hamza Mohamed Hamza | Egyptian Meteorological Authority Department of Air Pollution Study Egyptian Meteorological Authority P.O. Box 11784 – Cairo, Egypt |
| Amsterdam Island (France) | Jean Sciare Michel Ramonet | LSCE (Laboratoire des Sciences du Climat et de l'Environnement) UMR CEA-CNRS LSCE - CEA Saclay - Orme des Merisiers - Bat.701 91191 Gif-sur-Yvette, France |
| Mt. Kenya (Kenya) | Josiah Kariuki Murageh Jörg Klausen Stephan Henne | Kenya Meteorological Department Dagoretti Corner P.O. Box 30259 00100 Nairobi, Kenya |
| Cape Verde Observatory (Cape Verde) | Katie Read Zoë Fleming | Department of Chemistry, University of York, Heslington, York, YO10 5DD, United Kingdom |
| Funchal (Portugal) | Maria Amelia V.Lopes | Instituto de Meteorologia, I.P. Rua C-Aeroporto de Lisboa 1749-077 Lisboa Portugal |
| Assekrem (Algeria) | Mimouni Mohamed | Office National de la Meteorologie P.O. Box 31 Tamanrasset 11000, Algeria |
| REGION II (Asia) | | |
| Nagoya (Japan) | A. Matsunami | Research Center for Advanced Energy Conversion, Nagoya University Furo-cho, Chikusaku, Nagoya 464-8603, Japan |
| Minamitorishima Ryori Yonagunijima (Japan) | Daisuke KUBOIKE | Atmospheric Environment Division, Global Environment and Marine Department, Japan Meteorological Agency (JMA) 1-3-4 Otemachi, Chiyoda-ku, Tokyo 100-8122, Japan |

LIST OF CONTRIBUTORS (continued)

| Station Country/Territory | Name | Address |
|---|---|---|
| Cape Ochi-ishi Hateruma (Japan) | Hitoshi MUKAI | Center for Global Environmental Research, National Institute for Environmental Studies 16-2, Onogawa, Tsukuba-shi, Ibaraki 305-8506, Japan |
| Anmyeon-do (Republic of Korea) | Il-Young Lee Jeong-Sik Kim Im-Chul Shin Ki-Jun Park Sang-Hoon Kim | Korea Global Atmosphere Watch Center, Korea Meteorology Administration 1764-6, Seungen-Ri, Anmyeon-Eup, Taean-Kun, Chung Nam, 357-961, Republic of Korea |
| Gosan (Republic of Korea) | Jeong-Ah Yu Seung-Yeon Kim | National Institute of Environmental Research Environmental Research Complex, Gyeongseo-dong, Seo-gu, Incheon, 404-708, Republic of Korea |
| Hok Tsui King's Park (Hong Kong, China) | K.C. Tsui K.H. Tam Chan, Siu Wai | Hong Kong Observatory 134A Nathan Road, Kowloon, Hong Kong, China |
| Hok Tsui (Hong Kong, China) | Ka Se Lam | Department of Civil and Structural Engineering, Hong Kong Polytechnic University Hung Hom, Kowloon, Hong Kong, China |
| Tsukuba (Japan) | Kazumasa Mori | Lower Aerological Observations Division, Aerological Observatory, Japan Meteorological Agency (JMA) 1-2 Nagamine, Tsukuba, Ibaraki, 305-0052, Japan |
| Mikawa-Ichinomiya (Japan) | Koji Ohno | Aichi Air Environment Division 1-2 Sannomaru-3chome, Naka-ku, Nagoya, Aichi 460-8501, Japan |
| Mt. Waliguan (China) | Lingxi ZHOU | Professor, PI for Greenhouse Gases & Related Tracers Chinese Academy of Meteorological Sciences (CAMS) China Meteorological Administration (CMA) 46 Zhongguancun Nandajie Beijing 100081, China |
| Memanbetsu (Japan) | Michio Hirota | Geochemical Research Department, Meteorological Research Institute 1-1, Nagamine, Tsukuba, Ibaraki 305-0052, Japan |
| Tsukuba (Japan) | Michio Hirota Yousuke Sawa | Geochemical Research Department, Meteorological Research Institute 1-1, Nagamine, Tsukuba, Ibaraki 305-0052, Japan |
| Hamamatsu (Japan) | Mitsuo TODA | Shizuoka University 3-5-1 Jyohoku, Hamamatsu 432-8561, Japan |
| Bering Island Kotelny Island (Russian Federation) | Nina Paramonova | Main Geophysical Observatory (MGO) Karbyshev Street 7, St. Petersburg, 194021, Russian Federation |
| Kyzylcha (Uzbekistan) | | |

LIST OF CONTRIBUTORS (continued)

| Station Country/Territory | Name | Address |
|--|---------------------------------------|---|
| Everest - Pyramid (Nepal) | Paolo Cristofanelli Paolo Bonasoni | ISAC-CNR ISAC-CNR, VIa Gobetti 101-40129 Bologna, Italy |
| Takayama (Japan) | Shohei Murayama | Research Institute for Environmental Management Technology, National Institute of Advanced Industrial Science and Technology (AIST) AIST Tsukuba West, 16-1 Onogawa, Tsukuba, Ibaraki 305-8569, Japan |
| Gosan (Republic of Korea) | So-young Bang | Applied Meteorology Research Laboratory, Meteorological Research Institute (METRI), Korea Meteorological Administration (KMA) 460-18, Shindaebang-dong, Dongjak-gu, Seoul 156-720, Republic of Korea |
| Ship between Ishigaki Island and Hateruma Island (Japan) | Takakiyo Nakazawa Shuji Aoki | Center for Atmospheric and Oceanic Studies, Graduate School of Science, Tohoku University Aoba, Sendai 980-8578, Japan |
| Suita (Japan) | Tomohiro Oda | Division of Sustainable Energy and Environmental Engineering, Graduate School of Engineering, Osaka University 2-1 Yamadaoka, Suita, Osaka 565-0871, Japan |
| Issyk-Kul (Kyrgyzstan) | V. Sinyakov | Laboratory of Geophysics, Institute of Fundamental sciences at the Kyrgyz National University Manas Street 101, Bishkek, 720033, Kyrgyz Republic |
| Mt. Dodaira Kisai Urawa (Japan) | Yosuke MUTO | Center for Environmental Science in Saitama 914 Kamitanadare, Kisai-machi, Kita-Saitama-gun, Saitama 347-0115, Japan |
| REGION III (South America) | | |
| Arembepe (Brazil) | LuanaãS. Basso Luciana Vanni Gatti | IPEN Atmospheric Chemistry Laboratory Av. Prof. Lineu Prestes, 2242, Cidade Universitaria, Sao Paulo, SP- BRAZIL CEP 05508-900, Brazil |
| Huancayo (Peru) | Mutsumi Ishitsuka | Observatorio de Huancayo, Instituto Geofisico del Peru Apartado 46, Huancayo, Peru |

LIST OF CONTRIBUTORS (continued)

| Station Country/Territory | Name | Address |
|--|---|---|
| Ushuaia (Argentina) | Sergio Luppo | Servicio Meteorológico Nacional - Gobierno de Tierra del Fuego Estación VAG Ushuaia Subsecretaria de Ciencia y Tecnología, Ministerio de Educación, Cultura, Ciencia y Tecnología Gobierno de Tierra del Fuego 9410 Ushuaia, Tierra del Fuego, Argentina |
| REGION IV (North and Central America) | | |
| Alert | Doug Worthy | Environment Canada (EC) |
| Candle Lake | Lin Huang | 4905 Dufferin Street, Toronto, Ontario, Canada, M3H |
| Cape St. James | Peter C. Brickell | 5T4 |
| Chibougamau | | |
| East Trout Lake | | |
| Egbert | | |
| Estevan Point | | |
| Fraserdale | | |
| Lac La Biche (Alberta) | | |
| Sable Island (Canada) | | |
| Algoma | Mike Shaw | Environment Canada Meteorological Service of Canada |
| Bratt's Lake | | Air Quality Research Branch |
| Chalk River | | 4905 Dufferin Street, Toronto, Ontario, Canada M3H |
| Chapais | | 5T4 |
| Egbert | | |
| Experimental Lakes Area | | |
| Esther | | |
| Kejimikujik | | |
| Longwoods | | |
| Saturna | | |
| Sutton (Canada) | | |
| La Palma (Cuba) | Oswaldo Cuesta Santos | Institute of Meteorology, Atmospheric Environment Research Center Aptdo. 17032, Postal Code 11700, Havana 17, Cuba |
| REGION V (South-West Pacific) | | |
| Baring Head (New Zealand) | Antony Gomez Sylvia Nichol Gordon Brailsford Ross Martin | National Institute of Water & Atmospheric Research Ltd. 301 Evans Bay Parade, Greta Point, Private Bag 14-901, Kilbirnie, Wellington, New Zealand |
| Cape Grim (Australia) | Bruce Forgan Ian Galbally | Commonwealth Bureau of Meteorology 700 Collins St, Docklands GPO Box 1289K, Melbourne, Victoria 3001, Australia |

LIST OF CONTRIBUTORS (continued)

| Station Country/Territory | Name | Address |
|--|--|--|
| Danum Valley GAW Baseline Station Tanah Rata (Malaysia) | Lim Sze Fook Maznorizan Mohamad | Environmental Studies Division Malaysian Meteorological Department Jalan Sultan, 46667 Petaling Jaya, Selangor, Malaysia |
| Bukit Koto Tabang Jakarta (Indonesia) | Nurhayati | Bureau of Meteorology and Geophysics Jalan Angkasa 1 No.2 Jakarta 10720, Indonesia |
| Bukit Koto Tabang (Indonesia) | Nurhayati Ilahi, Asep Firman Jörg Klausen | Bureau of Meteorology and Geophysics Jalan Angkasa 1 No.2 Jakarta 10720, Indonesia |
| REGION VI (Europe) | | |
| Puszcza Borecka/Diabla Gora (Poland) | Anna Degorska | Institute of Environmental Protection Kolektorska 4 01-692 Warsaw, Poland |
| Kloosterburen Kollumerwaard (Netherlands (the)) | Arien Stolk Hans Berkhout | RIVM - Laboratory for Environmental Measurements (LVM) P.O. Box 1, 3720 BA Bilthoven, The Netherlands |
| Monte Cimone (Italy) | Attilio Di Diodato Riccardo Santaguida | Italian Air Force Meteorological Service C.A.M.M. Mt. CIMONE, Via delle Ville 40, 41029-Sestola (MO), Italy |
| Hohe Warte Stephansplatz (Austria) | August Kaiser | Department for Environmental Meteorology Central Institute for Meteorology and Geodynamics Postfach 342, Hohe Warte 38, A-1191 Wien, Austria |
| Iskrba Krvavec (Slovenia) | Brigita Jesenovec Marijana Murovec | Ministry of Environment and Spatial Planning - Environmental Agency of the Republic of Slovenia (EARS) Vojkova 1/b, SI-1000 Ljubljana, Slovenia |
| Jungfrauoch Payerne Rigi (Switzerland) | Brigitte Buchmann Martin K. Vollmer Martin Steinbacher Thomas Seitz Stefan Reimann | Empa, Swiss Federal Laboratories for Materials Testing and Research, Air Pollution / Environmental Technology Überlandstrasse 129, CH-8600 Dübendorf, Switzerland |
| Fundata Semenic Stîna de Vale (Romania) | Daniela ZISU | National Research and Development Institute for Environmental Protection Splaiul Independentei nr. 294, sector 6, 77703 Bucuresti, Romania |
| Kamenicki Vis (Serbia) | Dragan Djordjevic | Republic Hydrometeorological Service, Environmental Control Department Kneza Visislava 66, 11030 Belgrade, Serbia |

LIST OF CONTRIBUTORS (continued)

| Station Country/Territory | Name | Address |
|---|--|---|
| Burgas Plovdiv Pleven Sofia Varna (Bulgaria) | Ekaterina Batchvarova | National Institute of Meteorology and Hydrology 66 Tzarigradsko chaussee, 1784 Sofia, Bulgaria |
| Jarczew Leba Suwalki (Poland) | Eugeniusz Brejnak | Institute of Meteorology and Water Management; Laboratory for Research and Monitoring of Air Pollution 61 Podlesna Street, 01-673 Warszawa, Poland |
| Sniezka (Poland) | Eugeniusz Brejnak Krzaczkowski Piotr, MSc | Institute of Meteorology and Water Management; Laboratory for Research and Monitoring of Air Pollution 61 Podlesna Street, 01-673 Warszawa, Poland |
| Fundata (Romania) | Florin Nicodim | National Meteorological Administration Sos. Bucuresti-Ploiesti nr. 97, 71552 Bucharest, Romania |
| Lampedusa (Italy) | Florinda Artuso Salvatore Chiavarini Salvatore Piacentino Alcide di Sarra | Italian National Agency for New Technology, Energy and the Environment (ENEA) ENEA ACS-CLIMOSS, Via Anguillarese 301, 00060 S.Maria di Galeria, Rome, Italy. |
| Plateau Rosa (Italy) | Francesco Apadula Daniela Heltai Andrea Lanza | Ricerca sul Sistema Energetico - RSE S.p.A. via Rubattino 54, 20134 Milano, Italy |
| Site J (Denmark) | Gen Hashida Shinji Morimoto Shuji Aoki | National Institute of Polar Research Kaga 1-9-10, Itabashi-ku, Tokyo 173-8515, Japan |
| Mace Head (Ireland) | Gerard Spain | National University of Ireland, Galway (NUI) Mace Head Research Station Carna, Co. Galway, Ireland |
| Hohe Warte Stephansplatz (Austria) | Guenther Schermann | Municipal Department 22 - Environmental Protection Air quality subdepartment, City of Vienna Ebendorferstrasse 4, A-1082 Vienna, Austria |
| Vindeln (Sweden) | Hakan Blomgren | IVL Swedish Environmental Research Institute P.O. Box 5302S-400 14 Goteborg, Sweden |
| Wank Peak Zugspitze (Germany) | Hans-Eckhart Scheel | Fraunhofer-Institute for Atmospheric Environmental Research, Forschungszentrum Karlsruhe, IMK-IFU D-82467 Garmisch-Partenkirchen, Germany |
| Danki Shepelevo (Russian Federation) | Irina Brouskina | |

LIST OF CONTRIBUTORS (continued)

| Station Country/Territory | Name | Address |
|---|----------------------------|--|
| BEO Moussala (Bulgaria) | Ivo Kalapov | INRNE Institut fo Nuclear Research and Nuclear Energy Tsarigradsko chaussee Blvd. 1784 Sofia Bulgaria |
| Doñana La Cartuja Logroño Mahón Noia Roquetes San Pablo de los Montes (Spain) | J.M. Saenz | Servicio de Desarrollos Medioambientales, Instituto Nacional de Meteorologia, Ministerio de Medio Ambiente Leonardo Prieto Castro, 8, 28071 Madrid, Spain |
| Zeppelinfjellet (Ny-Alesund) (Norway) | Johan Strom | Department of Applied Environmental Science (ITM), Stockholm University SE-106 91 Stockholm, Sweden |
| Pallas-Sammaltunturi (Finland) | Juha Hatakka Timo Salmi | Finnish Meteorological Institute P.O. Box 503, FI-00101 Helsinki, Finland |
| Brotjackkriegel Deuselbach Neuglobsow Schauinsland Westerland Waldhof Zingst Zugspitze Zugspitze / Schneefernerhaus (Germany) | Karin Uhse | Umweltbundesamt (UBA, Federal Environmental Agency) Air Monitoring Network Paul-Ehrlich-Strasse 29 D-63225 Langen, Germany |
| Hegyhatsal K-pusztá (Hungary) | Laszlo Haszpra | Hungarian Meteorological Service P.O. Box 39, H-1675 Budapest, Hungary |
| Angra do Heroismo Beja Bragança Castelo Branco Lisboa / Gago Coutinho Monte Velho Penhas Douradas Viana do Castelo (Portugal) | Maria Amelia V.Lopes | Instituto de Meteorologia, I.P. Rua C-Aeroporto de Lisboa 1749-077 Lisboa, Portugal |
| Kovk Zavodnje (Slovenia) | Marijana Murovec | Environmental Agency of Republic of Slovenia Environment Office Sektor za kakovost zraka / Air Quality Division Vojkova 1b, 1001 Ljubljana, p.p. 2608, Slovenia |

LIST OF CONTRIBUTORS (continued)

| Station Country/Territory | Name | Address |
|---|---|---|
| Dobele Rucava Zoseni (Latvia) | Marina Frolova | Observation Network Department, Latvian Environment, Geology and Meteorology Centre, Ministry of Environmental 165 Maskavas str. LV-1019, Riga, Latvia |
| Sonnblick (Austria) | Marina Fröhlich Wolfgang Spangl Elisabeth Friedbacher | Federal Environment Agency Austria Spittelauer Lände 5, A-1090 Wien, Austria |
| Ivan Sedlo (Bosnia and Herzegovina) | Martin Tais | Meteoroloski zavod Bosne i Hercegovine Bardakcije 12, 71000 Sarajevo, Bosnia and Herzegovina |
| Ile Grande Pic du Midi Puy de Dome (France) | Michel Ramonet | LSCE (Laboratoire des Sciences du Climat et de l'Environnement) UMR CEA-CNRS LSCE - CEA Saclay - Orme des Merisiers - Bat.701 91191 Gif-sur-Yvette, France |
| Finokalia (Greece) | | |
| Mace Head (Ireland) | | |
| Begur (Spain) | | |
| Kosetice (Czech Republic) | Milan Vana | Czech Hydrometeorological Institute, Kosetice Observatory Na Sabatce 17, 143 06 Praha 4 - Komorany, Czech Republic |
| Ocean Station Charlie Teriberka (Russian Federation) | Nina Paramonova | Main Geophysical Observatory (MGO) Karbyshev Street 7, St. Petersburg, 194021, Russian Federation |
| Zeppelinfjellet (Ny-Alesund) (Norway) | Ove Hermansen | Norwegian Institute for Air Research (NILU) P.O. Box 100 Instituttveien 18, N-2027 Kjeller, Norway |
| Monte Cimone (Italy) | Paolo Bonasoni jgor arduini | ISAC-CNR ISAC-CNR, Via Gobetti 101-40129 Bologna, Italy |
| Eskdalemuir (United Kingdom of Great Britain and Northern Ireland) | Peter Kuria | Air and Environment Quality Division, DEFRA 4/F15, Ashdown House 123 Victoria StreetLondon, SW1E 3DE, United Kingdom |
| Giordan Lighthouse (Malta) | Raymond Ellul | Atmospheric Research Unit / Physics Department /University of Malta Msida MSD 06, Malta |

LIST OF CONTRIBUTORS (continued)

| Station Country/Territory | Name | Address |
|--|--|---|
| Jungfrauoch (Switzerland) | Sander van der Laan | Postdoc, Physics Institute, Climate and Environmental Physics, University of Bern Sidlerstrasse 5 CH-3012 Bern, Switzerland |
| Hohenpeissenberg Zugspitze / Schneefernerhaus (Germany) | Stefan Gilge Christian Plass-Duelmer Wolfgang Fricke | Deutscher Wetterdienst (DWD, German Meteorological Service) Meteorologisches Observatorium Hohenpeissenberg Albin-Schwaiger-Weg 10D-82383 Hohenpeissenberg, Germany |
| Lazaropole (The Former Yugoslav Republic of Macedonia) | Suzana Alcinova Monevska | Hydrometeorological Service Skupi bb, 1000 Skopje, The former Yugoslav Republic of Macedonia |
| Kosetice (Czech Republic) | Sverre Solberg | Norwegian Institute for Air Research P.O. Box 100NO-2027 Kjeller, Norway |
| Pallas-Sammaltunturi Utö (Finland) | | |
| Donon La Tardiere Peyrusse Vieille (France) | | |
| Brotjacklriegel Waldhof Schmuecke Zingst (Germany) | | |
| Starina (Slovakia) | | |
| Campisabalos (Spain) | | |
| Ähtäri Oulanka Utö Virolahti (Finland) | Timo Salmi | Finnish Meteorological Institute Erik Palmenin aukio 1, P.O. Box 503, FIN-00101 Helsinki, Finland |

LIST OF CONTRIBUTORS (continued)

| Station Country/Territory | Name | Address |
|---|---|--|
| ANTARCTICA | | |
| Arrival Heights (New Zealand) | Antony Gomez Sylvia Nichol Gordon Brailsford Ross Martin | National Institute of Water & Atmospheric Research Ltd. 301 Evans Bay Parade, Greta Point Private Bag 14-901, Kilbirnie, Wellington, New Zealand |
| Jubany (Italy) | Claudio Rafanelli Luigi Ciattaglia | ICES (Int'l Center for Earth Sciences) c/o CNR-Istituto di Acustica-Area della Ricerca di Roma Tor Vergata,via Fosso del Cavaliere 100, 00133 Rome, Italy |
| Syowa Station (Japan) | Koji Kawashima | Office of Antarctic Observations, Japan Meteorological Agency (JMA) 1-3-4 Otemachi, Chiyoda-ku, Tokyo 100-8122, Japan |
| Neumayer (Germany) | Rolf Weller | Alfred Wegener Institute Am Handelshafen 12, 27570 Bremerhaven, Germany |
| Mizuho (Japan) | Takakiyo Nakazawa | Center for Atmospheric and Oceanic Studies, Graduate School of Science, Tohoku University Aoba, Sendai 980-8578, Japan |
| Syowa Station (Japan) | Takakiyo Nakazawa Gen Hashida Shinji Morimoto | Center for Atmospheric and Oceanic Studies, Graduate School of Science, Tohoku University Aoba, Sendai 980-8578, Japan |
| MOBILE STATION | | |
| Aircraft Observation of Atmospheric trace gases by JMA (Japan) | Daisuke KUBOIKE | Atmospheric Environment Division, Global Environment and Marine Department, Japan Meteorological Agency (JMA) 1-3-4 Otemachi, Chiyoda-ku, Tokyo 100-8122, Japan |
| NOPACCS - Hakurei Maru - WEST COSMIC - Hakurei Maru No.2 - (Japan) | General Environmental Texhnos | The General Environmental Technos Co., Ltd. 1-3-5, Azuchi machi, Chuo-ku, Osaka 541-0052, Japan |
| INSTAC-I (International Strato/Tropospheric Air Chemistry Project) (Japan) | Hidekazu Matsueda | Geochemical Research Department, Meteorological Research Institute Nagamine 1-1, Tsukuba, Ibaraki 305-0052, Japan |
| Comprehensive Observation Network for TRace gases by AIRLiner (CONTRAIL) (Japan) | Hidekazu Matsueda Toshinobu Machida | Geochemical Research Department, Meteorological Research Institute Nagamine 1-1, Tsukuba, Ibaraki 305-0052, Japan |

LIST OF CONTRIBUTORS (continued)

| Station Country/Territory | Name | Address |
|---|--|---|
| MRI Research, Mirai, R/V (Japan) | Hisayuki Yoshikawa-Inoue | Laboratory of Marine and Atmospheric Geochemistry Graduate School of Environmental Earth Science Hokkaido University N10W5, Kita-ku, Sapporo 060-0810, Japan |
| northern and western Pacific (Japan) | Kentaro Ishijima Shuji Aoki Takakiyo Nakazawa | Japan Agency for Marine-earth Science and Technology (JAMSTEC) 3173-25 Showamachi, Kanazawa-ku, Yokohama, 236-0001, Japan |
| Santarem (Brazil) | Luciana Vanni Gatti Luana S. Basso Alexandre Martinewski | IPEN Atmospheric Chemistry Laboratory Av. Prof. Lineu Prestes, 2242, Cidade Universitaria, Sao Paulo, SP- BRAZIL CEP 05508-900, Brazil |
| MRI Research, Hakuho Maru, R/V MRI Research, Kaiyo Maru, R/V MRI Research, 1978-1986, R/V MRI Research, Natushima, R/V MRI Research, Ryofu Maru, R/V MRI Research, Wellington Maru, R/V (Japan) | Masao Ishii | Geochemical Research Department, Meteorological Research Institute Nagamine 1-1, Tsukuba, Ibaraki 305-0052, Japan |
| Aircraft: Orleans (France) | Michel Ramonet | LSCE (Laboratoire des Sciences du Climat et de l'Environnement) UMR CEA-CNRS LSCE - CEA Saclay - Orme des Merisiers - Bat.701 91191 Gif-sur-Yvette, France |
| Observation of Atmospheric Chemistry Over Japan The Observation of Atmospheric Methane Over Japan The Observation of Atmospheric Sulfur Hexafluoride Over Japan (Japan) | Michio Hirota | Geochemical Research Department, Meteorological Research Institute 1-1, Nagamine, Tsukuba, Ibaraki 305-0052, Japan |
| Pacific Ocean (New Zealand) | Sylvia Nichol Gordon Brailsford | National Institute of Water & Atmospheric Research Ltd. 301 Evans Bay Parade, Greta Point Private Bag 14-901, Kilbirnie, Wellington, New Zealand |

LIST OF CONTRIBUTORS (continued)

| Station Country/Territory | Name | Address |
|---|------------------|---|
| Alligator liberty, M/V Keifu Maru, R/V Kofu Maru, R/V Ryofu Maru, R/V (Japan) | Takayuki Tokieda | Pollutants Chemical Analysis Center, Marine Division, Climate and Marine Department, Japan Meteorological Agency (JMA) 1-3-4 Otemachi, Chiyoda-ku, Tokyo 100-8122, Japan |
| Soyo Maru, R/V Wakataka-Maru (Japan) | Tsuneo Ono | Hokkaido National Fisheries Research Institute 116 Katsurakoi, Kushiro 085-0802, Japan |

LIST OF CONTRIBUTORS (continued)

| Station Country/Territory | Name | Address |
|---|---|--|
| NOAA/ESRL Flask Network | | |
| Assekrem (Algeria) | Bruce Vaughn** (¹³ CH ₄ , N ₂ O and SF ₆) | (*)NOAA/ESRL Global Monitoring Division 325 Broadway R/GMD1 Boulder, CO 80305-3328, U.S.A |
| Tierra del Fuego (Argentina) | Bruce Vaughn** James White** (¹³ CO ₂ and C ¹⁸ O ₂) | (**)Institute of Arctic and Alpine Research (INSTAAR) INSTAAR, Univ. of Colorado 1560, 30th Street |
| Cape Grim (Australia) | Edward J. Dlugokencky* (CH ₄) | UCB 450 Boulder, CO 80309, U.S.A. |
| Ragged Point (Barbados) | Paul C. Novelli* (CO and H ₂) | |
| Arembepe (Brazil) | Thomas J. Conway* (CO ₂) | |
| Alert Lac La Biche Mould Bay (Canada) | Detlev Helmig** Jacques Hueber** (VOCs) | |
| Easter Island (Chile) | | |
| Lulin Shangdianzi Mt. Waliguan (China) | | |
| Summit (Denmark) | | |
| Pallas-Sammaltunturi (Finland) | | |
| Amsterdam Island Crozet (France) | | |
| Hohenpeissenberg Ochsenkopf (Germany) | | |
| Hegyhatsal (Hungary) | | |
| Heimaey (Iceland) | | |
| Bukit Koto Tabang (Indonesia) | | |

LIST OF CONTRIBUTORS (continued)

| Station Country/Territory | Name | Address |
|---|------|---------|
| Mace Head (Ireland) | | |
| Sede Boker (Israel) | | |
| Lampedusa (Italy) | | |
| Syowa Station (Japan) | | |
| Sary Taukum Plateau Assy (Kazakhstan) | | |
| Mt. Kenya (Kenya) | | |
| Christmas Island (Kiribati) | | |
| Kaashidhoo (Maldives) | | |
| Dwejra Point (Malta) | | |
| Mex High Altitude Global Climate Observation Center, Mexico (Mexico) | | |
| Ulaan Uul (Mongolia) | | |
| Gobabeb (Namibia) | | |
| Arrival Heights Baring Head Lauder Kaitorete Spit (New Zealand) | | |
| Ocean Station "M" Zeppelinfjellet (Ny-Alesund) (Norway) | | |
| Baltic Sea (Poland) | | |

LIST OF CONTRIBUTORS (continued)

| Station Country/Territory | Name | Address |
|---|------|---------|
| Terceira Island (Portugal) | | |
| Tae-ahn Peninsula (Republic of Korea) | | |
| Black Sea (Romania) | | |
| Mahe Island (Seychelles) | | |
| Cape Point (South Africa) | | |
| Izaña (Tenerife) (Spain) | | |
| Ascension Island St. David's Head Tudor Hill Halley Bay Bird Island (United Kingdom of Great Britain and Northern Ireland) | | |
| Akademik Korolev, R/V Argyle Atlantic Ocean St. Croix Barrow Cold Bay Cape Meares Discoverer 1983 & 1984, R/V Drake Passage Discoverer 1985, R/V Guam Grifton John Biscoe, R/V Key Biscayne Korolev, R/V Kitt Peak Cape Kumukahi Park Falls Long Lines Expedition, R/V McMurdo Station Sand Island Mauna Loa Mexico Naval H-02, R/V Niwt Ridge (T-van) | | |

LIST OF CONTRIBUTORS (continued)

| Station Country/Territory | Name | Address |
|------------------------------|------|---------|
| Niwot Ridge (Saddle) | | |
| Oceanographer, R/V | | |
| Olympic Peninsula | | |
| Pacific-Atlantic Ocean | | |
| Polar Star, R/V | | |
| Pacific Ocean | | |
| Palmer Station | | |
| Point Arena | | |
| South China Sea | | |
| Southern Great Plains | | |
| Shemya Island | | |
| La Jolla | | |
| Tutuila (Cape Matatula) | | |
| South Pole | | |
| Ocean Station Charlie | | |
| Surveyor, R/V | | |
| Trinidad Head | | |
| Wendover | | |
| West Branch | | |
| Moody | | |
| Western Pacific | | |
| (United States of America) | | |

NOAA/ESRL/HATS Network

| | | |
|---------------------------------|---|--|
| Tierra del Fuego (Argentina) | Geoffrey S. Dutton James W. Elkins Stephen A. Montzka | Halocarbons and Other Atmosphere Trace Species Group (HATS)/NOAA/ESRL Global Monitoring Division 325 Broadway R/GMD1 Boulder, CO 80305-3328, U.S.A |
| Cape Grim (Australia) | | |
| Alert (Canada) | | |
| Summit (Denmark) | | |
| Mace Head (Ireland) | | |
| BACPAC 99 | | |
| BLAST1 | | |
| BLAST2 | | |
| BLAST3 | | |
| Barrow | | |
| CLIVAR 01 | | |
| Gas Change Experiment | | |
| Harvard Forest | | |
| HATS Ocean Projects | | |
| Grifton | | |
| Cape Kumukahi | | |
| Park Falls | | |

LIST OF CONTRIBUTORS (continued)

| Station Country/Territory | Name | Address |
|------------------------------|------|---------|
| Mauna Loa | | |
| Niwot Ridge (C-1) | | |
| PHASE I-04 | | |
| Palmer Station | | |
| Tutuila (Cape Matatula) | | |
| South Pole | | |
| Trinidad Head | | |
| (United States of America) | | |

NOAA/ESRL Surface Ozone Network

| | | |
|----------------------------|-------------|--|
| Ragged Point (Barbados) | Sam Oltmans | NOAA/ESRL Global Monitoring Division 325 Broadway R/GMD1 Boulder, CO 80305-3328, U.S.A |
|----------------------------|-------------|--|

Summit
(Denmark)

Heimaey
(Iceland)

Arrival Heights
Lauder
(New Zealand)

Tudor Hill
(United Kingdom of Great
Britain and Northern
Ireland)

Barrow
McMurdo Station
Mauna Loa
Niwot Ridge (C-1)
Niwot Ridge (Saddle)
Tutuila (Cape Matatula)
South Pole
Trinidad Head
(United States of America)

LIST OF CONTRIBUTORS (continued)

| Station Country/Territory | Name | Address |
|------------------------------|------|---------|
|------------------------------|------|---------|

CSIRO Flask Network

| | | |
|--|-----------------|---|
| Aircraft (over Bass Strait and Cape Grim) | Ray Langenfelds | Commonwealth Scientific and Industrial Research Organisation (CSIRO) |
| Cape Ferguson | Paul Krummel | CSIRO Marine and Atmospheric Research |
| Cape Grim | Paul Steele | Private Bag 1 |
| Casey Station | Colin Allison | Aspendale, Vic 3195, Australia |
| Mawson | | |
| Macquarie Island (Australia) | | |

Alert
Estevan Point
(Canada)

Cape Rama
(India)

Shetland
(United Kingdom of Great
Britain and Northern
Ireland)

Mauna Loa
South Pole
(United States of America)

ALE/GAGE/AGAGE Network

| | | |
|----------------------------|----------|--|
| Cape Grim (Australia) | Ray Wang | School of Earth and Atmospheric Sciences, Georgia Institute of Technology 311 Ferst Drive |
| Ragged Point (Barbados) | | School of Earth and Atmospheric Sciences Georgia Institute of Technology Atlanta, GA 30332-0340, U.S.A |

Adrigole
Mace Head
(Ireland)

Zeppelinfjellet
(Ny-Alesund)
(Norway)

Jungfrauoch
(Switzerland)

Cape Meares
Tutuila (Cape Matatula)
Trinidad Head
(United States of America)

GLOSSARY

ATMOSPHERIC SPECIES:

| | |
|--------------------------------------|--|
| CCl₄ | tetrachloromethane (carbon tetrachloride) |
| CFC-11 | chlorofluorocarbon-11 (trichlorofluoromethane, CCl ₃ F) |
| CFC-12 | chlorofluorocarbon-12 (dichlorodifluoromethane, CCl ₂ F ₂) |
| CFC-113 | chlorofluorocarbon-113 (1,1,2-trichlorotrifluoroethane, CCl ₂ FCFClF ₂) |
| CFCs | chlorofluorocarbons |
| CH₃Cl | chloromethane (methyl chloride) |
| Halon-1211 | chlorodifluorobromomethane (CBrClF ₂) |
| Halon-1301 | bromotrifluoromethane (CBrF ₃) |
| HCFC-141b | hydrochlorofluorocarbon-141b (1,1-dichloro-1-fluoroethane, CH ₃ CCl ₂ F) |
| HCFC-142b | hydrochlorofluorocarbon-142b (1,1-difluoro-1-chloroethane, CH ₃ CClF ₂) |
| HCFC-22 | hydrochlorofluorocarbon-22 (chlorodifluoromethane, CHClF ₂) |
| HCFCs | hydrochlorofluorocarbons |
| HFC-134a | hydrofluorocarbon-134a (1,1,1,2-tetrafluoroethane, CH ₂ FCF ₃) |
| HFC-152a | hydrofluorocarbon-152a (1,1-difluoroethane, CHF ₂ CH ₃) |
| HFCs | hydrofluorocarbons |
| CH₄ | methane |
| CH₃CCl₃ | trichloroethane (methyl chloroform) |
| CO | carbon monoxide |
| CO₂ | carbon dioxide |
| N₂O | nitrous oxide |
| NO | nitrogen monoxide |
| NO₂ | nitrogen dioxide |
| NO_x | nitrogen oxides |
| O₃ | ozone |
| SF₆ | sulphur hexafluoride |
| SO₂ | sulphur dioxide |

UNITS:

| | |
|------------|--------------------|
| ppb | parts per billion |
| ppm | parts per million |
| ppt | parts per trillion |

Others:

| | |
|-------------|------------------------------|
| ENSO | El Niño-Southern Oscillation |
| M/V | merchant vessel |
| R/V | research vessel |

LIST OF WMO WDCGG PUBLICATIONS

DATA REPORTING MANUAL:

WDCGG No. 1 January 1991

WMO WDCGG DATA REPORT:

(period of data accepted)

| | | | | | | | |
|--------------------|-----------|------|-----------|------|---|-----------|------|
| WDCGG No. 2 Part A | October | 1992 | October | 1990 | ~ | August | 1992 |
| WDCGG No. 2 Part B | October | 1992 | October | 1990 | ~ | August | 1992 |
| WDCGG No. 3 | October | 1993 | September | 1992 | ~ | March | 1993 |
| WDCGG No. 5 | March | 1994 | April | 1993 | ~ | September | 1993 |
| WDCGG No. 6 | September | 1994 | September | 1993 | ~ | March | 1994 |
| WDCGG No. 7 | March | 1995 | April | 1994 | ~ | December | 1994 |
| WDCGG No. 9 | September | 1995 | January | 1995 | ~ | June | 1995 |
| WDCGG No.10 | March | 1996 | July | 1995 | ~ | December | 1995 |
| WDCGG No.11 | September | 1996 | January | 1996 | ~ | June | 1996 |
| WDCGG No.12 | March | 1997 | July | 1996 | ~ | November | 1996 |
| WDCGG No.14 | September | 1997 | December | 1996 | ~ | June | 1997 |
| WDCGG No.16 | March | 1998 | July | 1997 | ~ | December | 1997 |
| WDCGG No.17 | September | 1998 | January | 1998 | ~ | June | 1998 |
| WDCGG No.18 | March | 1999 | July | 1998 | ~ | December | 1998 |
| WDCGG No.20 | September | 1999 | January | 1999 | ~ | June | 1999 |
| WDCGG No.21 | March | 2000 | July | 1999 | ~ | December | 1999 |
| WDCGG No.23 | September | 2000 | January | 2000 | ~ | June | 2000 |
| WDCGG No.25 | March | 2001 | July | 2000 | ~ | December | 2000 |

WMO WDCGG DATA CATALOGUE:

| | | |
|-------------|----------|------|
| WDCGG No. 4 | December | 1993 |
| WDCGG No.13 | March | 1997 |
| WDCGG No.19 | March | 1999 |
| WDCGG No.24 | March | 2001 |

WMO WDCGG DATA SUMMARY:

| | | |
|-------------|---------|------|
| WDCGG No. 8 | October | 1995 |
| WDCGG No.15 | March | 1998 |
| WDCGG No.22 | March | 2000 |
| WDCGG No.26 | March | 2002 |
| WDCGG No.27 | March | 2003 |
| WDCGG No.28 | March | 2004 |
| WDCGG No.29 | March | 2005 |
| WDCGG No.30 | March | 2006 |
| WDCGG No.31 | March | 2007 |
| WDCGG No.32 | March | 2008 |
| WDCGG No.33 | March | 2009 |
| WDCGG No.34 | March | 2010 |
| WDCGG No.35 | March | 2011 |

WMO WDCGG CD-ROM:

(period of data accepted)

| | | | | | | | |
|--------------|-------|------|---------|------|---|----------|------|
| CD-ROM No. 1 | March | 1995 | October | 1990 | ~ | December | 1994 |
| CD-ROM No. 2 | March | 1996 | October | 1990 | ~ | June | 1995 |
| CD-ROM No. 3 | March | 1997 | October | 1990 | ~ | June | 1996 |
| CD-ROM No. 4 | March | 1998 | October | 1990 | ~ | December | 1997 |
| CD-ROM No. 5 | March | 1999 | October | 1990 | ~ | December | 1998 |
| CD-ROM No. 6 | March | 2000 | October | 1990 | ~ | December | 1999 |
| CD-ROM No. 7 | March | 2001 | October | 1990 | ~ | December | 2000 |
| CD-ROM No. 8 | March | 2002 | October | 1990 | ~ | January | 2002 |
| CD-ROM No. 9 | March | 2003 | October | 1990 | ~ | December | 2002 |

| | | | | | | | |
|--------------|-------|------|---------|------|---|----------|------|
| CD-ROM No.10 | March | 2004 | October | 1990 | ~ | December | 2003 |
| CD-ROM No.11 | March | 2005 | October | 1990 | ~ | December | 2004 |
| CD-ROM No.12 | March | 2006 | October | 1990 | ~ | December | 2005 |
| CD-ROM No.13 | March | 2007 | October | 1990 | ~ | November | 2006 |
| CD-ROM No.14 | March | 2008 | October | 1990 | ~ | November | 2007 |

WMO WDCGG DVD:

(period of data accepted)

| | | | | | | | |
|-----------|-------|------|---------|------|---|----------|------|
| DVD No. 1 | March | 2009 | October | 1990 | ~ | November | 2008 |
| DVD No. 2 | March | 2010 | October | 1990 | ~ | November | 2009 |
| DVD No. 3 | March | 2011 | October | 1990 | ~ | November | 2010 |
| DVD No. 4 | March | 2012 | October | 1990 | ~ | November | 2011 |